





# HIV alters the expression of miRNA hsa-miR-200c-3p in B-cells, leading to enhanced migration of lymphoma cells

**Presented for MSc (Med) in Haematology (PTY7023W)**
**Candidate: Miss Beatrice Relebogile Ramorola (RMRBEA001)**
**Supervisor: Dr Shaheen Mowla**
**Co-Supervisor: Dr Karen Shires**
**Department of Pathology**
**Division of Haematology**
**Faculty of Health Sciences**
**University of Cape Town**

**Name: Beatrice Relebogile Ramorola**

**Student Number: RMRBEA001**

**MSc Med by Dissertation (PTY7023W – Haematology)**

# Declaration

I, **Beatrice Relebogile Ramorola**, hereby declare that the work on which this dissertation (MSc(Med)) is based is my original work (except where acknowledgements indicate otherwise) and that neither the whole work nor any part of it has been, is being, or is to be submitted for another degree in this or any other University.

I have used the Harvard convention for citation and referencing. Each contribution to, and quotation in, this MSc (Med) Dissertation from the work(s) of other people has been attributed, and has been cited and referenced.

I empower the University to reproduce for the purpose of research either the whole or any portion of the contents in any manner whatsoever.

**Signature** Signed by candidate

**Date** 25/04/2018

# Abstract

**Background:** The sub-Saharan African region is one that is affected most by the HIV/AIDS pandemic, with South Africa being the country with the highest number of infected individuals at 7.06 million. Infection with HIV is often associated with co-morbidities, including HIV-associated Non-Hodgkin's Lymphomas (HIV-NHLs). Burkitt's lymphoma (BL), a highly aggressive cancer, is one of the most common NHLs associated with HIV infection. Despite receiving highly active anti-retroviral therapy, the prognosis for this HIV-associated lymphoma remains poor and the incidence keeps on increasing in this group of patients. Recent studies have shown that microRNA (miRNA) dysregulation play essential roles in the pathogenesis of many cancers, including NHLs. While several human pathogenic viruses have been shown to deregulate cellular miRNAs, to date, no comprehensive studies have been carried out to determine whether HIV infection can lead to miRNA dysregulation in B-cells, which may contribute to the development of HIV-associated lymphomas.

**Objective**: This research project aimed to validate the differential expression of selected miRNAs which were identified as potentially important in a PCR array, and characterise their roles in Burkitt's lymphoma cells exposed to an attenuated strain of HIV-1, compared to control cells.

**Methods:** Single-tube TaqMan miRNA assays were used to validate the previously observed differential expression of four selected miRNAs in Burkitt's lymphoma cell lines (Ramos and BL41) exposed to HIV-1 compared to matched-microvesicle treated (control) cells. Following validation, the role of miRNA hsa-miR-200c-3p in the development of HIV-associated BL was investigated. This was done by using online bioinformatic prediction tools, as well as literature searches, to identify gene targets. Thereafter, the differential expression of a selected gene target was investigated by qPCR and western blotting. The functional significance of the observed changes in miRNA and gene expression was investigated by performing cell viability and migration assays.

**Results:** Three upregulated (hsa-miR-575, hsa-miR-363-3p and hsa-miR-222-3p) and one downregulated (hsa-miR-200c-3p) miRNAs that were significantly deregulated by 2-fold or more ($p<0.05$) in the PCR array were selected for validation. Thereafter, the miRNA hsa-miR-200c-3p was selected for further analysis. Upon exposure to attenuated HIV-1, hsa-miR-200c-3p was downregulated in the BL cell line Ramos, and this was reproducible in a second BL cell line BL41. The transcription factors ZEB1 and ZEB2, which are involved in cancer cell migration, were identified as targets of hsa-miR-200c-3p. Contrary to what is expected, the mRNA expression of both genes was found to be significantly downregulated in Ramos and BL41 exposed to attenuated HIV-1. At the protein level, in the Ramos cells, ZEB1 and ZEB2 matched what was observed for the mRNA. In contrast, both ZEB1 and ZEB2 protein were upregulated in BL41 cells under the same treatment conditions. At the functional level, the

migration of both cell lines was enhanced when exposed to attenuated HIV-1, compared to control cells.

**Conclusions:** The present study has demonstrated that HIV-1 has the ability to modulate cellular miRNA expression in Burkitt's lymphoma cells. Of these miRNAs, hsa-miR-200c-3p is consistently downregulated when two BL cell lines were exposed to HIV. The ZEB transcription factors ZEB1 and ZEB2, which promote Epithelial-to-Mesenchymal Transition (EMT) through enhancing cellular migration, were investigated as hsa-miR-200c-3p targets. The mRNA levels of ZEB1 and ZEB2 were downregulated in both cell lines under the same experimental conditions. This is contrary to what is expected, since miRNAs lead to the attenuation of transcription or translation of their target genes and a downregulation of a miRNA should lead to an upregulation of its target. However, protein expression rather than mRNA expression has been described as a more accurate indication of target validation for miRNAs. The protein expression levels for ZEB1 and ZEB2 correlated with the mRNA expression results observed in the Ramos cells. In the BL41 cells, ZEB1 and ZEB2 protein levels were upregulated. Furthermore, in both cell lines, an increase in migratory ability was observed when cells were exposed to attenuated HIV-1. These results demonstrate that exposure to HIV enhances the cancer phenotype and that this is potentially due to changes in cellular miRNA expression brought about by the virus or viral components. Future studies should focus on gain-of-function and loss-of-function studies to determine whether the increase in cell migration is specifically due to a decrease in hsa-miR-200c-3p.

# Acknowledgements

*"F.E.A.R has two meanings: Forget Everything and Run OR Face Everything and Rise. The Choice is yours"*

-Zig Ziglar

There were many times in my journey when I was questioning my decision-making skills, trying to find my "why". Why did I choose to fall in love with science? Why did I choose to go against what people think is the norm? And then I look around me. I see so many wonderful people who inspire me to do more, to be more confident in owning and expressing my passion for research and science. During my honours year, my supervisor, Dr Shaheen Mowla, once described me as "quiet but potent". Although I did not know what it meant at the time, I have grown to realise that I am stronger than I think, and that I should have more faith in myself.

To Dr Shaheen Mowla, I would like to thank you for all the love, kindness and compassion you have expressed towards me. I truly appreciate all the support you have given me so far in my journey. I admire your strength, passion and positive attitude, which is evident in all that you do. Thank you for guiding me and sharing your valuable knowledge with me.

I would also like to express my gratitude to the following people for making my Masters journey more pleasant:

- My co-supervisor, Dr Karen Shires. I admire the amount of passion you have when you talk about your work/research. Thank you for your support, advice and encouragement when times were tough
- A special thanks to Leo and Lungile, for the laughs and long chats. To Grant, Gift and Taahira, thank you for all the wisdom and sound advice
- To the Haematology lab staff for their kindness and support
- The Centre for Proteomic and Genomic Research (CPGR) and Dr Nicki Adams for assistance while using the Applied Biosystems 7900HT Fast Real-Time PCR system machine.
- Prof Dave Sandeep for kindly donating the BL41 cell line
- Prof Jeff Lifson and Dr Wendy Burgers for kindly donating the attenuated HIV-1 and matched microvesicles
- The South African Medical Research Foundation and the Marion Beatrice Waddell Bursary (University of Cape Town) for assisting me financially and making the journey less stressful

Lastly, I would like my family and friends for their continued love and support, as well as their encouragement and prayers.

# Table of Contents

# List of figures

# List of tables

# Abbreviations

3’-UTR – 3’ untranslated regions
Ago – Argonaute
AID – Activation-induced cytidine deaminase
BCA – Bicinchonic acid
BCL6 – B -Cell Lymphoma protein 6
BL – Burkitt ’s lymphoma
BLID – BH3-like motif-containing cell death inducer
BSA – bovine serum albumin
c-ART - combination Anti-Retroviral Therapy
CPGR – Centre for Proteomic and Genomic Research
CSR – Class Switch Recombination
DGCR8 – DiGeorge Syndrome Critical Region 8
DMSO – Dimethyl sulfoxide
DNA – deoxyribose nucleic acid
dsRNA – double-stranded RNA
EBNA2 – Epstein Barr Virus Nuclear Antigen 2
EBV – Epstein Barr Virus
E-Cad – endothelial Cadherin
EcTRs – E-cadherin transcriptional repressors
EMT – Epithelial-to-Mesenchymal Transition
ERα – Oestrogen Receptor α
Exp5 – Exportin 5
HAART – Highly Active Antiretroviral Therapy
HCV – Hepatitis C Virus
HIV-1 – Human Immuno-Deficiency Virus subtype 1
HIV/AIDS – Human Immuno-Deficiency Virus/Acquired Immuno-Deficiency Syndrome
HIV/NHLs – Human Immuno-Deficiency Virus associated Non-Hodgkin’s Lymphomas
KS – Kaposi’s Sarcoma
KSHV – Kaposi’s Sarcoma associated Herpes Virus
MAPK/ERK – mitogen-activated kinases/ extracellular signal-regulated kinases
MCL – Mantle cell lymphoma
miR-genes – miRNA encoding genes
mi-RISC – miRNA containing RNA Induced Silencing Complex
MiRNA – microRNA
MGB – Minor groove binder
mRNA – messenger RNA
MR-EMT – Master Regulators of Epithelial-to-Mesenchymal Transition
MV – Microvesicles
NFQ – nonfluorescent quencher

NHLs – Non-Hodgkin's Lymphoma
NIH – National Institutes of Health
NK – Natural Killer
OncomiR – oncogenic miRNA
PBMC – Peripheral blood mononuclear cells
PCAF – P300/CBP-associated factor
pre-miRNA – precursor microRNA
pri-miRNA – primary microRNA
Ran-GTP – Ras related Nuclear-GTPase protein
RISC – RNA Induced Silencing Complex
RNA – Ribonucleic acid
rpm – Revolutions per minute
RPMI – Rosswell Park Memorial Institute
SDS-PAGE – Sodium dodecyl sulphate polyacrylamide gel electrophoresis
SHM – Somatic hypermutation
SIP – Smad Interacting protein
TRBP – trans-activation response RNA binding protein
UNAIDS – United Nations programme on HIV and AIDS
WHO – World Health Organisation
qPCR – quantitative polymerase chain reaction
ZEB1/2 – Zinc finger E-box binding protein 1/2

# Chapter 1

# Introduction

## Background

### 1.1 MicroRNAs

MicroRNAs (miRNAs) are small non-coding single-stranded ribonucleic acid (RNA) that can negatively regulate gene expression (Ambros et al., 2003). The first members of this class of RNA molecules were discovered in *Caenorhabditis elegans*, where they were shown to be spatially and temporally expressed and involved in regulating development (Wightman et al., 1993, Lee et al., 1993). Recently, more miRNAs have been identified in a wide range of plants and animals (Luo et al., 2013, Lee et al., 2007, Altuvia et al., 2005). Due to their fairly recent discovery, many miRNAs still do not have functions assigned to them. However, thus far, miRNAs have been found to be involved in normal cellular processes such as proliferation, growth, differentiation and apoptosis. Importantly, the deregulation of miRNA expression has been linked to several pathological processes, one of which being cancer (Ranganathan and Sivasankar, 2014, Cheng et al., 2005).

### 1.1.1 MicroRNA Biogenesis

The biogenesis of miRNAs has been well studied and described in the literature. Two processing events are involved in the most widely accepted model for miRNA biogenesis. As Figure 1.1 indicates, the first processing event occurs in the nucleus while the final processing event occurs in the cytoplasm. Primary miRNAs (pri-miRNAs), which are 70-100 nucleotides long, are transcribed from the miR-genes (Nathans et al., 2009). The pri-miRNAs then fold to form hairpin structures, which can be recognised and cleaved by the microprocessor complex. This complex mainly consists of the RNase III endonuclease enzyme Drosha and its co-factor DiGeorge syndrome critical region 8 (DGCR8) (Roth et al., 2013, Han et al., 2004, Gregory et al., 2004). The resulting product is referred to as the precursor miRNA (pre-miRNA), which is a 60-70 nucleotides long double-stranded molecule (Ranganathan and Sivasankar, 2014, Roth et al., 2013, Han et al., 2004, Gregory et al., 2004).

The processed pre-miRNA is then recognised by the karyopherin Exportin 5 (Exp5) transporter protein. Nuclear export by Exp5 is dependent on the cofactor Ran-GTP (Yi et al., 2003). In the cytoplasm, the pre-miRNA is recognised by the RNase III endonuclease enzyme Dicer and its cofactor, the HIV-1 trans-activation response (TAR) RNA binding protein (TRBP) (Haase et al., 2005). Dicer performs the second processing step, resulting in a short double-stranded RNA (dsRNA) product, denoted as miRNA/miRNA*. The dsRNA duplex consists of the miRNA that will become the mature guide (as indicated by the red strand in Figure 1) for the RNA induced silencing complex (RISC), and the other passenger strand (miRNA*) that will be degraded. The Dicer-TRBP dimer, while bound to the miRNA/miRNA* duplex can recruit one of four argonaute (Ago) proteins to form the RISC (Lee et al., 2006, Chendrimada et al., 2005, Gregory

et al., 2004). Once the mature miRNA is incorporated, the mi-RISC is ready to bind to the 3'-UTR of target mRNAs to induce degradation or inhibit translation.

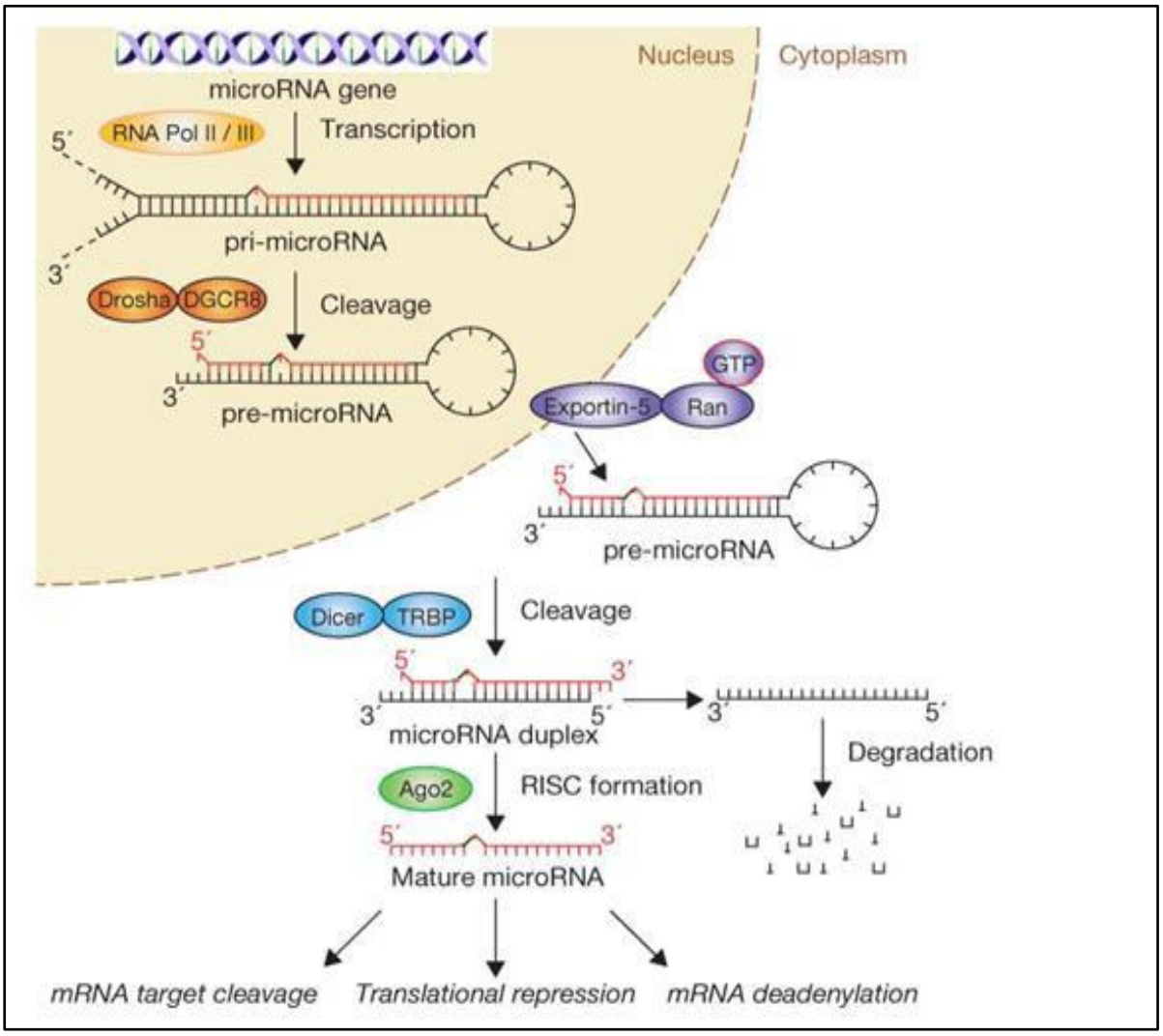


**Figure 1.1: Pathway of miRNA biogenesis and mechanism of action** (Adapted from Velu et al., 2012).

Gene silencing occurs in specialized cytoplasmic regions called processing bodies (P-bodies), which contain proteins essential for mRNA degradation and/or those with 5'- and 3'-exonuclease activity (Nathans et al., 2009). A stretch of 7-8 nucleotides in the guide miRNA referred to as the "seed region" can bind complementarily to the 3'-UTR of the target mRNA. Perfect complementarity between the seed region and the target mRNA results in degradation while imperfect complementarity is enough to induce translational inhibition (MacFarlane and Murphy, 2010, Iorio et al., 2005). The small size of the seed region allows one miRNA to have multiple mRNA targets. Since these small molecules regulate essential cellular processes, their deregulation can have detrimental effects that results in diseases, including cancer formation and progression.

### 1.1.2 Mechanisms of MiRNA Regulation

As already mentioned, miRNAs are essential for many biological functions which require stringent modulation by different effectors. Therefore, more clarity on the underlying molecular mechanisms regulating miRNA expression levels is needed to understand the variations in protein-coding gene expression (Gulyaeva and Kushlinskiy, 2016). There are various levels in this pathway that can be regulated. These regulatory factors may be promoted or inhibited by various physiological and pathological stimuli (hormones, cytokines), as well as external factors (diet and lifestyle). As shown in Figure 1.2, these regulatory levels can either be transcriptional or post-transcriptional. At the transcriptional level, the methylation status of the miRNA-encoding genes (miR-genes) as well as activating or inhibitory transcription factors acting on the promoter and regulatory regions of the miR-genes affect their expression. Hypermethylation of CpG islands or regions enriched in CpG residues may result in transcriptional silencing (Morales et al., 2017), and therefore less pri-miRNA hairpins to be processed by the Drosha microprocessor complex. For example, work by Vera *et al* has shown that methylation of miR-7 in platinum-sensitive patients could be used as a clinical tool for predicting a poorer response to platinum-based treatment regimens (Vera et al., 2017).

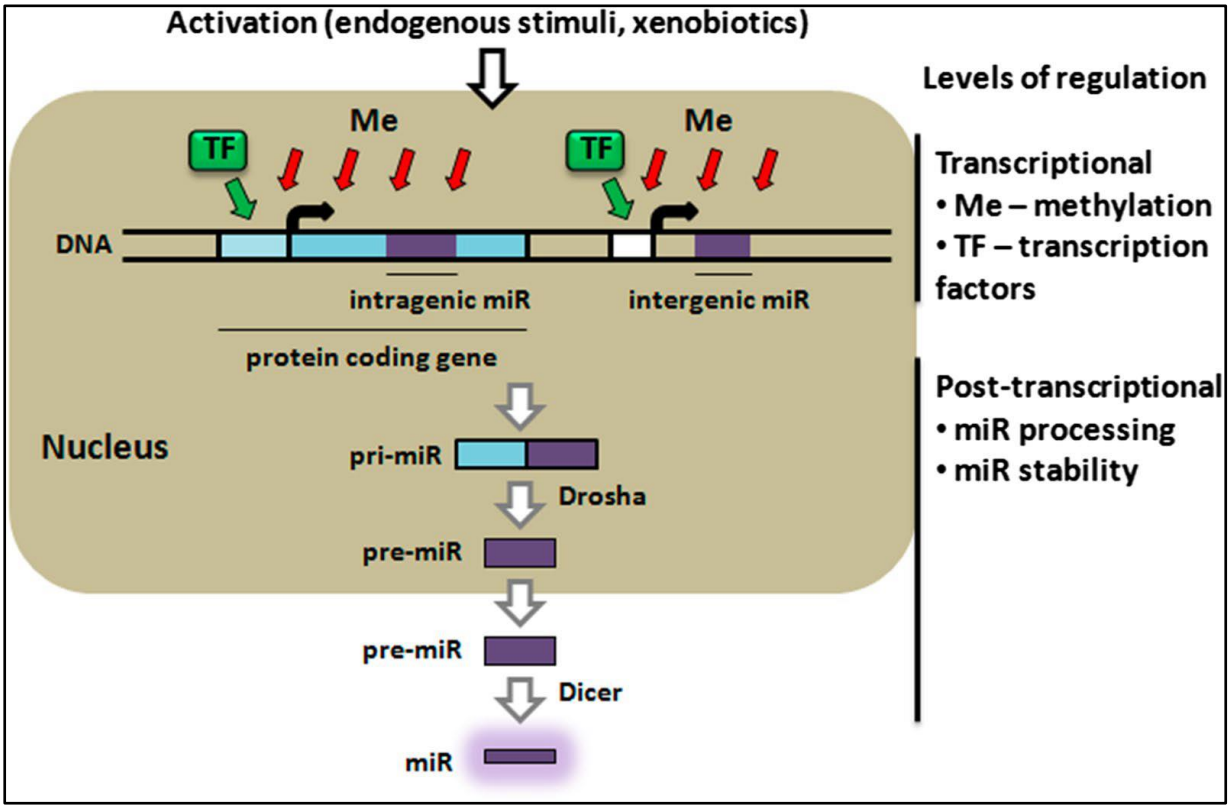


**Figure 1.2: Levels of regulation of miRNA expression** (Adapted from Gulyaeva and Kushlinsky, 2016).

At the post-transcriptional level, miRNAs can be affected by changes in expression or activity of dsRBD-containing proteins that interact with them, namely, the processing enzymes Drosha and Dicer as well as their cofactors. For instance, the c-Myc oncogene is known to

regulate the expression of certain miRNAs directly at the transcriptional level and indirectly through transcriptional regulation of Drosha (Wang et al., 2013, Guo et al., 2013). The Dicer cofactor TRBP has been shown to be phosphorylated by the mitogen-activated kinases/ extracellular signal-regulated kinases (MAPK/ERK) pathway as well as the S6 kinases (Paroo et al., 2009, Warner et al., 2016). Hyper-phosphorylation of TRBP activates and stabilizes it, resulting in increased binding to Dicer and thereby increased processing of growth-promoting miRNAs (Blahna and Hata, 2013, Paroo et al., 2009).

As with protein-coding genes in the genome, miRNA gene expression can also be affected by mutations. Furthermore, miRNA genes have been found to be frequently located at fragile sites and hotspots for chromosomal abnormalities or cancer susceptibility loci that correlate with tumorigenesis (Calin and Croce, 2006, Calin et al., 2002).

## 1.2 miRNAs and cancer

Cancer is a group of diseases which develop from abnormal cell division. These group of diseases can develop from any cell type and are caused by changes in gene expression, function and regulation, usually brought upon by genetic mutations. Normal cell division and differentiation depends on the balance and stringent regulation of several cellular processes involving proto-oncogenes, tumour suppressor genes and DNA repair genes. If the homeostasis of a cell is disrupted, the expression of these different genes can be altered in a manner that favours cancer formation and progression. It has recently become evident that miRNA biogenesis is one of the cellular pathways altered in cancer development.

As mentioned earlier, miRNAs are expressed in a way that is specific to particular tissues or developmental stages and their expression patterns have been found to be altered in several human diseases, including cancers (Velu et al., 2012). By comparing miRNA expression levels between normal and tumour tissue one can determine which miRNAs may be involved in the development and pathogenesis of these cancers (Iorio et al., 2005). These differentially expressed miRNAs can act in a similar manner to protein proto-oncogenes and tumour suppressors in regulating cancer development and progression. miRNAs that can act as oncogenes, termed “oncomiRs”, are upregulated in tumours compared to normal tissues. These oncomiRs negatively regulate tumour suppressor genes, thereby contributing to the cancer phenotype, for instance by halting cell differentiation and evading apoptosis (Ullah et al., 2015). On the other hand, miRNAs that are downregulated in cancers can be called tumour suppressors. These can negatively regulate oncogenes; thus, their suppression is essential in cancer progression. Calin and co-workers determined that miR-15 and miR-16, which are located in the 13q14 region that is often lost in chronic lymphocytic leukaemia (CLL), can act as tumour suppressors by controlling normal CD5+ B cell homeostasis (Calin et al., 2002). Therefore, the loss of these two miRNAs is essential for the formation and pathogenesis of CLL. In a bid to determine a miRNA signature for breast cancer, a genome wide miRNA expression profile was done in normal and breast cancer samples using microarrays (Iorio et al., 2005). The study found that miR-21 and miR-155 were significantly upregulated in breast

cancer tissues and cell lines compared to normal tissue samples, whereas miR-10b, miR-125b and miR-145 were downregulated.

Another example was illustrated in hepatocellular carcinoma (HCC), where miR-122a was identified as a target for Cyclin G1, which is usually upregulated in these cancers to inhibit the function of the tumour suppressor p53 (Gramantieri et al., 2007). Therefore, miR-122a is usually downregulated in HCC and indirectly causes the downregulation of p53 and increased chromosomal instability. These and many other studies show that miRNAs expression profiles can potentially be used for diagnostic, prognostic and therapeutic purposes (Velu et al., 2012). Through further studies, miRNAs can be characterised and classified based on the type of cancer, and can potentially be used as biomarkers in diagnosis and prognosis of these specific cancers.

According to GLOBOCAN estimates, there was an estimated 14.1 million new cancer cases and 8.2 million cancer deaths in 2012 (Torre et al., 2015). Southern African had the 4$^{th}$ highest incidence of new cancer cases at 82 900 (Figure 1.3). The increase in the incidence of cancer in developing countries such as South Africa emphasises the need for more research centred around these African population. The focus of our research group is Non-Hodgkin's lymphomas. Of interest are those that are associated with the Human immunodeficiency virus (HIV), including Diffuse Large B-cell Lymphoma (DLBCL) and Burkitt's lymphoma (BL).

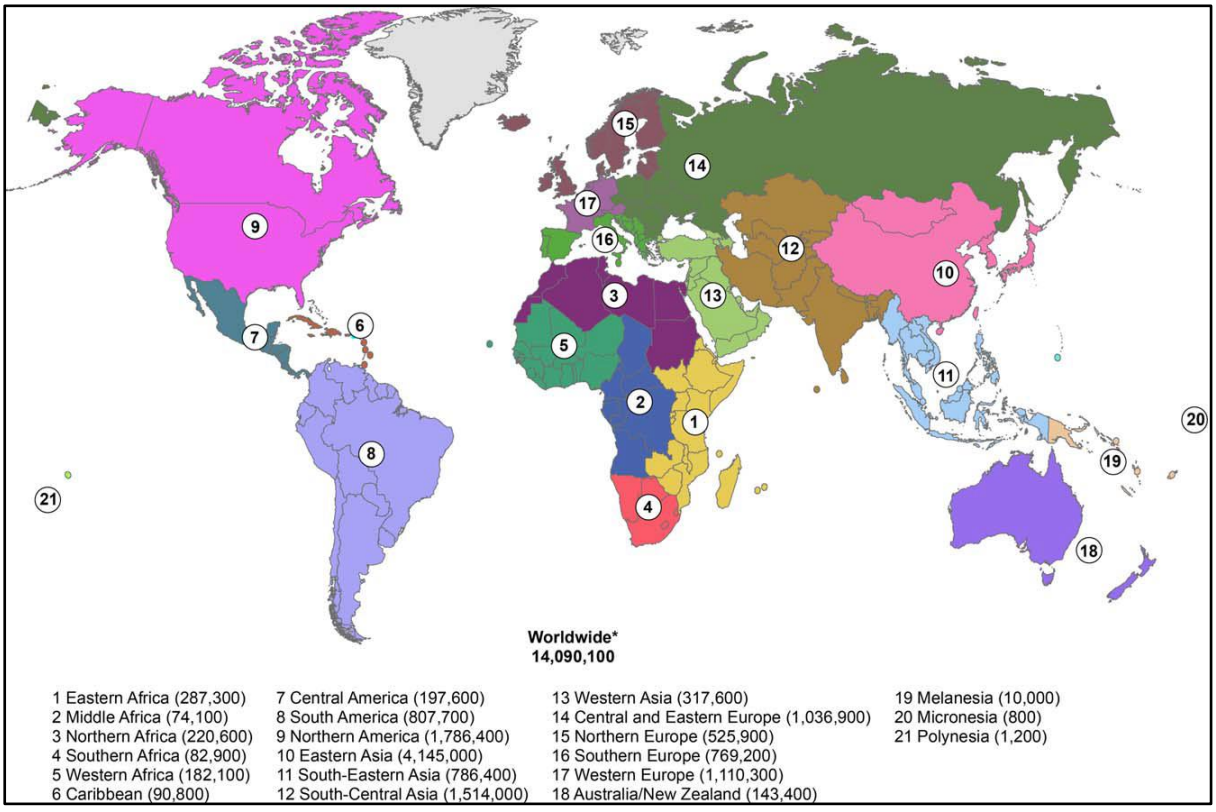


**Figure 1.3: Estimated new cancer cases in the world for 2012** (Adapted from Torre *et al.*, 2015).

### 1.2.1 Non-Hodgkin's lymphomas

Lymphomas are a type of cancer that originates from lymphocytes, which are white blood cells of the immune system. Lymphomas can be of B-cell, T-cell or natural killer (NK) cell origin and have varying degrees of aggressiveness. Since most B-cells are located in the lymph nodes, most of the B-cell lymphomas are associated with enlarged lymph nodes and other lymphatic organs. These cancers can be broadly grouped into two, namely, Hodgkin's lymphomas (HLs) and Non-Hodgkin's Lymphomas (NHLs). It is very important to diagnose the exact subtype of lymphoma and stage, using clinical means, imaging, laboratory investigations and specific tests on the tissue, including immunohistochemical staining, cytogenetics and molecular profiling, as they require different treatment strategies and doses. There are many subtypes of B-cell derived NHLs and because some morphological and clinical features overlap, there is continuous need for the identification of new diagnostic and prognostic biomarkers.

Burkitt's lymphoma (BL) is a high-grade lymphoma and its common molecular feature is the translocation of the oncogene c-MYC (t(8;14) (q24;q32)), leading to its constitutive expression. Table 1 provides a summary of the three variants of this NHL subtype. As with other cancers, the WHO 2008 classification criteria is used to accurately diagnose BL cases, which includes analysis of cell morphology, where the characteristic starry background is observed. The pathologic specimens are also examined for CD20 positivity, expression of germinal centre markers CD10 and B-Cell Lymphoma (BCL) 6, a Ki-67 proliferation index of over 95%, BCL2 negativity and genetic features such as the presence of c-MYC rearrangements and/or translocations. (Sissolak et al., 2017, Campo et al., 2011). Furthermore, staging of the disease depends on lymph and organ involvement using the Ann Arbor staging system (Armitage, 2005). Currently, there is no standard approach to treating BL cases. Depending on the stage of the disease upon diagnosis, treatment strategies include Lymphome Malins de Burkitt (LMB) 86 (cytoreduction with low-dose cyclophosphamide, vincristine, and prednisone followed by induction with vincristine, methotrexate, cyclophosphamide, doxorubicin and prednisone) (Stefan and Rabeen Lutchman, 2014), hyper-CVAD (hyperfractionated cyclophosphamide, vincristine, doxorubicin, dexamethasone, methotrexate, and cytarabine), Stanford regimen (cyclophosphamide, doxorubicin, vincristine, and prednisone and high-dose methotrexate with leucovorin rescue on day 10 with accompanying prophylactic IT chemotherapy) and the CHOP-like (cyclophosphamide, doxorubicin, vincristine, and prednisone) regimen (Sissolak et al., 2017). The outcome of these cases greatly depends on the subtype, age and stage of the disease at diagnosis. The more advanced and aggressive the cancer, the lower the rate of survival.

Of interest in South Africa is the immunodeficiency associated variant. Although very rare in the general population, BL is one of the most common NHL subtypes associated with HIV infection and often presents as more aggressive with poor prognosis. Therefore, more research on the molecular pathogenesis of BL, in the presence of HIV needs to be conducted in order to get a better understanding of cellular processes and mechanisms that drive the disease. This will aid in the development of improved treatment strategies.

**Table 1.1: Variants of Burkitt's lymphoma**

| | Common Characteristics |
|---|---|
| **Endemic** | - Found in Malaria endemic areas<br>- EBV in almost all cases<br>- Mostly in children, the jaw bone is often affected |
| **Sporadic** | - ''non-African'' variant. In areas where malaria is not endemic<br>- Rarely associated with EBV<br>- Most common site is the ileocecal region |
| **Immunodeficiency-associated** | - Associated with HIV infection or post-transplant patients on immunosuppressive drugs |

References: (Pannone et al., 2014), (Magrath, 2012), (Dunleavy et al., 2013)

In recent years, HIV has been directly implicated in cancer. One potential mechanism is that HIV may alter cellular processes in favour of lymphoma development is through miRNA biogenesis. Studying the deregulation of miRNA expression profiles brought upon by the presence of HIV may provide the valuable information needed to better understand these HIV-associated BL cases.

### 1.3 Deregulation of miRNAs by viruses

RNA interference (RNAi) or silencing can be activated as a host defence mechanism against viral (RNA or DNA) infections (Triboulet et al., 2007). However, some miRNAs have been shown to be deregulated as a result of viral infections. For instance, infection with Hepatitis C virus (HCV), a causative agent of liver cancer, results in a downregulation of miR-130a. Moreover, re-introduction of this miRNA into cells resulted in restoration of the innate immune system through the upregulation of the interferon proteins; causing a downregulation of another miRNA, miR-122, and a decrease in HCV replication (Li et al., 2014). This indicates that the virus down-regulates miR-130a as the latter can act as a tumour suppressor and hinder effective viral replication.

Some viral infections are prerequisites for the development of certain cancers. These viruses infect the host cells and remain latent until physiological conditions change to favour their reactivation, which can then lead to cellular transformation (Massimelli et al., 2015). The Epstein Barr Virus (EBV), a member of the herpes virus family has been found in variants of BL that are associated with immunosuppression. Recently, through modified computational prediction methods, it was found that EBV has 7 pre-miRNA sequences (Pfeffer et al., 2005). This is an indication that viruses are evolving to exploit the RNAi mechanism to their own advantage. Furthermore, the EBV-encoded protein EBNA2 was shown to increase levels of

mature cellular miR-21, a known oncomiR, and downregulate miR-146a, which regulates immune-related genes (Rosato et al., 2012). Another example is the Kaposi's Sarcoma associated Herpes Virus (KSHV), which expresses multiple viral miRNAs in its latent cycle (Gottwein et al., 2011). KSHV is predominantly latent in Kaposi Sarcoma (KS), aiding in host immune evasion. One of the ways that viral latency is maintained is through the inhibition of the replication and transcription activator (RTA) protein by the host miR-1258, which is activated by the HIV-1 accessory protein Nef (Yan et al., 2014). In addition, one of the viral miRNAs (KSHV-miR-K12-11) encoded by the virus is an ortholog of the cellular miRNA miR-155. Since both miRNAs share 100% seed sequence homology, KSHV-miR-K12-11 can target miR-155 gene targets such as BACH-1 (Skalsky et al., 2007).

### 1.3.1 MicroRNA deregulation by HIV

The Human Immunodeficiency Virus (HIV) is the cause of one of the most detrimental diseases to affect humankind. Thus far there is no cure; however, the lives of individuals with the virus can be prolonged through the use of Highly Active Antiretroviral Therapy (HAART). According to the United Nations Programme on HIV and AIDS (UNAIDS) Global report (http://www.unaids.org) as well as the World Health Organisation (WHO) global health observation data, approximately 36.7 million people were living with HIV as of June 2017 (http://www.who.int/gho/hiv/en/). As highlighted in Figure 1.4, the sub-Saharan Africa region is the most affected region. In South Africa specifically, the Statistics South Africa mid-year report estimated the prevalence of HIV to be approximately 12.6% of the country's population at 7.06 million (http://www.statssa.gov.za).

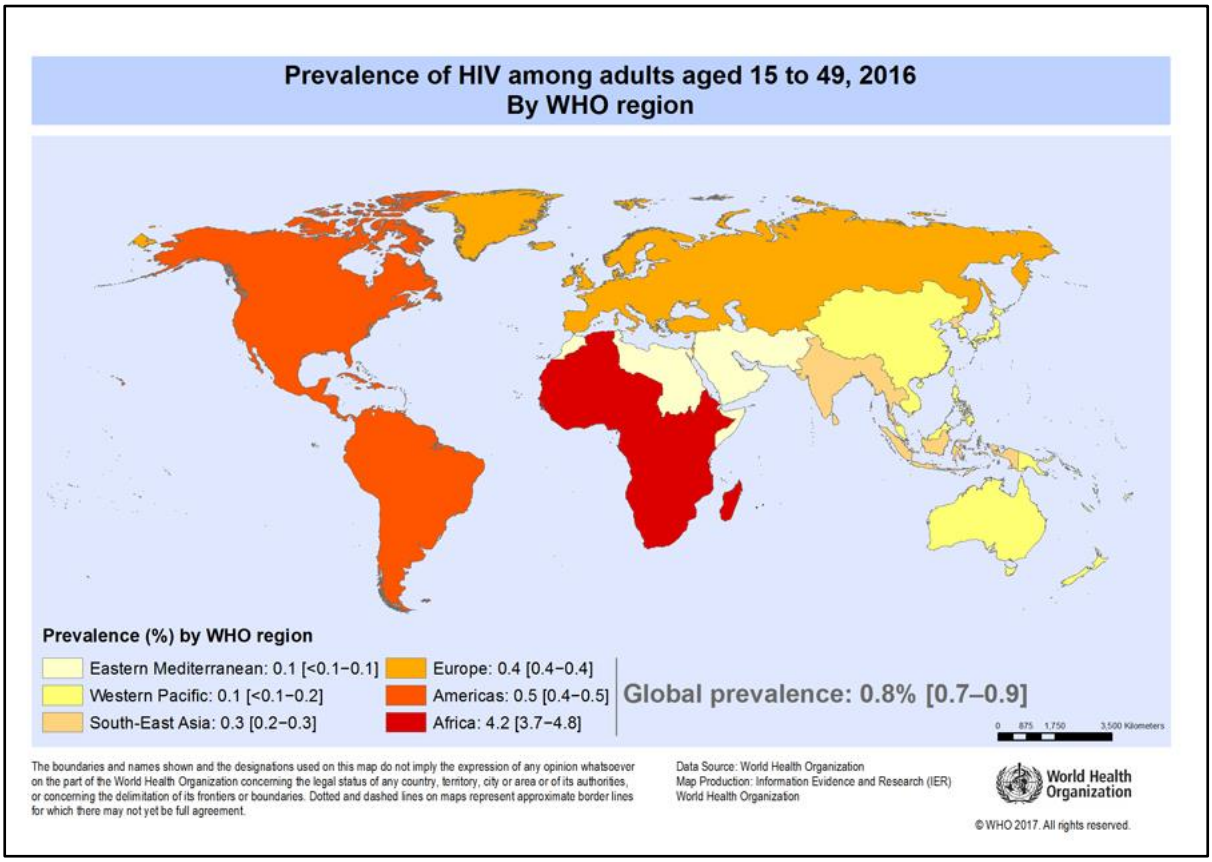

**Figure 1.4: Prevalence of HIV in the world according to UNAIDS 2016 Global Statistics report** (Adapted from http://www.who.int/gho/hiv/en/, http:www.unaids.org).

HIV can affect various cellular processes in the host, including cellular miRNA expression patterns. A study by Houzet et al (2008) showed from patients' peripheral blood mononuclear cell (PBMC) samples that each stage (I-IV, based on viral load and CD4+ count) of the disease is associated with different miRNA expression profiles (Houzet et al., 2008). It was further noted that most of the miRNAs that were downregulated were T-cell specific. This observation indicates that miRNAs may have anti-viral effects and that the virus alters their expression somehow to evade detection by the host. Because the HIV-1 genome is so small, the virus needs some host proteins for efficient replication and survival. The host can manipulate this dependency and target specific proteins through RNAi. An example is the P300/CBP-associated factor (PCAF), which is an endogenous protein that is a co-factor of HIV-1 Tat. The miR-17-92 cluster targets PCAF, making it unavailable to bind the Tat protein and resulting in inefficient HIV-1 transactivation (Triboulet et al., 2007).

## 1.4 HIV and cancer

The high prevalence of HIV within the South African population has resulted in an increased incidence of HIV-associated co-morbidities, including certain types of cancers. These cancers are termed HIV-associated or AIDS-defining cancers. While a compromised immune system is known to lead to the development of cancers, new evidence has emerged pointing to a more direct role of HIV in carcinogenesis. The most common AIDS-defining cancers include KS, cervical cancer and subtypes of NHLs, including BL and DLBCL. Furthermore, a study by Abayomi *et al* (2011) noted that there is a difference between the prevalence of certain lymphoma types in the presence and absence of HIV (Abayomi et al., 2011). For example, BL cases are more prevalent in the HIV positive population, whereas its occurrence is very rare in the HIV negative population (Figure 1.5). As mentioned earlier, the research in our laboratory focusses on understanding the pathology of HIV-associated BL and DLBCL.

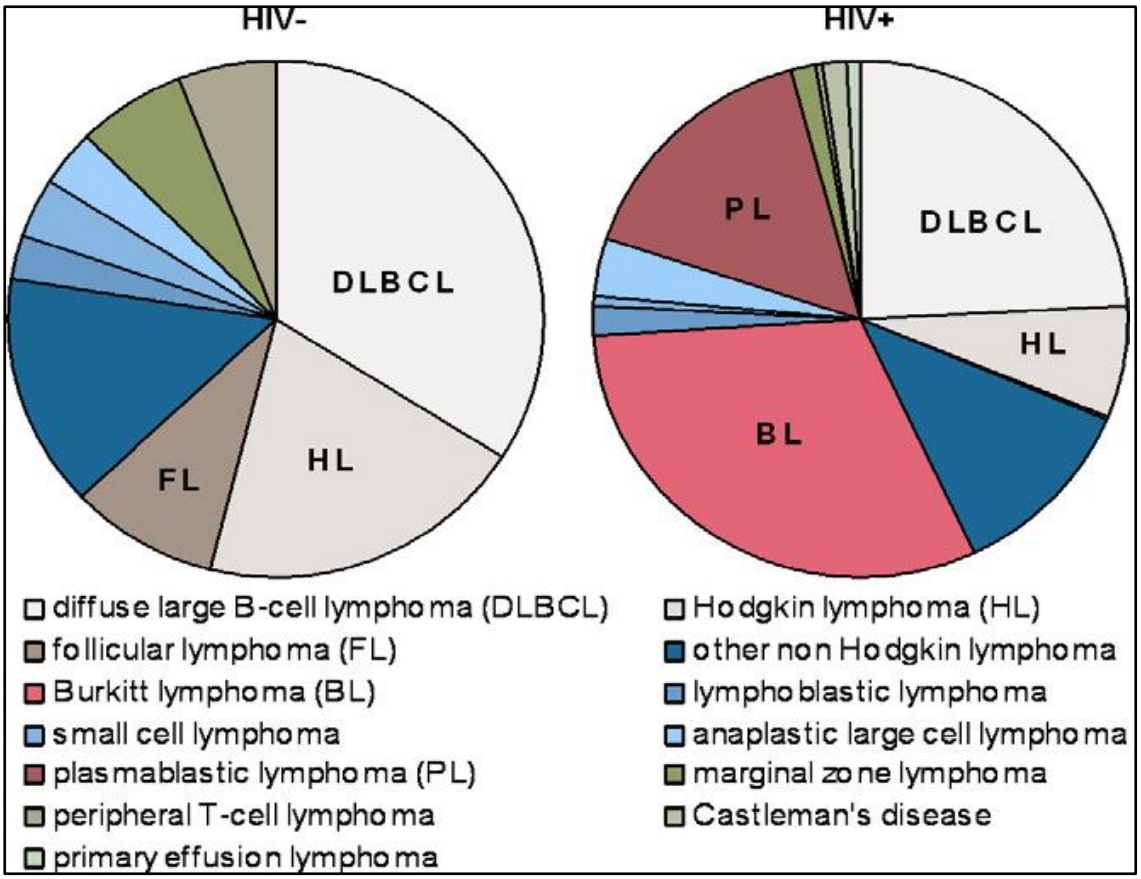


**Figure 1.5: The distribution of types of lymphomas in the HIV-positive and HIV-negative populations** (Adapted from Abayomi *et al*., 2011).

### 1.4.1 miRNAs in HIV-associated Non-Hodgkin's lymphomas

HIV-positive individuals have a 60- to 200-fold higher chance of developing NHLs (Dunleavy and Wilson, 2012). Even with chemotherapy, the patients have lower survival rates compared to their HIV-negative counterparts (Gloghini et al., 2013). The presence of HIV makes treatment of these lymphomas more difficult as, although the virus does not infect B-cells, it directly affects B-cell maturation and activation. In vitro studies confirm that exposure of isolated peripheral B-cells with HIV-1 increases their survival and proliferation rates, changing the ratios of B-cell subpopulations and inducing activation of naïve B-cells (Perise-Barrios et al., 2012). Additionally, the study showed that the full integrity of the HIV-1 virus particle is essential to overexpression of the activation-induced cytidine deaminase (AID) gene, an enzyme which induces class switch recombination (CSR) and somatic hypermutation (SHM), but when overexpressed, lead to cellular transformation.

The presence of HIV causes a greater risk and complication for these lymphomas, which are already challenging to treat with current chemotherapy regimens, as overlapping toxicity and pharmacokinetic factors must be taken into consideration. As a result, some physicians opt to suspend HAART during chemotherapy cycles and resumed after the treatment regimen is complete; this is a better way to reduce HIV drug resistance as opposed to a stop-and-start strategy (Little and Dunleavy, 2013, Dunleavy and Wilson, 2012). Another treatment strategy

is combination anti-retroviral therapy (c-ART), where chemotherapy is administered simultaneously with HAART. The latter option is the general standard of practice in South Africa (Patel et al., 2015). Better understanding of the molecular pathogenesis of these NHLs in the presence of HIV is needed, which could improve the current treatment regimens and prognosis of these cases. For instance, a retrospective study by Lim et al (2005) showed that even in the HAART era, CHOP (cyclophosphamide, hydroxydoxorubicin, vincristine (onovin), prednisone) and M-BACOD (methotrexate, bleomycin, cyclophosphamide, etoposide) treatment regimens, which are normally used for NHL cases in HIV-negative individuals, did not improve the survival of HIV-BL patients (Lim et al., 2005).

The added challenge of HIV to these NHLs further highlights the urgent need for more diagnostic and prognostic molecular markers. In addition, there should be more emphasis on studying these cases in the context of HIV, as there may be distinct pathological features that may be affected by or caused by the virus. There is, as yet, no data available to show whether HIV causes miRNA deregulation in B-cells which may ultimately lead to the development and/or progression of NHLs in HIV-positive individuals. It is this gap in HIV-associated NHL research which is hoped to be addressed in the current project. With the use of microarray and quantitative PCR (qPCR)-based methods, novel miRNAs that are deregulated due to HIV can be identified and characterised in the context of their role in B-cell derived lymphomagenesis. The identified miRNAs can then be further characterised, with regards to their targets and functions in carcinogenesis. Ultimately, this information can be used to identify miRNAs as biomarkers, which is of particular interest as this may lead to earlier diagnosis and better prognosis.

## 1.5 Previous work

A customised miRNA PCR array was performed as part of a fellow student's (Goolam Hoosen, 2017) research project in our laboratory to identify the differentially expressed miRNAs in lymphoma cells when exposed to HIV-1, compared to control cells. Attenuation of the virus was achieved by treatment with the chemical aldrithiol – 2, 2 dithiopyridine (AT-2), which covalently modifies zinc fingers in the nucleocapsid protein, thus eliminating the virus' ability to infect while maintaining the structure and integrity of the envelope glycoproteins (Rossio et al., 1998). Control cells were treated with matched microvesicle (Rossio et al., 1998). Both the attenuated HIV and matched microvesicles control were kindly provided by Dr Jeff Lifson of the National Institutes of Health (NIH, Maryland, USA).

Following extensive statistical analysis, a total of 32 miRNAs were identified to be deregulated by 2-fold or more (Figure 1.6) (Goolam Hoosen, 2017). This project focuses on the validation and characterisation of four miRNAs selected from that list.

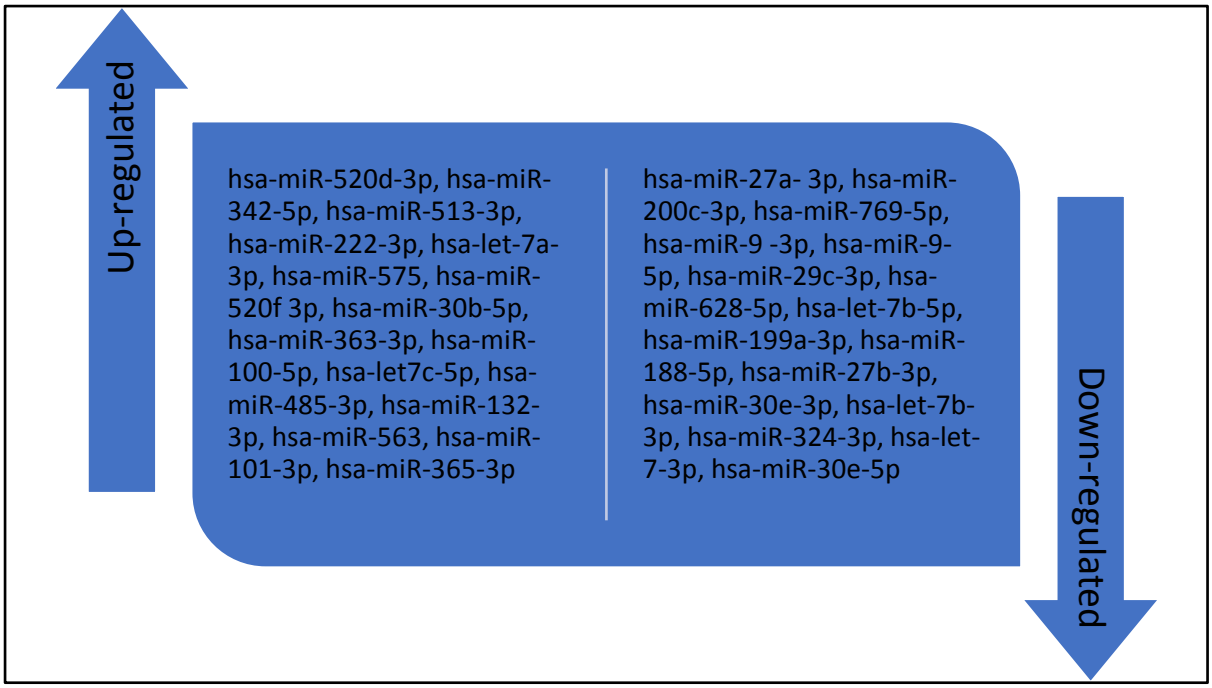


**Figure 1.6: Complete list of selected miRNAs that were deregulated in HIV-treated compared to microvesicle-treated Ramos cells in the PCR array experiment** (Adapted from Goolam Hoosen, 2017)

### 1.5.1 Project aims

The aim of this research project was to validate the differential expression of four miRNAs (hsa-miR-200c-3p, hsa-miR-222-3p, hsa-miR-363-3p and hsa-miR-575), that were found to be significantly deregulated upon exposure of BL cells to HIV-1 in a PCR array. Thereafter, the role of hsa-miR-200c-3p in the pathogenesis of HIV-associated BL was further characterised. Literature and bioinformatic tools were then used to identify potential gene targets of hsa-miR-200c-3p. The functional role of the selected miRNA and gene targets in the context of lymphoma development was thereafter, examined using various cellular biology techniques.

# Chapter 2

# Materials and Methods

## 2.1 Cell culture

### 2.1.1 Cell lines and storage

The cell lines Ramos and BL41 were used in this research project. The Ramos cell line was purchased from the American Type Culture Collection (ATTC®, Virginia, USA). This cell line is an EBV negative human lymphoblastic cell line established from a 3-year-old Caucasian male with Burkitt's lymphoma. The second cell line, BL41 was kindly donated by Professor Dave Sandeep, from Duke University (North Carolina, USA). The BL41 cell line is also EBV negative and was established from an 8-year-old Caucasian male. The cells were cryopreserved in freezing media (consisting of 10% dimethyl sulfoxide (DMSO), Roswell Park Memorial Institute (RPMI) media (Sigma Aldrich, Missouri, USA), fetal bovine serum (FBS)) and stored in liquid nitrogen.

### 2.1.2 Thawing, expansion and freezing

Complete growth medium was prepared using RPMI-1640 media (Sigma Aldrich, Missouri, USA), FBS and penicillin/streptomycin (P/S) solution. Once all the reagents were brought to room temperature, they were cleaned with 70% Ethanol and placed in a biosafety level one fume hood. The growth medium (complete medium) was composed of 10% FBS and 1% P/S in RPMI (Appendix A). 5 ml of the complete medium was added to a T25 flask and warmed in the $CO_2$ incubator (5% $CO_2$, 37$^{\circ}$C) while 4 ml was added to a 15 ml Falcon tube and placed in the Fume Hood. One vial of cryopreserved cells was removed from liquid nitrogen and thawed by hand. Once thawed the contents of the vial were added to the complete medium in the 15 ml Falcon tube and centrifuged at 1000 revolutions per minute (rpm) for 5 minutes in order to pellet the cells. The supernatant was removed and the pelleted cells were resuspended in 1 ml of the warmed media from the T25 flask. The cells were then added to the flask and placed in the incubator. Both cell lines were maintained and expanded by adding fresh growth media every 2-3 days and depopulated as needed. The cells grew best and were maintained at a density of between 2 X $10^5$ and 1 X $10^6$ viable cells/ml. Once the volume in the T25 flask exceeded 20 ml, the cells were transferred to a bigger flask.

For freezing of cells, the freezing medium consisting of RPMI (Sigma Aldrich, Missouri, USA), 10% FBS and 10% DMSO (Appendix A) was prepared and place on ice (in the fume hood). The expanded cells were transferred from T25 or T75 flasks to 15 ml Falcon tubes (about 10 ml in each), and centrifuged at 1000 rpm for 10 minutes. The supernatant was removed and the pelleted cells were resuspended in the freezing medium (the final density of the cell suspension was approximately 1 X $10^6$ cells/ml). The resuspended cells were distributed to cryovials (1ml each), which were placed in a freezing container with isopropanol. The container was placed in a -80$^{\circ}$C freezer overnight. The added isopropanol in the container

allows the cells to cool down at a rate close to 1˚C/minute, ensuring that fewer crystals are formed. The cryovials were transferred into liquid nitrogen for long term storage the following day.

### 2.1.3 Mycoplasma testing

The cells were tested for mycoplasma contamination prior to treatment and at regular intervals during the project. 1 X $10^6$ cells/ml were suspended in P/S free media (containing only RPMI and 10% FBS) and plated in a 35 mm tissue culture dish. The cells were allowed to expand for 2-3 days in the antibiotic-free medium before being prepared for the test. A microscope slide was cleaned thoroughly with 70% ethanol and about 3 µl of the cell suspension was smeared on it with a pipette tip. The slide was allowed to air dry before the fixative (Appendix A) was added to the cells (enough to cover the cells). After two minutes the fixative was washed off with distilled water and stained with Hoechst stain (0.5 µg/ml) (Sigma Aldrich, Missouri, USA) for 5-8 minutes. The stain was washed off with distilled water and excess water was blotted out with tissue paper. A drop of mounting fluid (Appendix A) was added to the cells and a clean cover slip was carefully placed on top. The cells were visualised using a fluorescent microscope at 40X magnification (Zeizz Axiovert 200M, Carl Zeizz Microimaging, Germany).

The Hoechst stain, a blue fluorescent stain, can bind nuclei material biosynthetically. Mycoplasma contamination of cells were indicated by the presence of blue fluorescent dots in the cytoplasm and on the cell membrane. Contaminated cells were disposed of properly as they could not be used in further experiments. A negative mycoplasma result was indicated by the stain being present only in the nuclei of the cells.

### 2.1.4 Cell treatment

Following binding to the primary cellular receptor CD4, HIV uses the CCR5 and CXCR4 chemokine co-receptors to enter its host cell and replicate. Although HIV does not infect B-cells (due to lack of CD4), it has been shown to interact with the cells as they express the CXCR4 chemokine co-receptor as well as other surface receptors that the virus can use (Moir and Fauci, 2009, Nie et al., 2004). The HIV virions used in this project were the HIV-1 (HIV-$1_{NL4-3}$ and HIV-$1_{BAL}$; lot P4244), which was kindly donated by Professor Jeff Lifson (NIH, Maryland, USA) and Dr Wendy Burgers (Division of Medical Virology, Department of pathology, UCT). The virions were treated with Alrithiol-2 (AT-2), a mild oxidising agent which inactivates the virus' ability to infect cells by breaking down sulphide bonds between cysteine residues of the nucleocapsid proteins (Rossio et al., 1998). This reaction does not affect the structural integrity of the glycoproteins on the surface of the virus, ensuring that it is still able to interact with cell surface receptors. As the virions are non-infectious, they are safe for experimental use in the laboratory. As a precautionary measure, all cell treatments were performed in a biosafety level two fume hood. Microvesicles (MV), which are non-virion material co-purified with the attenuated virion, were used as matched controls for the cell treatment experiments (SUPT1-CCR5 (MV-CCR5; lot P4287).

Prior to treatment, cells were thoroughly resuspended and 10 µl was used for cell counting using a haemocytometer. Viable cells were counted in four 1 $mm^2$ squares and the obtained number was converted to cell number per ml. 8 X $10^6$ cells/ml were plated in 35mm wells approximately 16 hours before treatment in low serum media (consisting of 0.5% FBS, 1% P/S and RPMI) (Appendix A). A predetermined number of wells were treated with 500ng/ml of AT-2 inactivated HIV-1 virions while an equal number of wells were treated with the equivalent amount of microvesicles. The plate(s) were covered with foil and incubated at 37˚C (in the $CO_2$ incubator) for 3 hours.

## 2.2 RNA isolation and quantification

### 2.2.1 RNA isolation for miRNA Validation studies

In preparation for RNA extraction, all plasticware to be used was treated with water containing 0.1% diethyl pyrocarbonate (DEPC) (Appendix A), an effective nuclease inhibitor, and autoclaved thereafter. The working bench was wiped thoroughly with decon (Thermo Fisher Scientific™, Massachusetts, USA) or diluted bleach, followed by 70% ethanol. The water used was also treated with DEPC (unless the water required was RNAse-free, provided in the kit used). Furthermore, sterile techniques were used and gloves were worn at all times.

After treatment, the cells were removed from the wells and placed in 15ml Falcon tubes. The wells were rinsed with cold 1X phosphate-buffered saline (PBS) (Appendix A) to remove remaining cells. The cells were centrifuged at 1000 rpm (Measuring and Scientific Equipment (MSE), Essex, UK) and the supernatant was discarded. The cell pellets were washed twice with cold 1X PBS. The cells were transferred to 1.5 ml centrifuge tubes for the final wash step. The *mir*Vana™ miRNA Isolation kit (Thermo Fisher Scientific™, Massachusetts, USA) was used for small RNA isolation for initial experiments. The manufacturer's instructions were followed. The kit combines both the organic and solid-phase extraction methods. In summary, the pelleted cells were lysed by adding the lysis/binding solution after the PBS wash supernatant was discarded. The cells were vortexed to obtain a homogenous lysate before the miRNA homogenate additive was added. The mixtures were incubated on ice for 10 minutes. Thereafter, Acid-Phenol:Chloroform (125:24:1) was added to the cell lysates and mixed by vortexing for 30-60 seconds. The cell lysates were then centrifuged at maximum speed for 5 minutes to separate the aqueous and organic phases. The upper aqueous was carefully removed and transferred to fresh 1.5ml centrifuge tubes. 100% ethanol (at room temperature) was added and the contents of the centrifuge tubes were mixed thoroughly and then transferred onto a filter cartridge prior to centrifugation at 10 000 rpm for 15 seconds to allow the mixture to pass through the filter. The filtrate was discarded and the filter was washed once with the first RNA wash solution and twice with the second one. The RNA was eluted with nuclease-free/DEPC-treated water in DEPC-treated centrifuge tubes, quantified, aliquoted and stored at -80˚C.

### 2.2.2 Total RNA isolation for miRNA and target expression studies

The Roche High Pure RNA Isolation Kit (Roche Applied Sciences, Penzberg, Germany) was used for total RNA isolation of treated cells as per the protocol provided. The cells were treated as in Section 2.14. Thereafter, the treated cells were transferred to 15 ml Falcon tubes, pelleted and washed twice with cold 1X PBS. The cells were then resuspended in 200 µl of the cold 1X PBS in 1.5 ml centrifuge tubes. 400 µl of the Lysis/Binding buffer was added to the resuspended cells and vortexed for 15 seconds. The cell lysates were pipetted onto the High Pure Filter tubes, which were centrifuged at 8000xg for 15 seconds. The flow through was discarded and DNase I solution was added to the filter tubes. The samples were incubated for 15 minutes at room temperature. Thereafter, the filter was washed once with the wash buffer I and twice with the wash buffer II. The first 2 washes were done with 500 µl of each solution, centrifuged at 8000xg for 15 seconds while the last wash was done with 200 µl of the buffer, centrifuged at maximum speed for 2 minutes. The RNA was eluted in the elution buffer provided (nuclease-free water), quantified, aliquoted and stored at -80˚C.

### 2.2.3 RNA quantification

Quantification of the isolated RNA was performed using the NanoDrop™ 1000 spectrophotometer (Thermo Fisher Scientific™, Massachusetts, USA). This machine uses ultra-violet (UV) spectrophotometry to determine the concentration of nucleotides as well as the level of contamination using the 260/280 and 260/230 ratios. Generally, nucleotides are detected at 260 nm while protein and organic (phenol) contamination can be detected at 280nm and 260nm, respectively. Briefly, 1 µl of each RNA sample was used for analysis on the NanoDrop™. Prior to measuring the samples, 1 µl of nuclease-free, DEPC-treated water or elution buffer was used to blank the machine.

### 2.2.4 Gel electrophoresis of RNA

The integrity of the isolated RNA was checked using gel electrophoresis. The gel tray, comb and chamber were soaked in DEPC-treated water with sodium hypochlorite (~10%) for at least 3 hours to prevent RNA degradation. A 1% or 1.5% agarose gel was prepared with 1X TBE buffer containing 0.5mg/ml ethidium bromide (EtBr) (Sigma Aldrich, Missouri, USA). The RNA samples were prepared for loading onto the gel by adding 5 µl of 2X RNA loading buffer (Appendix A) to 5 µl of RNA in clean (DEPC-treated) 1.5 ml centrifuge tubes. The RNA was denatured by incubating the samples at 55˚C for 5 minutes. Thereafter, the samples were centrifuged briefly and loaded onto the wells. The gel was electrophoresed at 100 volts for 35-45 minutes and visualised over a UV trans-illuminator (Uvitec, UK).

## 2.3 TaqMan® miRNA assays

To determine the expression levels of selected miRNAs under experimental conditions, single-tube TaqMan® miRNA assays (Applied Biosystems™, California, USA) were used. Assays for hsa-miR-200c-3p, hsa-miR-575, hsa-miR-222-3p, hsa-miR-363-3p as well as endogenous control assays for RNU48 and RNU6B were purchased (Table 2.1) The use of these single-tube assays is more advantageous as they are more specific and sensitive to the mature sequence of the selected miRNAs. Each assay contains two tubes, one containing specific stem-loop

primers for reverse transcription (RT) and the other containing forward and reverse primers for qPCR as well as the minor groove binder (MGB) probe, which is composed of the fluorescent reporter at the 5' end and the nonfluorescent quencher (NFQ) at the 3' end (Figure 2.1).

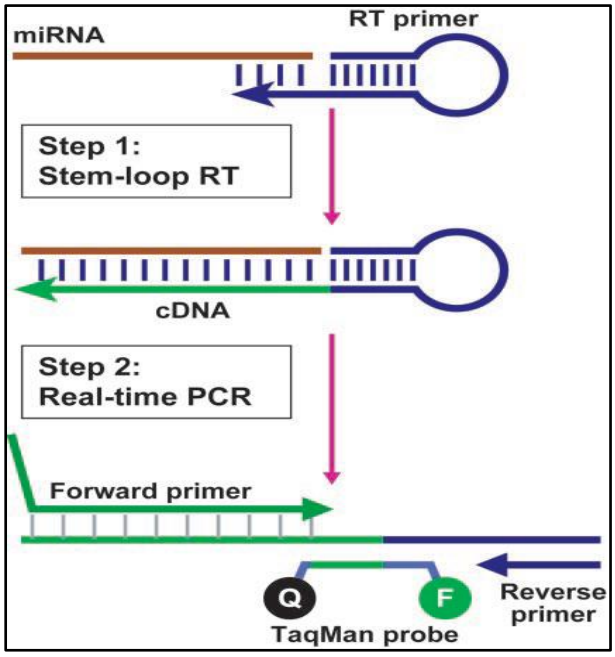


**Figure 2.1: Overview of the two-step process involved in TaqMan® miRNA assays.** The first step is reverse transcription, where a specific stem-loop primer binds to the 3' end if the miRNA, allowing the reverse transcriptase enzyme to bind and synthesize cDNA. The RT product is used in the second stem, where specific forward and reverse primers are used to amplify the product. The TaqMan® MGB probe allows for quantification while the RT product is being amplified (Chen et al., 2005).

### 2.3.1 Reverse transcription

Reverse transcription (RT) is the reaction used for synthesizing complementary DNA (cDNA) from RNA. In these single-tube assays, the stem-loop primers for the RT step are designed to be specific for the mature sequence of the selected miRNA. After RNA isolation, the RNA was diluted to 10 ng/µl as recommended by the kit. The kit components were allowed to thaw on ice and a master mix (Table 2.1) was prepared in a 1.5 ml centrifuge tube according to the TaqMan® miRNA Reverse Transcription kit (Applied Biosystems™, California, USA). The master mix was mixed and 7 µl was aliquoted to PCR tubes. Thereafter, 1 µl of diluted RNA (10ng/µl) was added to each reaction tube. The RT primers (3 µl) were added to each reaction tube respectively for each specific assay. Each reaction was made up to 15 µl with nuclease free water.

**Table 2.1: Components for the reverse transcription reaction using TaqMan® miRNA-specific RT stem-loop primers**

| Reagent | Volume (µl) for 1 reaction |
|---|---|
| **10 RT buffer** | 1.50 |
| **RNase Inhibitor (20 U/µl)** | 0.19 |
| **100Mm dNTPs** | 0.15 |
| **Multiscribe Reverse Transcriptase (50U/µl)** | 1.00 |
| **Nuclease-free water** | 4.16 |
| **Total Volume** | 7µl |

The cycling conditions were set as indicated in the protocol (Table 2.2) and the Labnet MultiGene™ Gradient PCR Thermal Cycler (Labnet International, California, USA) was used for the reaction. The reaction tubes were stored at -20˚C to be used in qPCR.

**Table 2.2: Cycling conditions for reverse transcription using TaqMan® miRNA-specific RT stem-loop primers**

| Step type | Time (minutes) | Temperature (˚C) |
|---|---|---|
| **Hold** | 30 | 16 |
| **Hold** | 30 | 42 |
| **Hold** | 5 | 85 |
| **Hold** | ∞ | 4 |

### 2.3.2 Quantitative real-time PCR

Quantitative real-time PCR (qPCR) is the laboratory technique used to quantify targeted nucleotide molecules as the amplification reaction occurs. The purchased tube miRNA assays include a TaqMan® MGB probe, which binds specifically to the cDNA generated from the RT step. As the amplification occurs, the probe will be cleaved by the DNA polymerase enzyme, which has 5'- exonuclease activity. The cleavage separates the quencher from the reporter, allowing fluorescence to be detected. The amount of fluorescence detected directly correlates with the amount of target DNA present in the reaction tube.

For the miRNA expression validation experiments, master mixes were prepared separately for each miRNA and controls in 1.5ml centrifuge tubes using the TaqMan® Universal PCR Master Mix (No AmpErase®, UNG 2X). The protocol was adjusted as follows: the total reaction volume was halved to 10µl (recommended by technician operating the platform) and each component was scaled down as needed (Table 2.3). The master mix was aliquoted to appropriate wells in a 384-well plate and the cDNA template was added individually to each well. The plate was sealed and centrifuged for 10 minutes (Eppendorf 5804, Hamburg, Germany). Thereafter, the plate was loaded into the Applied Biosystems 7900HT Fast Real-time PCR system machine (Applied Biosystems, California, USA), located at the Centre for

Proteomic & Genomic Research (CPGR, Observatory, Cape Town, South Africa). The cycling conditions were set (Table 2.4) as instructed in the protocol and the reaction was started.

**Table 2.3: Components for TaqMan® miRNA qPCR reaction using the Applied Biosystems 7900HT Fast Real-time PCR machine platform**

| Reagent | Volume (µl) for 1 reaction |
|---|---|
| **TaqMan Universal Master Mix X2** | 5.00 |
| **TaqMan 20X MicroRNA assay** | 0.50 |
| **Nuclease-free water** | 3.90 |
| **RT product (cDNA)** | 0.60 |
| **Total Volume** | 10 µl |

**Table 2.4: Cycling conditions for TaqMan® miRNA assay reactions**

| Step type | Time | Temperature (˚C) | Cycle |
|---|---|---|---|
| **Hold** | 10 min | 95 | 1 |
| **Denature** | 15 sec | 95 | 40 |
| **Anneal** | 45 sec | 60 | |

After one miRNA was selected for further investigation, the RotorGene Q platform (Qiagen, Hilden, Germany) was used for the TaqMan® single tube assay experiments that followed. The master mixes were prepared as in Table 2.5. 18.67 µl of the master mix was added to 0.1 ml reaction tubes provided by the manufacturer (Qiagen, Hilden, Germany). Thereafter, 1.33 µl of cDNAs template was added to corresponding reaction tubes. The tubes were mixed gently and loaded onto the RotorGene machine. The cycling conditions were set as in Table 2.4 and the run was started.

**Table 2.5: Components for TaqMan® miRNA qPCR reaction using the Roche Rotor-Gene Q platform**

| Reagent | Volume (µl) for 1 reaction |
|---|---|
| **TaqMan Universal Master Mix X2** | 10.00 |
| **TaqMan 20X MicroRNA assay** | 1.00 |
| **Nuclease-free water** | 7.67 |
| **RT product (cDNA)** | 1.33 |
| **Total Volume** | 20 µl |

### 2.3.2 Data analysis

The file containing the quantification data was obtained from the Applied Biosystems platform. The plate set up was analysed using SDS 2.3 (Applied Biosystems, California, USA) and thereafter, exported to RQ manager (Applied Biosystems, California, USA). Each amplification plot was analysed using RQ manager (Applied Biosystems, California, USA) software and the baseline and threshold Ct values were set. The data was then exported as a text file and opened using DataAssist™ version3.01 (Applied Biosystems, California, USA). The DataAssist™ software was used to view the Ct values for each replicate and to determine the

best endogenous control between RNU48 and RNU6B. After all the Ct values were visualised the data was exported as a Microsoft excel file.

Similarly, the data file from the Rotor-Gene Q platform was obtained after each run. The amplification plots were visualised using the Rotor-Gene Q series Software (Qiagen, Hilden, Germany). The software was used to visualise the amplification curves. The baseline and threshold Ct values were set and the data was exported to a Microsoft excel file.

Once the Ct values were in a Microsoft file, outliers were identified (difference of >1 amongst technical replicates) and excluded. The Ct data was analysed using the comparative method (ΔΔCt) of relative quantification to determine the fold expression of each miRNA. The miRNA of interest was normalised to the endogenous control and the fold change in expression was determined in the HIV relative to the microvesicle samples. The equation $2^{-(\Delta\Delta Ct)}$ was used to calculate fold induction. The data was represented as the average of fold changes, with error bars representing standard deviation, normalised to the microvesicle samples (set as 1). The Student t-test (Microsoft excel) was performed to determine statistical significance between the HIV-treated and the microvesicle control samples, which was set at $p<0.05$.

## 2.4 Bioinformatic analysis and gene target selection

After the qPCR data was analysed, one miRNA was selected for further investigation, namely, hsa-miR-200c-3p. The bioinformatics algorithms miRBase (http://www.mirbase.org), miRNADB (http://www.mirdb.org), microRNA.org (http://www.microrna.org), TargetScan (http://www.targetscan.org), miRTarBase (http://mirtarbase.mbc.nctu.edu.tw/index.php) and TarBase V8 (http://carolina.imis.athena-innovation.gr/diana_tools) were used to determine potential gene targets for the selected miRNA. These prediction tools search for complementarity between the seed region (6-8 nucleotides at the 5' end) of the miRNA and the 3' untranslated regions (3'UTR) of known genes. By convention, the gene target that was similar across two or three of the algorithms was selected (Kuhn et al., 2008a). To reduce the list obtained from each algorithm even further, a literature search (Pubmed, Google Scholar) was done to determine which targets have been validated for hsa-miR-200c-3p in other cancers.

## 2.5 Reverse transcription and qPCR of gene target

### 2.5.1 Primer design

The complete sequence for ZEB1 (NG_017048.1) and ZEB2 (NG_016431.1) were obtained from the NCBI database. The sequences were imported into the Primer3Plus program (http://www.bioinformatics.nl/cgi-bin/primer3plus/primer3plus.cgi). This program was used to design the forward and reverse primers according to specific parameters, such as primer length (18-25 base pairs (bp)), melting temperature (48-55°C) and GC content (40-60%). Oligoanalyzer (Integrated DNA Technologies, Iowa, USA) was used to analyse the possibility of the primers forming stable secondary structures. It was ensured that the ΔG for potential

secondary structures for the primer pair was kept lower than 3 kcal/mole. Thereafter, the selected primers were analysed for complementarity to the specific genes using the Basic Local Alignment Search Tool (BLAST) (http://blast.ncbi.nlm.nih.gov). The primer pair was selected if they showed 100% complementarity to the specific gene and less than 75% complementarity to non-related genes. The primer information is shown in Table 2.6.

**Table 2.6: Selected primer pairs for gene expression analysis**

| Primer | Sequence | Melting temperature (Tm) (˚C) | Amplicon size (bp) |
|---|---|---|---|
| **ZEB1_F** | 5'-GCCTGAAATCCTCTCTGAATG-3' | 59.8 | 95 |
| **ZEB1_R** | 5'-CACCTCTTGTCAAAC-3' | 58.6 | |
| **ZEB2_F** | 5'-GAAGAGACTGGAGATCACTC-3' | 51.0 | 93 |
| **ZEB2_R** | 5'-GCCATCTTCCATATTGTC-3' | 50.9 | |
| **GAPDH_F** | 5'-GAAGGCTGGGGCTCATTT-3' | 55.4 | 133 |
| **GAPDH_R** | 5'-CAGGAGGCATTGCTGATGAT-3' | 55.2 | |
| **RPL27_F** | 5'-ATCGCCAAGAGATCAAAGATAA-3' | 51.7 | 123 |
| **RPL27_R** | 5'-TCTGAAGACATCCTTATTGACG-3' | 52.1 | |

F – forward primer; GAPDH – Glyceraldehyde-3-Phosphate Dehydrogenase; R – reverse primer; RPL27 – 60S ribosomal protein 27; ZEB 1/2- Zinc Finger E-box Binding protein 1/2

### 2.5.2 Reverse transcription using OligodT and random hexamer Primers

The iScript™ cDNA Synthesis Kit (Bio Rad, California, USA) was used for reverse transcription according to the protocol provided. For each sample, the reaction was set up as indicated in Table 2.7 in 0.5 ml nuclease-free PCR tubes. Based on the concentrations obtained from the NanoDrop™ readings, 1 µg of RNA template was added to the reaction tubes for each RNA sample. The samples were made up to 20 µl with nuclease free water. The tubes were mixed and centrifuged briefly, after which they were loaded onto the Labnet MultiGene™ Gradient PCR Thermal Cycler (Labnet International, California, USA) and the cycling conditions used were as shown in Table 2.8. The cDNA was stored at -20˚C until use for qPCR.

**Table 2.7: Reagents for cDNA synthesis using the iScript™ cDNA synthesis kit**

| Reagent | Volume (µl) for 1 reaction |
|---|---|
| **5X iScript™ reaction mix** | 4.00 |
| **IScript Reverse Transcriptase** | 1.00 |
| **Nuclease-free water** | Variable |
| **RNA template (1 µg)** | Variable |
| **Total Volume** | 20 µl |

**Table 2.8: Cycling conditions for Reverse Transcription using the iScript™ kit**

| Step type | Time (minutes) | Temperature (˚C) |
|---|---|---|
| **Hold** | 5 | 25 |
| **Hold** | 30 | 42 |
| **Hold** | 5 | 85 |
| **Hold** | ∞ | 4 |

### 2.5.3 Endpoint PCR of gene targets

Endpoint PCR was performed to confirm the specificity of the selected primer pairs. The selected primers were synthesised (Department of Molecular and Cell Biology, UCT, South Africa) and the stock diluted to 10 µM. The reaction was prepared using the MyTaq™ DNA polymerase (Bioline, Tennessee, USA). The total reaction volume was halved to 25 µl and all the reagent volumes were adjusted as needed (Table 2.9). The master mix consisted of the buffer, DNA polymerase and nuclease-free water in a 1.5 ml centrifuge tube. The master mix was mixed thoroughly and centrifuged briefly. Thereafter, 23 µl was aliquoted to PCR tubes, were the primers and cDNA template were added individually. The reaction was mixed and centrifuged before loading onto the Labnet MultiGene™ Gradient PCR Thermal Cycler (Labnet International, California, USA). The parameters were set as shown in Table 2.10 and the reaction was run for

30 cycles.

**Table 2.9: Components for PCR using MyTaq™ DNA polymerase**

| Reagent | Volume (µl) for 1 reaction |
|---|---|
| **5X MyTaq™ Buffer** | 5.00 |
| **MyTaq™ DNA polymerase (50 U/µl)** | 0.25 |
| **Forward Primer (10µM** | 1.00 |
| **Reverse Primer (10µM)** | 1.00 |
| **cDNA template** | 1.00 |
| **Nuclease-free water** | 16.75 |
| **Total Volume** | 25 µl |

**Table 2.10: Cycling parameters for PCR using the My Taq™ DNA polymerase**

| Step type | Time | Temperature (˚C) | Cycle |
|---|---|---|---|
| **Initial denaturation** | 1 min | 95 | 1 |
| **Denaturation** | 15 sec | 95 | 30 |
| **Annealing** | 15 sec | 48 | |
| **Extension** | 15 sec | 72 | |
| **Hold** | ∞ | 4 | |

### 2.5.4 Gel electrophoresis of PCR products

Agarose gel electrophoresis was used to visualise the PCR products. A 1.5% gel was prepared with 1X TBE buffer (Appendix A) and EtBr (0.5 mg/ml). 2 µl of 5X DNA loading dye (Appendix A) was added to 15 µl of each PCR product sample. The samples were mixed and centrifuged briefly before loading onto the gel and 1Kb ladder (Thermo Fisher Scientific, Massachusetts, USA was added to the first lane (Appendix B). The gel was electrophoresed at 100 volts for 35 minutes. The gel was visualised under a UV trans-illuminator (Uvitec, UK)

### 2.5.5 qPCR of gene targets

Once the specificity of the designed primers and the optimum annealing temperature were confirmed, qPCR was performed using the KAPA SYBR® FAST qPCR Kit (Kapa Biosystems, Cape Town, SA). Glyceraldehyde-3-Phosphate Dehydrogenase (GAPDH) and 60S ribosomal protein 27 (RPL27) were included as endogenous controls to be used for normalisation. Master mixes, accounting for 3 technical replicates as well as a no template control, for each gene were prepared in 1.5 ml centrifuge tubes containing all the components except the cDNA (Table 2.11). The master mix was mixed thoroughly and centrifuged briefly. Thereafter, 19 µl was aliquoted to corresponding PCR tubes (Qiagen, Hilden, USA). The cDNAs template (1 µl) was added last to each PCR tube, which were mixed thoroughly before loading onto the Rotor-Gene Q (Qiagen, Hilden, Germany) machine. The cycling parameters were set as indicated in Table 2.12 and the reaction was run for 40 cycles. The data was exported and analysed using the comparative (ΔΔCt) method and student t-test as described in Section 2.3.2

**Table 2.11: Components for qPCR using the KAPA SYBR®FAST qPCR kit**

| Reagent | Volume (µl) for 1 reaction |
|---|---|
| **2X KAPA SYBR® FAST qPCRs Master Mix Universal** | 10.00 |
| **Forward Primer (10 µM** | 0.40 |
| **Reverse Primer (10 µM)** | 0.40 |
| **cDNA template** | 1.00 |
| **Nuclease-free water** | 8.2 |
| **Total Volume** | 20 µl |

**Table 2.12: Cycling conditions for qPCR using the KAPA SYBR® FAST qPCR kit**

| Step type | Time | Temperature (˚C) | Cycle |
|---|---|---|---|
| **Pre-incubation** | 3 min | 95 | 1 |
| **Denaturation** | 3 sec | 95 | 30 |
| **Annealing** | 20 sec | 48 | |
| **Extension (data acquisition)** | 20 sec | 72 | |
| **Cooling** | 10 sec | 40 | 1 |

## 2.6 Functional analysis of gene targets

### 2.6.1 Protein extraction

Protein was isolated using Radio-Immunoprecipitation Assay (RIPA) buffer (Appendix A) and 7X complete™, mini EDTA-free Protease inhibitor (Appendix A) (Roche Applied Science, Penzberg, Germany). The RIPA buffer contains detergents which lyse the cells while the Protease inhibitor prevents degradation of the isolated proteins. The RIPA buffer and Protease inhibitor solution was fresh placed on ice in the fume hood in preparation for the protein isolation. After cell treatment, the cells were transferred to 15 ml Falcon tubes and the wells were rinsed with cold 1X PBS. The cells were centrifuged at 2000 rpm (MSE, California, USA) for 5 minutes. The supernatant was discarded and the pelleted cells were washed three times by resuspending in cold 1X PBS (Appendix A) and centrifugation. Depending on the cell pellet, 200-500 µl of the RIPA/Protease inhibitor solution was used to resuspend the cells and the tubes were stored at -80˚C overnight for optimum lysis. The cells were then thawed on ice and centrifuged at 4˚C at 12 000 rpm (Beckman, London, UK) for 20 minutes, in order to pellet DNA, and the soluble proteins were transferred to a new tube, aliquoted and stored at -80˚C.

### 2.6.2 Protein quantification

The bicinchonic acid (BCA) reagent was used to determine the concentration of protein in the isolated samples. This was performed using the Pierce™ BCA assay kit (Thermo Fisher Scientific™, Massachusetts, USA). This sensitive colorimetric assay relies on two reactions. The first reaction, known as the biuret reaction, is the reduction of $Cu^{2+}$ to $Cu^{1+}$ by the protein peptide bonds in an alkaline environment. The second reaction occurs when BCA molecules chelates with the reduced $Cu^{1+}$ cations. These BCA/$Cu^{1+}$ complexes are soluble in water and the colour produced from this reaction is proportional to increasing protein concentrations. Briefly, the protein samples were thawed on ice and diluted in ratios of 1:2 and 1:5 using the RIPA buffer (total volume of 25 µl). The BCA working solution was prepared according to the protocol by mixing reagents A and B in a ratio of 50:1. In parallel, a standard curve was generated using the bovine serum albumin (BSA; 2 mg/ml) protein (provided in the kit) diluted in RIPA buffer at known concentrations (2000 µg/ml, 1000 µg/ml, 500 µg/ml, 125 µg/ml and 0 µg/ml (RIPA buffer blank)). In a 96-well plate, 10 µl of each protein sample as well as the standards were added to wells. 200 µl of the working reagent was added to the protein and standard samples in the wells, which was then covered with parafilm and the plate was incubated at 37˚C for 30 minutes and the intensity of the colour was measured at a wavelength of 560 nm using the Glo-Max®-Multi+ multiplate reader (Promega, Wisconsin, USA). The measurements were corrected by subtracting the average blank readings from the average readings for the other samples and standards. A curve was plotted using the corrected absorbance readings of the BSA samples. The equation from the standard curve generated was used to extrapolate the concentration of the diluted protein samples.

### 2.6.3 Western blot analysis

#### 2.6.3.1 SDS PAGE

Sodium dodecyl sulphate polyacrylamide gel electrophoresis (SDS-PAGE) was used to separate the proteins. SDS, an anionic detergent was used to denature and linearize the proteins. The proteins bind the amount of SDS in proportion to its molecular mass. The now negatively charged proteins become strongly attracted to the positively charged anode in an electric field. Since the mass-to-charge ratio in SDS-denatured proteins in nearly the same, the proteins will be separated solely based of their relative molecular mass. An 8% resolving gel (7.5 ml) and a 5% stacking gel (3 ml) was prepared according to the manufacturers protocol (Appendix A) using the Bio-Rad mini-PROTEAN 3 casting apparatus (Bio-Rad, California, USA). The samples were prepared as shown in Table 2.13 and incubated at 100˚C for 5 minutes and centrifuged briefly before loading onto the polyacrylamide gel.

**Table 2.13: Sample preparation for protein samples loaded onto the SDS-PAGE gel**

| Reagent | Volume (µl) for 1 reaction |
|---|---|
| **Protein sample (20 µg)** | Variable |
| **100 mM DTT** | 1.00 |
| **5X protein Loading dye** | 6.00 |
| **RIPA Buffer** | Up to 30 |
| **Total Volume** | 30 µl |

Once set, the polyacrylamide gel was set up in the electrode assembly cassette and placed inside the electrophoresis chamber (Bio-Rad, California, USA). 1X running buffer (Appendix A) was added to the chamber, ensuring that the wells were submerged. The comb was then removed carefully. The samples were carefully loaded into the wells, with 1 µl of the BenchMark™ Pre-stained 1 Kb Protein Ladder (Appendix B) being loaded into at least one well. The 5X protein loading dye (Appendix B) (6µl) was added to the empty wells to ensure that the proteins were separated evenly. The chamber was then closed and connected to the Bio-Rad power pack and electrophoresed for 2-2.5 hours at 100 volts (until the dye front reached the bottom of the gel).

#### 2.6.3.2 Protein transfer onto nitrocellulose membrane

After the proteins were separated, the polyacrylamide gel was prepared for transfer to a nitrocellulose membrane (Bio-Rad, California, USA). The nitrocellulose membrane was cut to size, labelled at the bottom left corner and soaked in cold 1X running buffer (Appendix A). The transfer was assembled by placing the fiber pad, filter paper, the gel and membrane as shown in Figure 2.2 in a cassette. The cassette was placed into the transfer assembly. The assembly was then placed into the electrophoresis chamber, with an ice pack on the side. The chamber was then filled with 1X transfer buffer (Appendix A), closed and connected to the Bio-Rad power pack. The transfer was done for 1 hour 30 minutes at 100 volts.

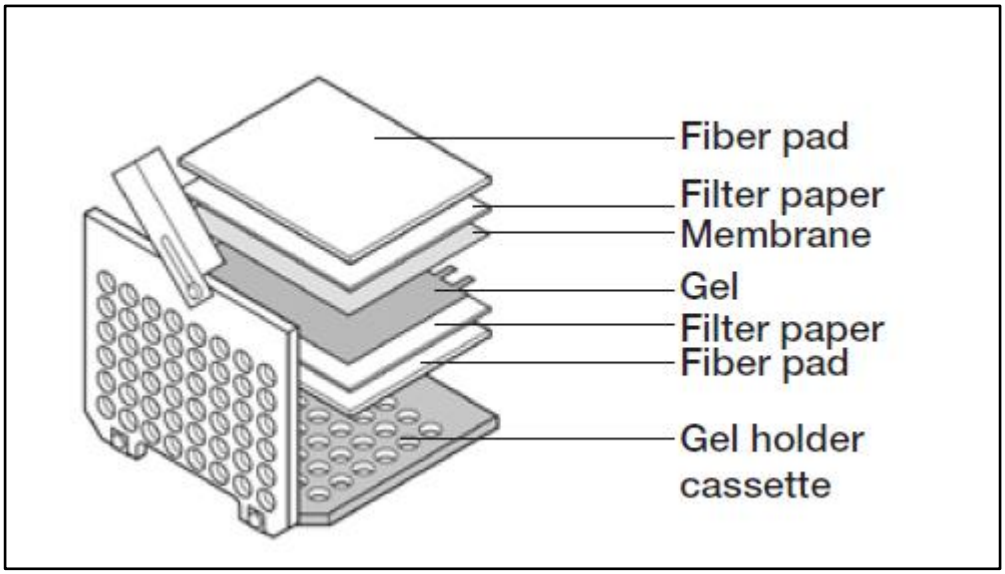


**Figure 2.2: Orientation of gel and nitrocellulose membrane in the cassette for protein transfer.** (Adapted from manual, Bio-rad, California, USA)

2.6.3.3 Antibody incubation and protein visualisation

Following transfer, the membrane was stained with Ponceau S (Sigma Aldrich, Missouri, USA) to confirm that the transfer was successful (Appendix A). The stain was then washed off with deionised water. The membrane was incubated, with gentle agitation, in blocking buffer (Appendix A) for one hour. The membrane was then incubated with blocking buffer containing primary antibody at 4˚C with gentle agitation overnight. The primary antibodies used were ZEB1 and SIP1 (ZEB2) (Santa Cruz Biotechnology, California, USA) and p38 (Bio-Rad, California, USA). The dilution used as well as secondary antibodies used are shown in Table 2.14.

**Table 2.14: Concentration of primary and secondary antibodies used for western blot analysis**

| Protein | Primary antibody | Secondary antibody |
|---|---|---|
| **ZEB1** | 1:1000 | 1:5000 (goat anti-rabbit) |
| **ZEB2** | 1:1000 | 1:5000 (goat anti-mouse) |
| **p38** | 1:5000 | 1:5000 (goat anti-rabbit) |

After overnight incubation, the membrane was washed with PBS/Tween (2 X 5 minute followed by 2 X 10 minutes) on the orbital shaker. The membrane was then incubated with the appropriate HRP-conjugated secondary antibody diluted in blocking buffer for two hours at room temperature on the orbital shaker. After incubation the membrane was washed as before and visualised by the chemiluminescence using the Clarity™ Western ECL substrate (Bio-Rad, California, USA). The two reagents provided in the kit were mixed in a ratio of 1:1 and the membrane was incubated in that solution for 1 minute. The membrane was then transferred to a transparency pocket and exposed to X-ray film in the dark. The film was

developed and fixed to visualise the protein signal. The developed film of the western blot was scanned and the intensity of the bands was quantified using the ImageJ software (National Institute of Health, Maryland, USA).

#### 2.6.3.4 Membrane stripping

After protein visualisation, the membrane was rinsed with PBS/Tween. The stripping buffer (Appendix A) was pre-heated at 55˚C. The stripping buffer was then added to the membrane in a small container and incubated at 55˚C for 30 minutes, with brief shaking every 15 minutes. Thereafter, the membrane was washed twice with PBS/Tween for 10 minutes. The membrane was then blocked again and reused to detect the loading control p38.

## 2.7 Transwell migration assays

Transwell® migration assays (Coning, New York, USA) were used to determine the migratory ability of cells. This technique involves the use of a chamber separated by a porous filter membrane, as depicted in Figure 2.4 (Hulkower and Herber, 2011). Briefly, the cells were plated in low serum media (0.5% FBS) and exposed to attenuated HIV-1 or matched microvesicles. The wells were gently shaken to evenly distribute the HIV or microvesicles as described in Section 2.1.4. 600µl of complete media (10% FBS) was added to the bottom chamber (12-well plate). The Transwell® chambers (8µm pore size) were carefully placed over the wells containing complete media using sterile forceps. 1 X $10^4$ cells (100 µl) of the HIV-exposed and microvesicle control cells were carefully seeded inside the respective chambers. The plate was covered with foil and incubated at 37˚C in the $C0_2$ incubator for 24 hours. The cells were then fixed by placing the chambers in 600 µl of 100% methanol in a 12-well plate for 5 minutes. The chambers were rinsed in distilled water and sterile cotton swabs were used to firmly wipe the upper side of the membrane and walls of the chambers in order to remove cells which were left behind and not migrated. The chambers were then placed in 0.2% crystal violet (Appendix A) to stain the migrated fixed cells for 30 minutes. As controls, some cell chambers were not wiped before staining. Excess stain was removed from the chambers with a pipette. The chambers were then rinsed thoroughly three times in distilled water. Thereafter, the upper side of the membrane and the walls were wiped with sterile cotton swabs to remove excess stain. The chambers were then rinsed again as before and the upper side of the membrane and walls were again wiped thoroughly with cotton swabs. The chambers were left overnight to dry completely. The chambers were carefully placed in 1.5 ml centrifuge tubes and the crystal violet stain of the migrated cells was solubilised in the chambers with 150 µl 50% acetic acid. 100 µl of the acetic acid washes were added to wells in a 96-well plate, which was read at 595 nm using the Glo-Max®-Multi+ multiplate reader (Promega, Wisconsin, USA).

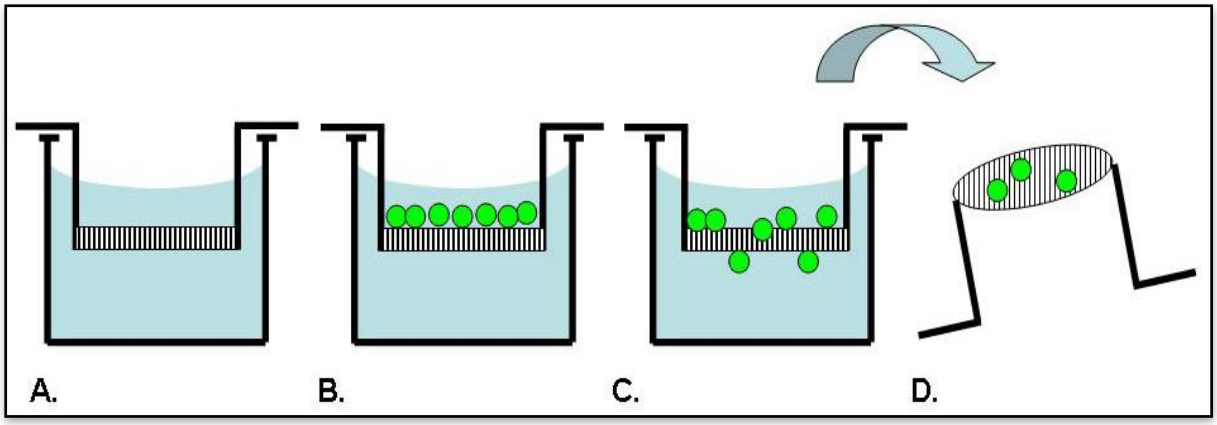


**Figure 2.4: Overview of the Transwell® migration assay.** (A) The membrane is inserted into a well to create two compartments. (B) Cells suspended in low-serum media are added to the upper compartment while serum-rich media is added to the well. (C) The cells migrate through the membrane during the incubation period. (D) The membrane is fixed and stained, and migrated cells can be counted on the lower side of the membrane. (Adapted from Hulkower and Herber, 2011)

# Chapter 3

# Validation of differentially expressed miRNAs

## 3.1 Introduction

Microarrays are used to study changes in expression of genes/miRNAs and have the advantage of allowing the large scale study of multiple genes/miRNAs simultaneously in one experiment (Chen et al., 2009). In cancer biology, these types of studies are useful as a screening tool to identify factors that may play significant roles in the disease, and hence become targets for therapy.

## 3.2 Aim

A custom miRNA PCR array experiment was performed in our laboratory to identify differentially expressed miRNAs in the Burkitt's lymphoma cell line Ramos when exposed to an attenuated form of HIV-1 (AT-2 treated) compared to microvesicle-treated (MV) cells as a control. The array identified 32 significantly up- and downregulated miRNAs (by 2-fold or more) of which, four miRNAs were selected for validation in this project. The four miRNAs, namely hsa-miR-200c-3p, hsa-miR-222-3p, hsa-miR-363-3p and hsa-miR-575 were selected because, although they have all been implicated in cancer, there is little to no information available in the literature on their role in lymphomas. The aim was to validate the expression of the selected miRNAs using TaqMan® miRNA single tube assays and miRNA-specific primers for both the RT and qPCR reactions (Chapter 2, Section 2.3) and the results are presented below.

## 3.3 Results

### 3.3.1 Cell treatment and RNA isolation

As was done for the PCR array, Ramos cells were treated with 500ng/ml of AT-2 inactivated HIV or matched microvesicles. Thereafter, total RNA was isolated using the *mir*Vana™ RNA isolation kit (Thermo Fisher Scientific, California USA; Chapter 2, Section 2.2.1) and quantified using the Nanodrop (Table 3.1). The 260/280 and 260/230 ratios displayed in the table indicated that the isolated RNA was free of significant protein and phenol contamination respectively. The RNA integrity was checked using agarose gel electrophoresis. As Figure 3.1 shows, the isolated RNA was of good integrity as no significant amount of degradation could be seen.

**Table 3.1: Quantification of the isolated RNA using the NanoDrop™ 1000**

| Sample | Concentration (ng/µl)* | 260/280 ratio | 260/230 ratio |
|---|---|---|---|
| **MV1** | 244.54 | 2.08 | 1.80 |
| **MV2** | 285.66 | 2.10 | 1.77 |
| **HIV1** | 206.10 | 2.12 | 1.97 |
| **HIV2** | 269.40 | 2.11 | 1.84 |

*1µl of RNA for measurement, RNAse-free water used as blank.

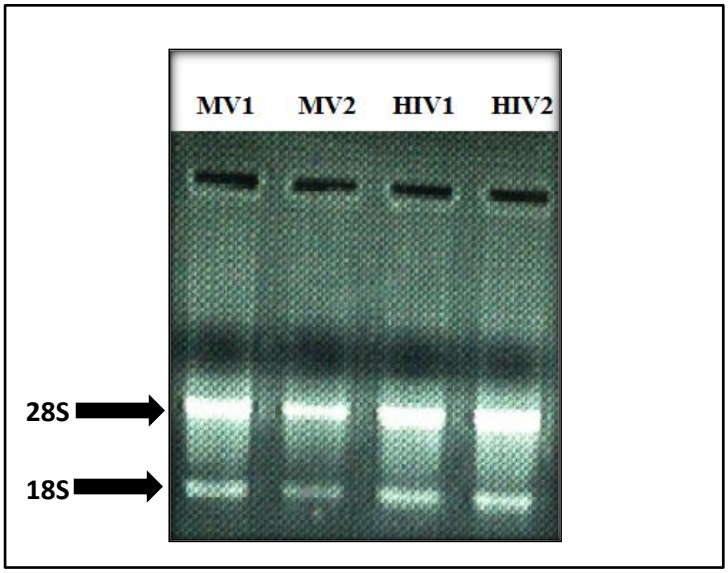


**Figure 3.1: Integrity of RNA isolated from Ramos cells exposed to either 500 ng/µl HIV or matched microvesicles**. 1% agarose gel (1X TBE) was electrophoresed at 100 volts for 35 minutes and visualised under UV light. 5µl of 2X RNA loading dye (Appendix A) was added to 1µg of the samples. Each sample was topped up to 15ml with DEPC-treated water and incubated at $55^0$C for 5 minutes before loading onto the wells. The RNA from microvesicles (MV) control cells are in lanes 1 and 2 while the RNA from HIV-exposed cells are in lanes 3 and 4.

One of the most widely used methods to validate array results is RT-qPCR, as it is the gold standard for measuring gene expression (Thomson et al., 2011, Morey et al., 2006). TaqMan® miRNA assays, which contain specific primers for both the reverse transcription and qPCR steps, were used to validate the differential expression of the four selected miRNAs.

### 3.3.2 Validation of Hsa-miR-200c-3p

Hsa-miR-200c-3p has been classified as a tumour suppressor in many types of cancers, including female reproductive cancers such as breast cancer, ovarian cancer and endometrial cancer (Cochrane et al., 2010). Along with other miRNAs in the miR-200 family, it's expression has been found to be a marker of the epithelial phenotype, as they target numerous

mesenchymal genes and inhibit tumour cell migration and invasion (Ibrahim et al., 2015, Elgaaen et al., 2014).

The aim was to determine if a similar trend is observed between the array and single-tube qPCR results. The small RNA molecules RNU48 and RNU6B were used as endogenous controls (Forte et al., 2012, Malumbres et al., 2009). The microvesicle-treated cells were used as the calibrator samples and the fold change in expression was determined. The experiments were performed at least twice (Appendix B) and Figure 3.2 depicts the results. A downregulation was observed in the HIV-treated cells (0.76-fold, p=0.16) compared to the microvesicle-treated ones. Therefore, we can confidently conclude that we have successfully validated the differential expression of hsa-miR-200c-3p in response to treatment with HIV compared to microvesicles.

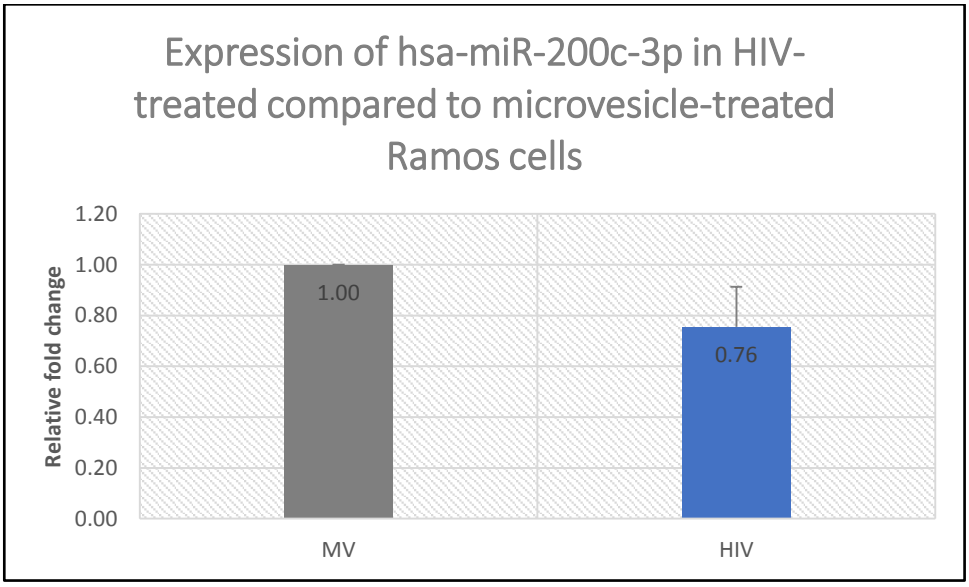


**Figure 3.2: Hsa-miR-200c-3p is downregulated in cells exposed to attenuated HIV compared to microvesicles control cells**. The qPCR data is represented as average fold change in HIV-exposed cells normalised to the microvesicle control, which has been set to 1. The small RNA molecule RNU48 was used as an endogenous control (Raw data in Appendix B). Each sample had three technical replicates. The error bars represent the standard deviation between the HIV-exposed and microvesicle control groups.

### 3.3.3 Validation of Hsa-miR-575

Hsa-miR-575 has recently been shown to be upregulated in non-small-cell lung cancer (NSCLC) (Wang et al., 2015). It was also found to be upregulated in miRNA profiling studies conducted in gastric, ovarian and oesophageal cancers (Drahos et al., 2016, Nam et al., 2016, Yao et al., 2009). Additionally, the BH3-Like Motif-Containing Cell Death Inducer (BLID) has recently been validated as a direct target of hsa-miR-575, thereby regulating cell proliferation, migration and invasion in cancer NSCLC cells (Wang et al., 2015).

As shown in Figure 3.3 below, in the single-tube assay, hsa-miR-575 found to be downregulated in Ramos cells exposed to attenuated HIV-1 compared to the microvesicle control. A fold change of 0.78 is observed compared to the microvesicle control set at 1. Furthermore, this particular result was not statistically significant. However, upon multiple repeats, a similar trend was observed but these results are not presented here as they were performed as part of another project which focussed on characterising the role of hsa-miR-575 in HIV-associated lymphoma (Goolam Hoosen, 2017).

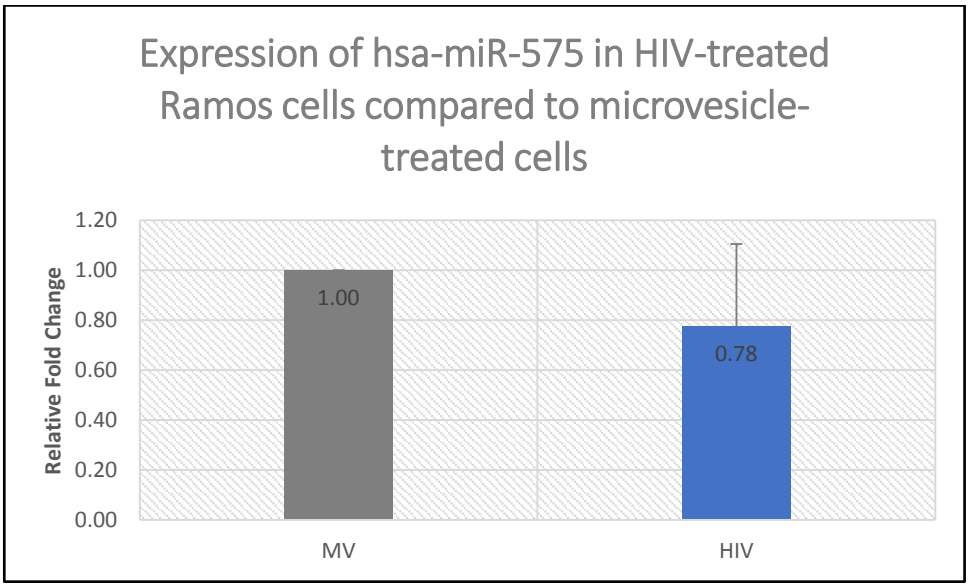


**Figure 3.3: hsa-miR-575 is downregulated in HIV-treated Ramos cells**. Data represented as average fold change in HIV-exposed cells normalised to control microvesicle. RNU48 was used as an endogenous control (Raw Data in Appendix B). The experiment was performed in triplicate and the error bar represents the standard deviation between the HIV and microvesicle group.

### 3.3.4 Validation of Hsa-miR-222-3p

Hsa-miR-222-3p has been classified as a tumour suppressor, as it has been found to be downregulated in many cancers, including breast cancer, tongue Squamous Cell Carcinoma and thyroid papillary carcinomas (Liu et al., 2009, Miller et al., 2008, Visone et al., 2007). Functional studies done on the miRNA also indicate that it is involved in inhibition of migration and invasion. Furthermore, hsa-miR-222-3p has also has oncogenic effects, as it been shown to inhibit apoptosis by directly targeting the cell cycle inhibitor p27 (Liu et al., 2009, Visone et al., 2007). The miRNA was also found to promote cell proliferation and invasion by directly targeting the Oestrogen Receptor α (ERα) in endometrial cancer cells (Liu et al., 2014).

Although the PCR array results indicate that this miRNA was upregulated, we could not successfully validate the differential expression of hsa-miR-222-3p. After multiple experiments, our results were inconclusive (Raw data in Appendix B).

### 3.3.5 Validation of Hsa-miR-363-3p

Hsa-miR-363-3p has been implicated in tumour metastasis in cancers, including Head and neck squamous cell carcinoma and neuroblasotoma (Sun et al., 2013, Qiao et al., 2013) It has been classified as a tumour suppressor as *in vitro* studies show that its overexpression results in a decrease in cancer characteristics such as anchorage-independent growth, cell invasion and metastasis (Sun et al., 2013, Qiao et al., 2013). Hsa-miR-363-3p was also found to be downregulated in gastric cancer and the miRNA was validated to directly target NOTCH1 (Song et al., 2015). Furthermore, hsa-miR-363-3p also has an antiapoptotic effects, as it has been found to target Caspase-3 and -9 as well as Bim (Floyd et al., 2014).

This miRNA was found to be upregulated in response to HIV treatment in the PCR array. However, despite numerous attempts, hsa-miR-363-3p was not detectable by qPCR in the single tube assays (Raw data in Appendix B).

## 3.4 Discussion

The validation of PCR array results is an essential step as array data can vary greatly depending on the platform and the procedures used. This is due to the shortcomings of microarrays such as different spot intensities and cross-hybridisation (Git et al., 2010). Additionally, in the case of miRNA arrays, some miRNAs are clustered in families that can differ by only one nucleotide. Therefore, Quantitative real-time PCR (qPCR) is often a common and often preferred method for validation. Although this technique also has its pitfalls, the results are likely to be less variable than microarray data because it focusses on amplifying one specific miRNA per reaction.

The first stage to ensuring optimum qPCR results is the amount and quality of RNA template used. As indicated in Table 3.1 and Figure 3.1, the RNA isolated was of good quality, integrity and of sufficient quantity, with little DNA contamination, in order to proceed with the qPCR. In general, RNA samples are considered "pure" if both the 280/260 and 230/260 ratios are approximately 2.00. According to the 260/230 ratios (Table 3.1), there was some organic contamination in the RNA samples, most likely from the reagents used in the isolation. As there is no consensus on the lower limit of this ratio, and it has been shown that the low ratio does not affect downstream processes, the RNA samples were used for downstream reverse transcription experiments (Ahlfen and Schlumpberger, 2010).

Single tube qPCR-based assays such as TaqMan® miRNAs have become very popular in miRNA studies. These assays are convenient as they contain specific primers for both the reverse transcription and qPCR steps. Validation of microarray results can be defined as obtaining similar quantitative and qualitative results for both the microarray and the qPCR (Morey et al., 2006). This means that one hopes to obtain a fold change in the same direction as well as similar amounts for both methods. By this definition, we did not successfully validate three of the four selected miRNAs, namely, hsa-miR-575, hsa-miR-222-3p and hsa-miR-363-3p (Table 3.2).

**Table 3.2: Comparison between fold change results obtained from the original miRNA PCR array and the single tube TaqMan® miRNA PCR assays**. (Both experiments were done on the same cell line-Ramos)

| MicroRNA | Microarray Results (FC) | Validation Results (FC) |
|---|---|---|
| **hsa-miR-200c-3p** | Downregulated (FC = 0.15) | Downregulated (FC = 0.76 ± 0.16) |
| **hsa-miR-575** | Upregulated (FC = 4.52) | Downregulated (FC = 0.78 ± 0.33) |
| **hsa-miR-222-3p** | Upregulated (FC = 6.74) | Inconclusive |
| **hsa-363-3p** | Upregulated (FC = 3.50) | Undetected |

Table 3.2 above summarises the single-tube assay results, and compares them side by side with The PCR array result obtained previously. For hsa-miR-575, the calculated fold changes are in opposite direction between the miRNA PCR array and the single tube assays. This miRNA was found to be upregulated by 4.52-fold in the PCR array. However, a mild downregulation was observed in the single-tube assays. On the other hand, hsa-miR-363-3p could not be detected using the TaqMan® miRNA assays. Unfortunately, there were no positive controls set up in the experiment to check whether the primers for this assay were functional. This was because it was assumed that the specificity of the primers had been tested and verified by the manufacturer (Applied Biosystems™, California, USA). Another factor to consider is the variability and difference between how the microfluidic array and single tube assays are set up. The array may give a lot of false positive results, due to factors such as cross hybridisation and spot quality (Chugh and Dittmer, 2012).

The results obtained for hsa-miR-222-3p were inconsistent, despite numerous biological and technical repeats. This can happen if a miRNA is present in very low levels. A different assay, with reported higher sensitivity could be used to check this. However, due to cost and time constraints, this was not possible.

Of the four miRNAs, hsa-miR-200c-3p was the only miRNA that was successfully validated as matching the results obtained in the PCR array experiment. It was therefore selected for further investigation. Hsa-miR-200c-3p has been classified as a tumour suppressor in various cancer types (Zhou et al., 2015, Prislei et al., 2013, Cochrane et al., 2010). The next chapter presents the results obtained upon further characterisation of the role of hsa-miR-200c-3p in lymphoma development.

# Chapter 4

# MicroRNA hsa-miR-200c-3p targets ZEB1 and ZEB2 to inhibit cell migration

## 4.1 Introduction

The miRNA hsa-miR-200c-3p is a member of the miR-200 family cluster. This family consists of five members which are transcribed in two polycistron clusters (Brabletz and Brabletz, 2010, Burk et al., 2008, Korpal et al., 2008). The first transcript consists of hsa-miR-200a, hsa-miR-200b and hsa-miR-429, which is found in chromosome 1. The second transcript is located in chromosome 12, and consists of hsa-miR-200c and hsa-miR-141. These miRNAs have been termed "the guardians of the epithelial phenotype", as they have been found to be enriched in epithelial tissues and epigenetically silenced in mesenchymal tissues (Cochrane et al., 2009, Peter, 2009). Numerous studies have shown the essential role that the miR-200 family plays in the inhibition of EMT and metastasis in tumour progression (Bracken et al., 2008, Korpal et al., 2008).

### 4.1.1 The ZEB family of transcription factors

One of the validated targets of hsa-miR-200c-3p, which is relevant to this project, is of the Zinc Finger E-box Binding (ZEB) family of transcription factors. The ZEB proteins are characterised by two zinc finger domains for DNA binding and a centrally located homeodomain (Vandewalle et al., 2009, Zhang et al., 2015). This group of transcription factors consist of two members, namely ZEB1 and ZEB2. The first member of this family, ZEB1, plays an essential role in tumour progression and metastasis as well as chemoresistance (Zhang et al., 2015, Zhang et al., 2014). ZEB1 has also been shown to have a regulatory role in T cell development and modulating adaptive immunity (Rojas-Marquez et al., 2015). ZEB2, also known as the Smad Interacting protein (SIP1), is the second member of the ZEB family and is involved in regulating multiple neurodevelopmental processes (Hegarty et al., 2015). Mutations in the ZEB2 gene causes the development of Mowat-Wilson syndrome, a rare disorder affecting many parts of the body, with dysmorphic features of the brain, head and face (Moore et al., 2016).

Along with the SNAIL and TWIST protein families, the ZEB genes are well characterised as master regulators of epithelial-to-mesenchymal transition (MR-EMT) (Hill et al., 2013, Browne et al., 2010). These factors play an essential role during embryonic development and cell differentiation (Sánchez-Tilló et al., 2011, Vandewalle et al., 2009). This transition process has also been shown to be an essential step in cancer metastasis. These genes induce or maintain EMT in various cancer types through suppression of epithelial specific genes such as E-cadherin (E-Cad). Furthermore, increased expression of the ZEB genes has been found to be linked to more aggressive and metastatic stages of these cancers. Other carcinogenic processes that these transcription factors are associated with include cancer cell stemness,

replicative senescence, tumour angiogenesis, and resistance to chemotherapy (Browne et al., 2010, Brabletz and Brabletz, 2010)

## 4.2 Aims

The validation studies of the PCR array, which was presented in the previous chapter, led to the selection of hsa-miR-200c-3p for further investigation. The current chapter presents results obtained from the attempts to define the role of hsa-miR-200c-3p in lymphoma development. The main questions that this chapter aims to answer are outlined in Figure 4.1.

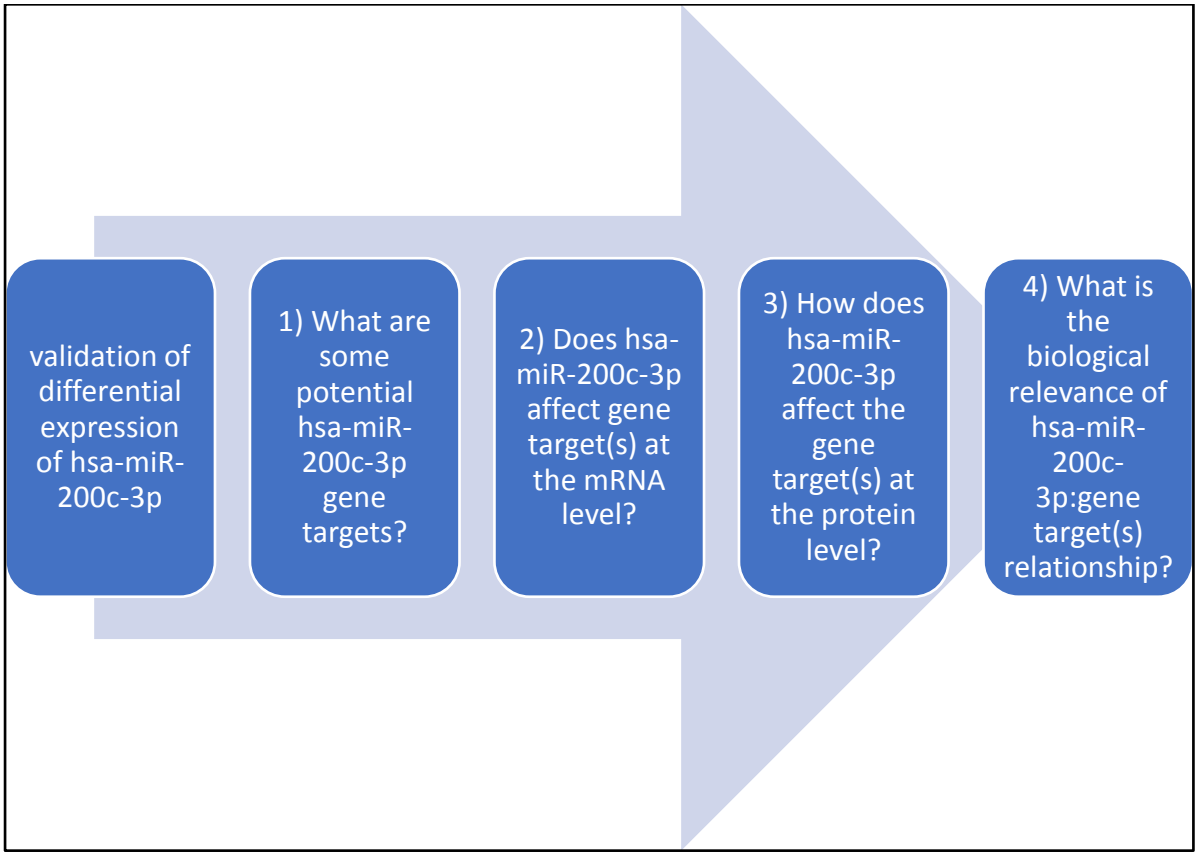


**Figure 4.1: Steps followed in Chapter 4 to better define the potential role of hsa-miR-200c-3p in the context of lymphomagenesis.**

## 4.3 Results

### 4.3.1 Hsa-miR-200c-3p is differentially expressed in two BL cell lines

As mentioned in Chapter 1, miRNAs tend to be differentially expressed in a spatio-temporal manner. Therefore, one would expect to observe a similar trend of deregulation in different samples of the same tissue, cell or cancer type. The BL cell line BL41 was selected to further validate the change in expression of hsa-miR-200c-3p observed. BL41 has similar characteristics to Ramos cells – both are EBV-negative and grow at similar rates. Therefore,

in order to ascertain the importance and relevance of hsa-miR-200c-3p in HIV-associated BL, its expression in this second BL cell line was investigated. Cells were cultured and exposed to attenuated HIV-1 as well as matched-microvesicles for controls as done previously (Chapter 2, Section 2.2). Ramos cells were also treated in parallel in order for the results to be directly comparative. Total RNA was isolated, quantified using the NanoDrop™ (Table 4.1), and acceptable 260/280 and 260/230 ratios were obtained. Furthermore, gel electrophoresis of the samples (Figure 4.2) indicate good RNA integrity. The hsa-miR-200c-3p expression levels in both cell lines (treated versus control) were determined using single-tube TaqMan miRNA assays as described in Section 2.3.

**Table 4.1: Quantification of RNA isolated from HIV/MV treatment using the Nanodrop™ 1000** (data represents one of several replicates)

| Sample | Concentration (ng/µl)* | 260/280 ratio | 260/230 ratio |
|---|---|---|---|
| **Ramos MV** | 211.1 | 2.09 | 2.25 |
| **Ramos HIV** | 185.2 | 2.09 | 2.18 |
| **BL41 MV** | 218.2 | 2.07 | 1.99 |
| **BL41 HIV** | 210.8 | 2.04 | 1.92 |

*1µl of each sample used for measurement. The elution buffer (nuclease-free water) provided in the High Pure kit (Roche Applied Sciences, Mannheim, Germany) was used as the blank.

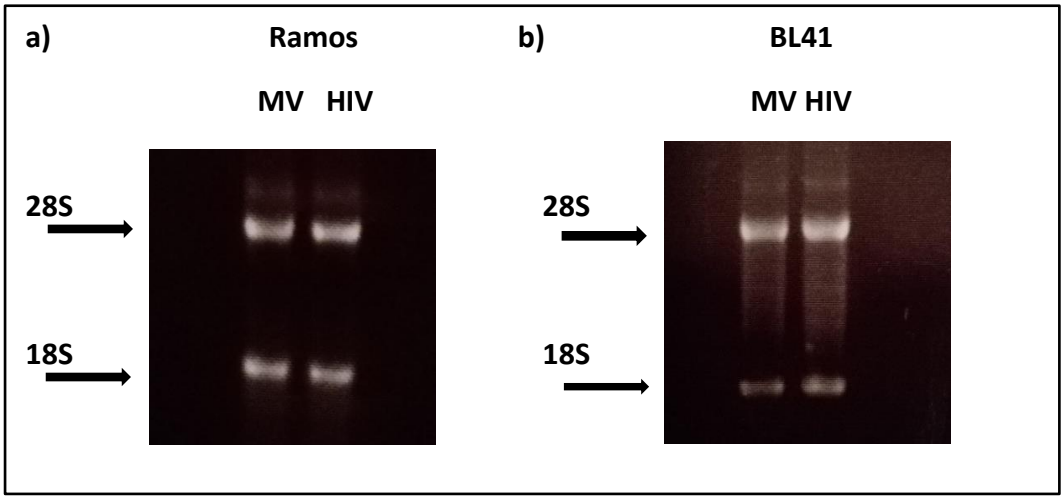


**Figure 4.2: Integrity of RNA isolated from Ramos and BL41 cells treated with HIV or matched microvesicles**. 1.5% agarose gel (in 1X TBE, EtBr (0.5mg/ml)) was electrophoresed at 100 volts for 35-45 minutes and visualised under UV light. 5µl of 2X RNA loading dye (Appendix A) was added to 5µl of each sample, which was then incubated at $55^0$C for 5 minutes before loading onto the wells.

### 4.3.2 hsa-miR-200c-3p is downregulated in both BL cell lines upon exposure to attenuated HIV

The TaqMan® miRNA assays (Section 2.3) were used to determine expression of hsa-miR-200c-3p in cells exposed to attenuated HIV, compared to controls, for both cell lines. The

small RNA molecules RNU48 and RNU6B were used as endogenous controls (Forte et al., 2012, Malumbres et al., 2009). The microvesicle-treated samples were used as the calibrator samples and the fold change in expression was determined. The results are shown in Figure 4.3 below and correlates with both the PCR array data (Chapter 3, Table 3.2) as well as the validation study (Chapter 3, Section 3.2.2). An approximately 2-fold decrease in hsa-miR-200c-3p expression is observed in both cell lines when the cells are exposed to attenuated HIV. It should be noted that the Roche High Pure RNA Isolation Kit (Roche Applied Sciences, Mannheim, Germany) was used in this instance, as opposed to the *mir*Vana™ miRNA Isolation Kit (Thermo Fisher Scientific™, Massachusetts, USA) used for the validation studies presented in Chapter 3. This is because the Roche High Pure RNA Isolation Kit (Roche Applied Biosciences, Mannheim, Germany) allows for detection of both miRNA expression as well as gene target expression (using messenger RNA (mRNA) as template). In addition, this kit has the added advantage of having a genomic elimination step, which ensures the accuracy of the qPCR result.

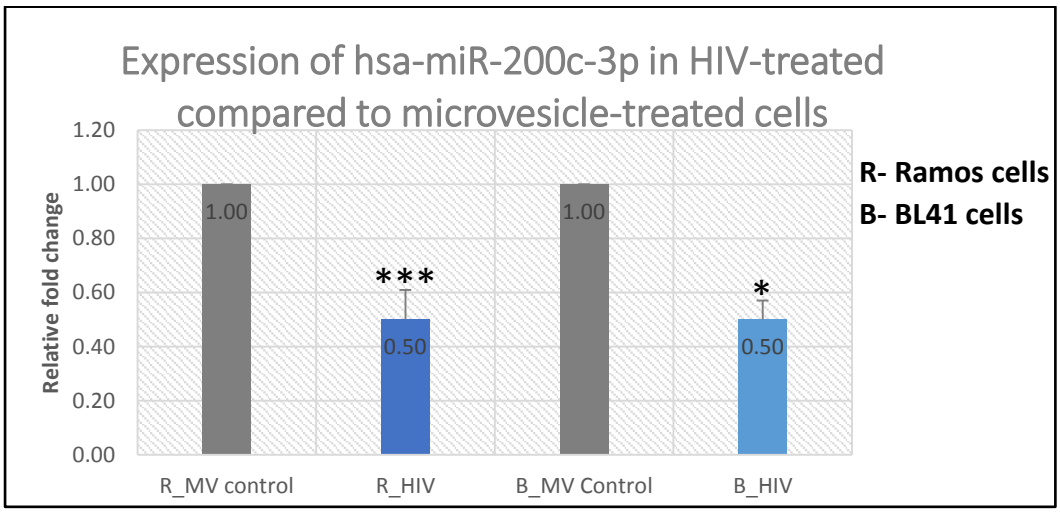


**Figure 4.3: Hsa-miR-200c-3p expression is downregulated in BL cells exposed to attenuated HIV.** Expression of hsa-miR-200c-3p in Ramos (R) and BL41 (B) cell lines exposed to attenuated HIV virions compared to matched microvesicle (MV) cells as control. Data represents one of at least 2 independent experiments. Each experiment was done in triplicate and error bars represent standard deviation between the HIV and MV groups (*p <0.05, ***p<0.001, t-test)

### 4.3.3 hsa-miR-200c-3p targets genes involved in the EMT Process

The next step in this research project was to identify potential gene targets of hsa-miR-200c-3p which are relevant in the context of our study, i.e., which play a role in lymphoma development. The use of predictive bioinformatic algorithms which are available online typically produce an extensive list of potential targets. As an example, a list of some predicted targets for hsa-miR-200c-3p are shown in Table 4.2 below, using the DIANA-TarBase Version 8 program (http://carolina.imis.athena-innovation.gr/diana_tools). To help narrow down this list, an extensive literature search was conducted in order to identify gene targets which have been validated using molecular tools such as qPCR, reporter assays, western blotting and others. The experimentally validated microRNA-target interactions database 7.0

(miRTarBase) (http://mirtarbase.mbc.nctu.edu.tw/index.php) was also used in this instance, as it provides links to updated literature and the techniques used to validate the gene targets. Some of these validated gene targets are presented in Table 4.3.

**Table 4.2: Summary of predicted gene targets for hsa-miR-200c-3p using the DIANA-TarBase V8 online program.**

| miRNA | Predicted gene target |
|---|---|
| **Hsa-miR-200c-3p** | KRAS |
| | MSN |
| | ZEB1 |
| | FN1 |
| | PPM1F |
| | NTRK2 |
| | LEPR |
| | CDH1 |
| | PMAIP1 |
| | ZEB2 |
| | VIM |
| | BCL2 |
| | ERRFI1 |
| | RHOA |
| | PKIA |
| | BMI |
| | ACVR2B |
| | HOXB5 |

**Table 4.3: Experimentally validated gene targets of hsa-miR-200c-3p and supporting literature**

| Gene target | Validation tool | Reference |
|---|---|---|
| **Tubulin Beta 3 Class III (TUBB3)** | Reporter assay, Western Blotting, qPCR | (Cochrane et al., 2009, Cochrane et al., 2010) |
| **Polycomb complex protein BMI 1 (BMI)** | Reporter assay, Western Blotting, qPCR | (Qiu et al., 2017, Liu et al., 2012) |
| **Zinc Finger E-box Binding Protein 1 (ZEB1)** | Reporter assay, Western Blotting, qPCR | (Zhou et al., 2015, Park et al., 2008) |
| **Zinc Finger E-box Binding Protein 2 (ZEB2)** | Reporter assay, Western Blotting, qPCR, NGS | (Zhou et al., 2015, Park et al., 2008) |
| **Fibronectin 1 (FN1)** | Reporter assay, Western Blotting, qPCR, NGS | (Howe et al., 2011, Zhang et al., 2017) |
| **Vascular endothelial growth factor A (VEGFA)** | Reporter assay, Western Blotting, qPCR | (Chuang et al., 2012, Erturk et al., 2015) |
| **Moesin (MSN)** | Reporter assay, Western Blotting, qPCR | (Howe et al., 2011) |
| **Fms Related Tyrosine Kinase1 (FLT1)** | Reporter assay, Western Blotting, qPCR | (Panda et al., 2012, Hur et al., 2013) |
| **Inhibitor of Nuclear Factor Kappa B Kinase Subunit Beta (IKBKB)** | Reporter assay, Western Blotting, qPCR | (Chuang and Khorram, 2014, Panda et al., 2012) |

### 4.3.4 ZEB1 and ZEB2 mRNAs expressions are downregulated in BL cell lines exposed to HIV

#### 4.3.4.1 ZEB primer design and testing using PCR

The open reading frame (ORF) sequence information for the human ZEB1 (NG_017048.1) and ZEB2 (NG_016431.1) were obtained from the NCBI nucleotide database (https://www.ncbi.nlm.nih.gov) and used for the design of gene specific primers to be used in quantitative real-time PCR assays. Primers were designed and optimised using Primer3Plus (http://www.bioinformatics.nl/cgi-bin/primer3plus.cgi) and Oligoanalyzer (Integrated DNA Technologies, Iowa, USA). The primer sequences, positions on the ORF, as well as transcript size are presented in Table 4.4 below. To test these primers, endpoint PCR was performed using cDNA as template, which was reverse transcribed from mRNA isolated from untreated Ramos cells (incubated in low serum media). The endpoint products were separated using gel electrophoresis and bands of the expected size were produced as shown in Figure 4.4.

**Table 4.4: Sequences of primer pairs designed for the ZEB1 and ZEB2 genes for qPCR analysis**.

| Gene | Primer pair sequences | Position on gene sequence | Transcript size (bp) |
|---|---|---|---|
| ZEB1 | **ZEB1_F** (5'-GCCTGAAATCCTCTCGAATG-3') | 3069-3088 | 95 |
| | **ZEB1_R** (5'-CATCCTCTTCCCTTGTCAAAC-3') | 3143-3163 | |
| ZEB2 | **ZEB2_F** (5'-GAAGAGACTGGAGATCACTC-3' | 4068-4088 | 93 |
| | **ZEB2_R** (5'-GCCATCTTCCATATTGTC-3') | 4144-4161 | |

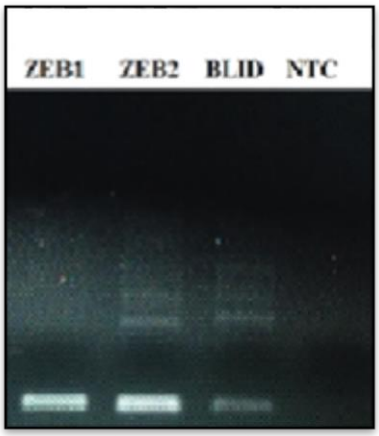


**Figure 4.4: ZEB1 and ZEB2 primers successfully amplify transcripts**. PCR products visualised on gel to determine the specificity of the designed primers. Agarose gel (1.5% in 1X TBE). Amplification bands for ZEB1 and ZEB2 are found in lanes 1 and 2 respectively. Lane 3 shows result using an unrelated primer set for the gene BLID and lane 4 shows the no template control (NTC).

#### 4.3.4.2 ZEB1 and ZEB2 mRNA expression is decreased in BL cells exposed to HIV

Once the ZEB primers were successfully tested using PCR, qPCR was then performed to determine the expression levels of the gene targets in cells exposed to attenuated HIV compared to the matched microvesicle control. cDNA was synthesised using the mRNA isolated from the Ramos and BL41 cells (Section 4.1.1), which were exposed to attenuated HIV and matched microvesicles (Chapter 2, Section 2.2). The results obtained indicate that both ZEB1 and ZEB2 are significantly downregulated in Ramos (Figure 4.5) and BL41 (Figure 4.6) cells. An approximately 2-fold decrease in the mRNA expression of both genes was observed in the Ramos cells exposed to HIV, relative to cells exposed to matched-microvesicles. The housekeeping gene GAPDH was used to normalise the result. Similarly, a decrease in the mRNA expression of both genes was observed the BL41 cells upon exposure to HIV, although to a lesser extent compared to what was observed in the Ramos cells.

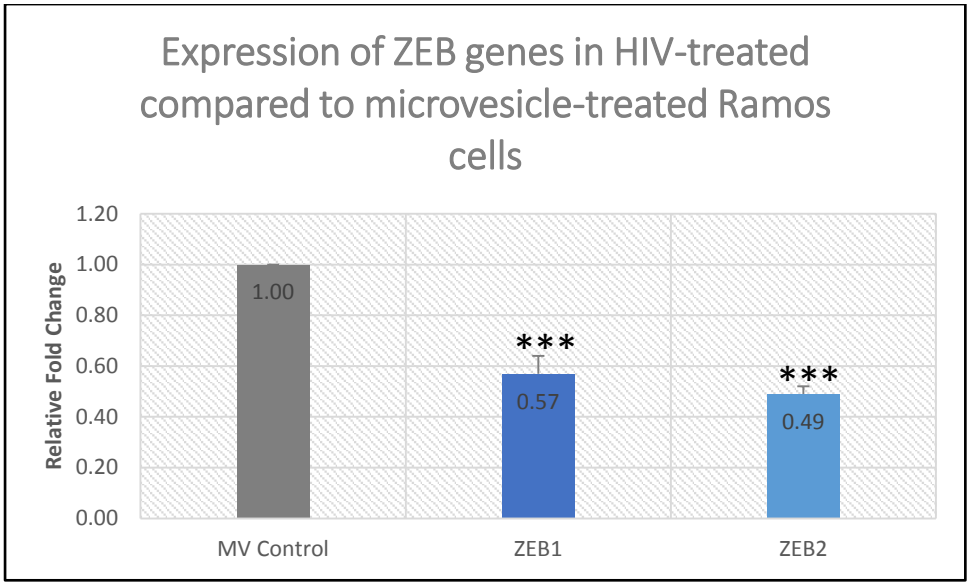


**Figure 4.5: ZEB1 and ZEB2 mRNA is downregulated in Ramos cells exposed to HIV**. Expression of ZEB1 and ZEB2 in Ramos cells exposed to attenuated HIV compared to cells exposed to matched microvesicles (MV control). Data represents one of at least 2 independent experiments. Each experiment was performed in triplicate and the error bars represent the standard deviation (***p <0.001, t-test)

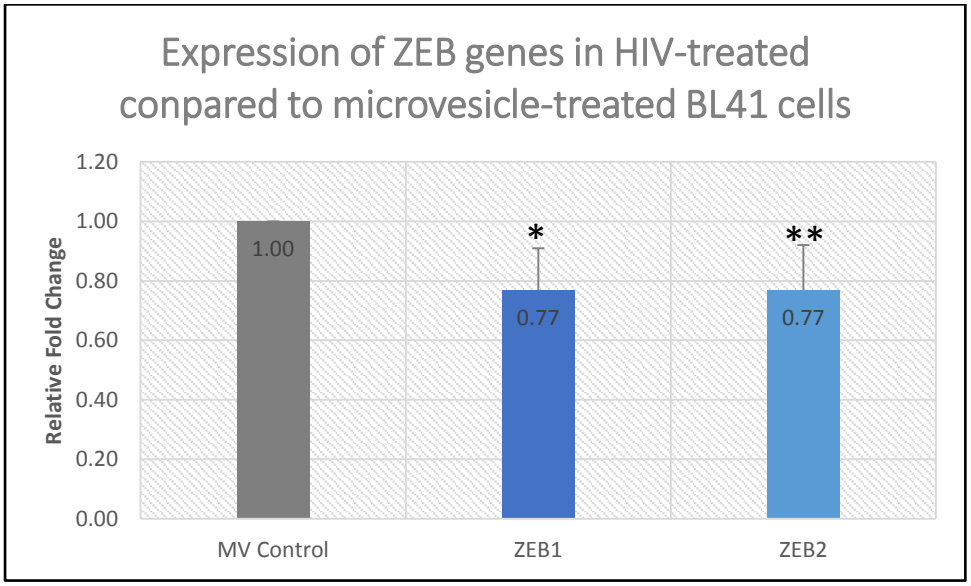


**Figure 4.6: ZEB1 and ZEB2 mRNA is downregulated in BL41 cells exposed to HIV**. Expression of ZEB1 and ZEB2 in BL41 cells exposed to attenuated HIV compared to cells exposed to matched microvesicles (MV) cells. Data represents one of at least 2 independent experiments. Each experiment was performed in triplicate and the error bars represent the standard deviation (*p <0.05, **p<0.01, t-test).

### 4.3.5 ZEB1 and ZEB2 protein levels are downregulated in Ramos, but upregulated in BL41 cells, exposed to HIV

To assess the functional significance of the altered expression of any miRNA, it is important to measure the downstream impact of changes in the protein expression of its potential gene targets. To this end, western blotting was performed using antibodies against ZEB1 and ZEB2 (Chapter 2, section 2.5). Cells were treated as previously described (Chapter 2, Section 2.2) and total protein was isolated using RIPA buffer (Appendix A). Thereafter, the protein was quantified using the BCA assay (Chapter 2, Section 2.5). The western blotting results for Ramos and BL41 cells are presented in Figure 4.7 and Figure 4.8 respectively. A clear and reproducible downregulation of both ZEB1 and ZEB2 proteins were observed in the Ramos cells exposed to attenuated HIV compared to those exposed to matched controls (Figure 4.7a). The result was normalised to p38, a constitutively expressed protein used as a loading control. The bar graphs below the blots represent densitometry readings generated from analysing the protein bands using ImageJ software (National Institute of Health, Maryland, USA). In contrast to what was observed in the Ramos cells, the expression of ZEB1 and ZEB2 protein increase in the BL41 cells upon exposure to attenuated HIV, compared to those exposed to matched microvesicles (Figure 4.8a).

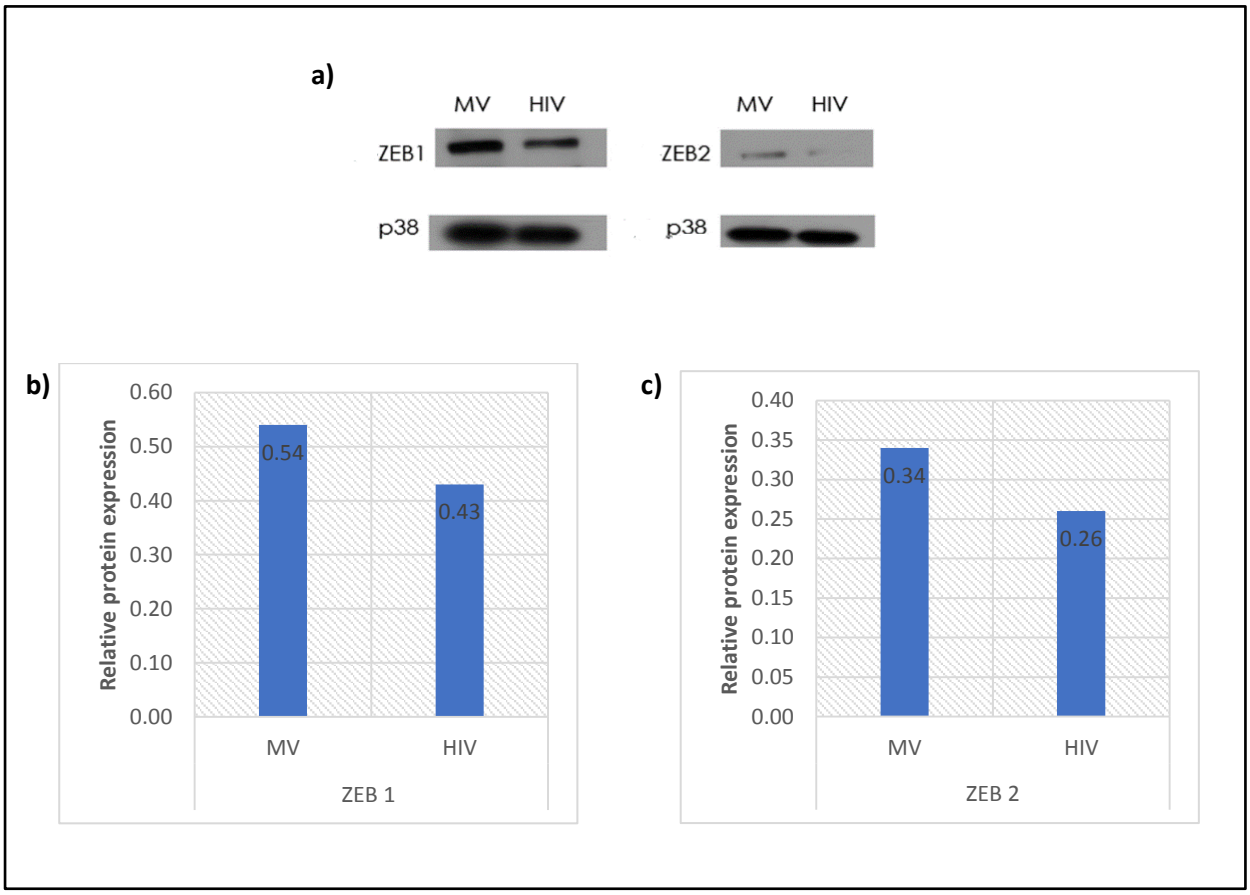


**Figure 4.7: ZEB1 and ZEB2 protein expressions are downregulated in HIV exposed Ramos cells.** Western blot analysis showing ZEB1 and ZEB2 expressions (both observed at ~ 200 kDa due to post-translational modification) in the Ramos cell line. Total protein was isolated from Ramos cells exposed to attenuated HIV and matched microvesicle controls. 20µg of protein was added to 6µl of the 5X SDS loading dye (Appendix A) and 1µl of DTT. The samples were topped up to 30µl with RIPA buffer and incubated at $100^0$C for 5 minutes before loading onto an 8% SDS-PAGE gel. The proteins were electrophoresed at 100V for 2 hours in 1X running buffer. The Proteins were then transferred to a nitrocellulose membrane (Bio-Rad, USA) for 1.5 hours in 1X transfer buffer. The membrane was then incubated with the Clarity™ Western ECL Blotting Substrate (Bio-Rad, USA) and exposed to X-ray film. The film was then developed and fixed to visualise the proteins. Protein bands for ZEB1 and ZEB2 (a) obtained from membrane exposed to X-ray film. (b and c) Quantification of band intensities using ImageJ software (normalised to p38 loading control). Data represents one of several repeats.

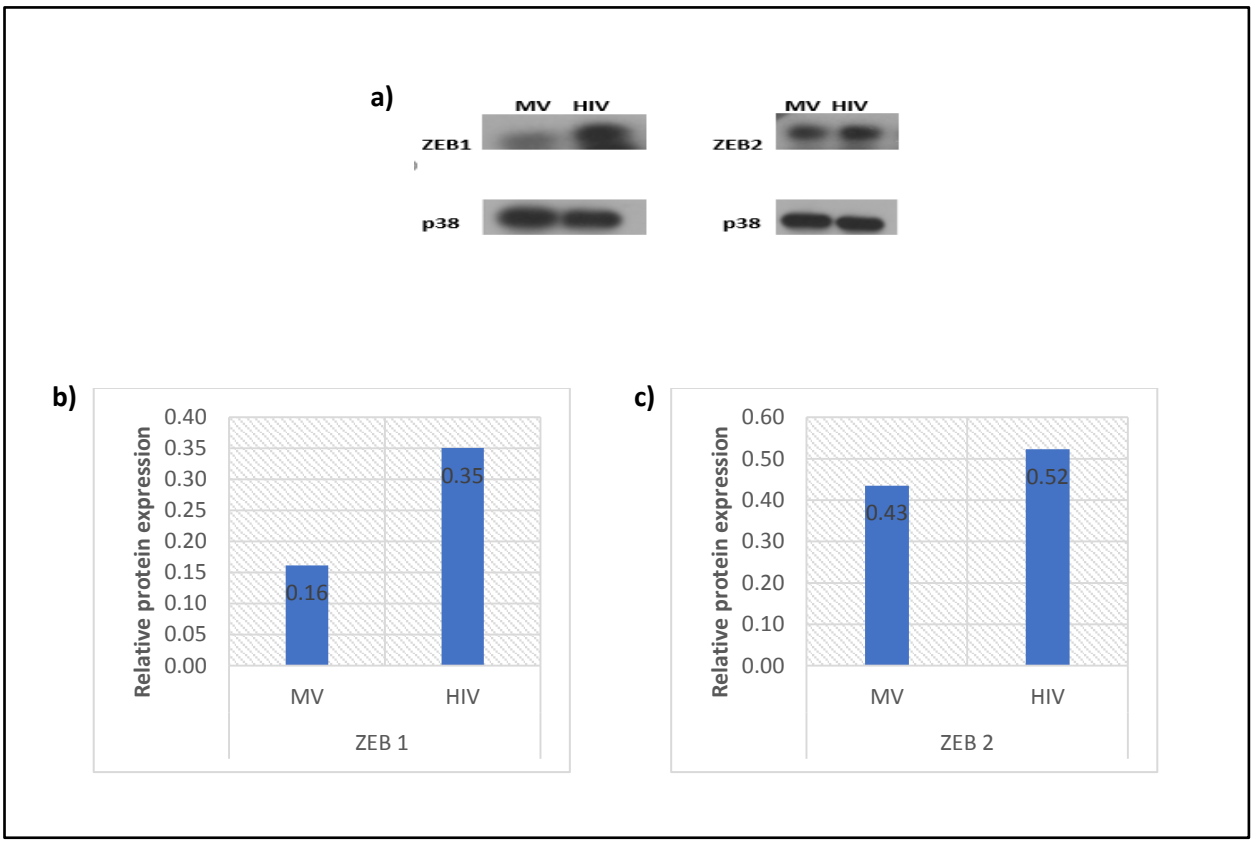


**Figure 4.8: ZEB1 and ZEB2 protein expressions are upregulated in HIV exposed BL41 cells.** Western blot analysis showing ZEB1 and ZEB2 expressions (both observed at ~ 200 kDa due to post-translational modification) in the BL41 cell line. Total protein was isolated from BL41 cells exposed to attenuated HIV and matched microvesicle controls. 20µg of protein was added to 6µl of the 5X SDS loading dye (Appendix A) and 1µl of DTT. The samples were topped up to 30µl with RIPA buffer and incubated at $100^0$C for 5 minutes before loading onto an 8% SDS-PAGE gel. The proteins were electrophoresed at 100V for 2 hours in 1X running buffer. The Proteins were then transferred to a nitrocellulose membrane (Bio-Rad, USA) for 1.5 hours in 1X transfer buffer. The membrane was then incubated with the Clarity™ Western ECL Blotting Substrate (Bio-Rad, USA) and exposed to X-ray film. The film was then developed and fixed to visualise the proteins. Protein bands for ZEB1 and ZEB2 (a) obtained from membrane exposed to X-ray film. (b and c) Quantification of band intensities using ImageJ software (normalised to p38 loading control). Data represents one of several repeats.

### 4.3.6 Burkitt's lymphoma cells migrate faster when exposed to HIV

One of the most well described roles of the ZEB family of transcription factors in cancer is in promoting cancer cell invasion through facilitating the EMT process (Brabletz and Brabletz, 2010). Tissue invasion and metastasis is one of the hallmarks of cancer, and to achieve this cancer cells found in solid tumours such as lymphomas have to untether themselves and degrade the extracellular matrix so that they can become mobile (Hanahan and Weinberg, 2011). To further characterise the role of hsa-miR-200c-3p in Burkitt's lymphoma, the transwell® migration assay was performed (Chapter 2, Section 2.6). This assay consists of a

two-chamber system separated by the cell membrane. The membrane contains pores which are blocked with a gel composed of components of the extracellular matrix, thus mimicking the physiological matrices that tumour cells encounter during the invasion process in vivo. The cells are placed on one side of the gel and a chemoattractant-usually a higher concentration of serum-is placed on the other side of the gel. The invasion potential of cells is determined by counting those cells that have traversed the cell-permeable membrane. Ramos and BL41 cells were plated as normal, and after attenuated HIV or matched microvesicles had been added to the medium, cells were transferred to the transwell® chambers and incubated for 24 hours, with complete medium (10% FBS) as a chemoattractant in the wells. The result is shown in Figure 4.9 below. For both cell lines, the ability of the cells to migrate was significantly enhanced upon exposure to HIV relative to the controls. The Ramos cells migrated ~32% faster, while the BL41 cells migrated ~37% faster.

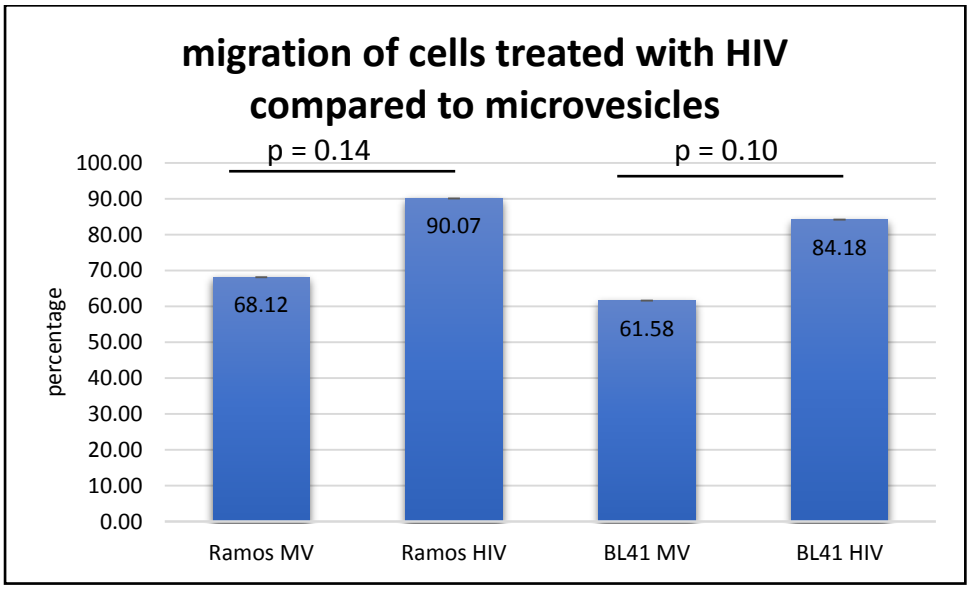


**Figure 4.9: Ramos and BL41 cells migrate faster when exposed to HIV**. The effect of HIV on the migratory ability of Ramos and BL41 cells were determined by using Transwell® migration assays. Ramos and BL41 cells were treated with attenuated HIV or matched microvesicles in low serum medium (containing 0.5% FBS). Thereafter, the cells were plated in the chambers (8µM pores), while complete medium (containing 10% FBS) was added to the wells. The number of cells that passed through the membrane pores were stained with 0.2% crystal violet. The stain was then solubilised with 50% acetic acid and the intensity, which correlates to the number of migrated cells, was measured using the GloMax®-Multi microplate reader (Promega, USA). The data was normalised to the total number of cells plated, which was determined by counting cells in both the upper and lower chambers. Data represents one of 3 independent experiments (p values displayed on graph, t-test).

## 4.4 Discussion

In order to define the role of hsa-miR-200c-3p in HIV-associated BL, a specific series of steps were followed, based on published guidelines. A review paper by Kuhn and colleagues outlined guidelines to follow to successfully validate miRNA gene targets (Kuhn et al., 2008b).

These guidelines are essential as bioinformatic tools use different methods to predict gene targets, however, these targets must be validated experimentally. In addition, it may be possible for a miRNA to not affect a selected gene in the cell/tissue type of interest. Therefore, it is always essential to confirm experimentally in the tissue/cells of interest, the effect a differentially expressed miRNA in a predicted gene targets.

To further support the concept that hsa-miR-200c-3p is relevant in Burkitt's lymphoma development among HIV-infected individuals, its expression was investigated in a second BL cell line. BL41 is similar to Ramos in that they both do not harbour EBV. Additionally, in our laboratory conditions, they both grow at a similar rate. Both cell lines were derived from a male child who developed BL (Lenoir et al., 1985, Klein et al., 1975). As shown in Figure 4.3, hsa-miR-200c-3p is downregulated in both cell lines when exposed to attenuated HIV-1. Therefore, this strengthens our initial data that hsa-miR-200c-3p plays a potentially important role in the development and/or progression of BL in people who are HIV positive and therefore warranted further investigations

Hsa-miR-200c-3p has been classified as a tumour suppressor miRNA in various cancers. In fact, members of the miR-200 family have been named as the "guardians of the epithelial phenotype", as they target mesenchymal-specific genes to inhibit EMT (Ibrahim et al., 2015). Some of the genes this miRNA family targets are the E-cad transcriptional repressors (EcTRs) (Sánchez-Tilló et al., 2011). ZEB1 and ZEB2 are two of the transcription factors that were selected to be investigated further in this research project. These were chosen because they were predicted targets of hsa-miR-200c-3p by at least 2 bioinformatic algorithms and this interaction was validated experimentally in other cancers (Table 4.3).

An inverse correlation in expression exists between a miRNA and its specific gene targets and hence one would expect the ZEB genes to have been upregulated under the treatment conditions used. At the mRNA level, both ZEB1 and ZEB2 were significantly downregulated in cells exposed to attenuated HIV-1 for both cell lines (Figure 4.5 and Figure 4.6). This may be indicative that hsa-miR-200c-3p not influencing the genes at the transcriptional level. This may also mean that under our experimental conditions, other factors are contributing to the suppression of the ZEB gene expression at the mRNA level.

Interestingly, a double-negative feedback loop has been observed between the ZEB transcription factors and the miR-200 family (Figure 4.10) (Brabletz and Brabletz, 2010). These transcription factors can bind to conserved recognition sequences (paired E-box elements) in the promoter regions of the two miR-200 genes (in chromosome 1 and 12) to inhibit transcription of the primary polycistron transcripts. Conversely, the 3'-UTRs of the ZEB genes contain eight and nine conserved sites, for ZEB1 and ZEB2 respectively, where the miR-200 members can bind to inhibit translation (Brabletz and Brabletz, 2010). This interaction is advantageous as it allows cells to reversibly switch between epithelial and mesenchymal characteristics, depending on extracellular signals (Hill et al., 2013). Recently, a similar feedback loop was described in B-cells between hsa-miR451 and the c-Myc oncogene (Ding

et al., 2018). Hsa-miR-451 can directly repress c-Myc by interaction with its 3'-UTR, but the oncoprotein can inversely regulate hsa-miR-451 by directly binding to its promoter. A disruption of this loop contributes to lymphomagenesis and there is a strong possibility that the same is the case with the hsa-miR-200c-ZEB family feedback loop.

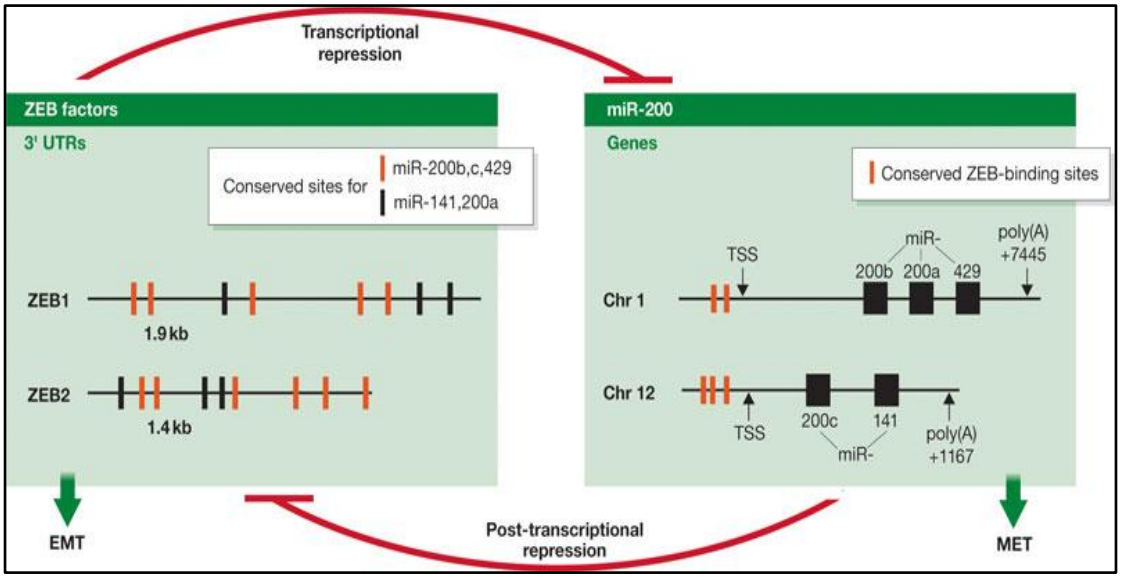


**Figure 4.10: The double-negative feedback loop observed between the ZEB and miR-200 families.** The ZEB factors are able to bind to E-box sequences to repress transcription of the miR-200 precursor miRNA genes (located in Chromosomes 1 and 12) while the miR-200 family can bind to conserved seed sequences in the 3'-UTR of the ZEB genes to inhibit their expression at the post-transcriptional level. (Adapted from *Brabletz and Brabletz, 2010*)

Ultimately, changes in protein and not in mRNA expression is a better indicator of functional impact. Western blot analysis, using antibodies against the ZEB proteins were performed. While protein expression correlated with the mRNA expression in the Ramos cells, in the BL41 cells, an increase in ZEB proteins was noted (Figures 4.7 and 4.8). Once again, this discrepancy between mRNA and protein could be explained by the feedback loop. Nevertheless, an increase in migratory ability was observed in both cell lines as measured by Transwell® assays (Figure 4.9). These results give further evidence that the presence of HIV can directly affect cellular functions in B-cells. The enhanced migration observed in both cell lines suggest that HIV may promote cellular processes in these B-cells that favour a more motile and invasive phenotype, thereby leading to a more metastatic and aggressive form of lymphoma.

# Chapter 5

# Summary and Conclusions

## 5.1 Summary

Of late, studies on the role of miRNAs in cancer research have become prominent as these small molecules are potentially powerful novel candidates for therapeutic intervention. Infection with HIV has been linked to a significantly increased incidence of certain types of cancers, including aggressive forms of NHLs. In recent years, it has become evident that HIV plays a direct role in the pathogenesis of some of these HIV-associated cancers, including lymphomas. Viruses and viral components have been found to alter cellular biological pathways, and gene expression, in various ways. One of these biological processes that viruses may alter to promote disease is the miRNA biogenesis pathway. This is, to the best of our knowledge, the first study where the ability of HIV to alter the expression of cellular miRNAs in lymphoma cells is being reported, and the downstream functional consequences in the cancer phenotype is being investigated.

The first objective was to validate the differential expression of selected miRNAs when lymphoma cells were exposed to HIV-1, compared to control cells. The result of these are presented in Chapter 3. The four selected miRNAs, namely, hsa-miR-200c-3p, hsa-miR-575, hsa-miR-222-3p and hsa-miR-363-3p, were chosen as from a custom miRNA PCR array performed in our laboratory and the selection criteria for these miRNAs was based on published reports on their involvement in other types of cancers, as well as having a 2-fold or more change in expression in the array. Following validation using single-tube qPCR assays, hsa-miR-200c-3p was selected for further investigation and characterisation. The downregulation of this miRNA was also further confirmed in a second BL cell line (BL41), thereby indicating that it may potentially act as a tumour suppressor.

A single miRNA can have multiple gene targets, as the recognition seed sequence is about eight bases long (Lewis et al., 2005). In addition, some miRNAs (groups/families) can have similar seed sequences, which allows for one gene to be repressed by multiple miRNAs. Furthermore, many of the genes that a specific miRNA targets are often involved in the same pathway or cellular process (Hashimoto et al., 2013). Among the multiple targets of hsa-miR-200c-3p (Table 4.3), the zinc finger transcription factors ZEB1 and ZEB2 were chosen for further investigation. This was because, aside from being experimentally validated targets of this miRNA (Zhou et al., 2015), the ZEB proteins have a well-defined role in cancer progression, and are associated with aggressive and advanced stage cancers as they facilitate cancer cell migration and metastasis. These transcription factors directly inhibit the transcription of epithelial genes, including the cell adhesion molecule E-Cad, resulting in the cells losing epithelial characteristics such as polarity and cell-cell adhesion, and dedifferentiating to gain mesenchymal ones (Brabletz and Brabletz, 2010).

Chapter 4 outlines the findings about the expression of the ZEB genes in the two BL cell lines, when exposed to attenuated HIV-1. Both ZEB1 and ZEB2 were found to be downregulated at the mRNA level. This was not unexpected, as there is an inverse correlation between miRNA and gene target expression. Nevertheless, these results are physiologically valid as it is possible for a miRNA's negative effect on its gene target to be observed at the protein level (i.e. the miRNA inhibits translation, without targeting the mRNA for degradation). In the Ramos cells, the ZEB protein expressions were also found to be downregulated. In contrast, both proteins were upregulated in response to exposure to attenuated HIV-1 in the BL41 cells. As the ZEB factors play an essential role in EMT, it was important to determine whether exposure of cells to attenuated HIV affected their migratory ability. Both cell lines were observed to have enhanced migration when exposed to attenuated HIV. As depicted in Figure 5.1, cells in the tumour microenvironment switch between the epithelial and mesenchymal phenotypes depending on what the tumour needs. In the initial stages of metastasis, there is increased levels of ZEB 1 and ZEB2, thereby promoting EMT and the mesenchymal phenotype. This will result in more tumour metastasis. As the cells reach a secondary site, the cells will lose their mesenchymal traits. As there is a need for the new solid tumour to form, miR-200c levels may increase to repress the ZEB factors post-transcriptionally. This will cause an increase in epithelial markers such as E-cadherin, resulting in more cells differentiating to become epithelial, and forming a solid tumour. Although this explanation is specific to epithelial tumours, a similar scenario may occur in the case of lymphomas, as they are also solid tumours and can migrate to other sites.

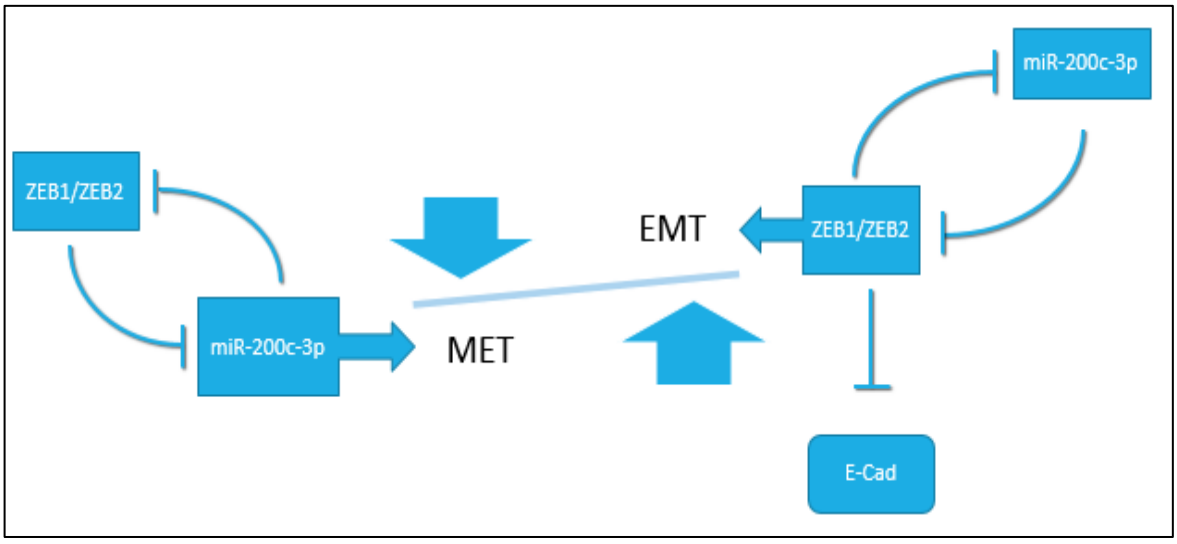


**Figure 5.1: Summary of the miR-200c/ZEB double negative feedback loop and its interaction with the reversible EMT process.**

## 5.2 Role of the ZEB genes in lymphomas

As already mentioned, the ZEB genes have well defined roles in carcinomas. These transcription factors promote tumour invasion and metastasis mainly through the process of EMT. However, there is not much information available on their involvement in lymphomas. One particular study showed that expression of ZEB1 was upregulated by the Wnt signalling

pathway in Mantle cell lymphoma (MCL) (Sanchez-Tillo et al., 2014). The study further elucidated to ZEB1 promoting cell proliferation and resistance to apoptosis in this type of lymphoma. In some cases of DLBCL, specific mutations in the "seed region" mature sequence of hsa-miR-142-3p were identified which resulted in the miRNA gaining novel binding sites for the 3'-UTR of both ZEB1 and ZEB2 (Kwanhian et al., 2012). Furthermore, the miRNA lost the ability to regulate its known gene targets. Unfortunately, the group did not conduct further functional studies to investigate the relevance of this interaction in promoting lymphomas.

Consequently, the work on the ZEB genes presented in this research project provides novel information on their potential role in lymphomas, specifically HIV-associated BL. The expression of these genes may also contribute towards the aggressive nature of this subtype of lymphoma. Ultimately, further research needs to be performed looking into the significance of these two transcription factors in lymphoma development and progression.

## 5.3 Limitations

Some of the limitations that were encountered during this research project include the challenge of detecting hsa-miR-363-3p using the TaqMan® miRNA assays and failing. Another limitation was the discrepancies between the PCR array and single-tube assay results obtained, which may have been due to using different platforms and experimental set up. When using the Applied Biosystems 7900HT Fast Real-time PCR system machine, the reaction volume was scaled down as the reaction was performed in a 384-well plate. This may have increased the chance of technical errors occurring from pipetting small volumes. Evaporation of samples may have occurred as the plate was not closed for an extended period during preparation of numerous samples.

## 5.4 Conclusions and Future Work

In line with the aim, this project has shown that HIV alters miRNA expression levels in lymphoma cells. Hsa-miR-200c-3p was found to be downregulated in response to HIV-1 exposure in two Burkitt's lymphoma cell lines, Ramos and BL41. The selected gene targets ZEB1 and ZEB2 were also found to be downregulated at the mRNA level in cells exposed to HIV. The gene expression results of the ZEB factors correlated with protein expression in the Ramos cells under the same experimental conditions. However, both genes were found to be upregulated in the BL41 cells exposed to HIV. The cells exposed to HIV also exhibited enhanced migratory ability relative to control cells. Future work should investigate whether the ZEB factors are indeed involved in the enhanced migration of these cells under HIV-1 exposure. This can be done by either enhancing (overexpressing) or inhibiting (using siRNA) their expression and repeating the Transwell® migration assays as before. Similarly, experiments can be performed using hsa-miR-200c-3p mimics or inhibitors to establish whether this miRNA is involved in the enhanced migration observed. Furthermore, other hsa-miR-200c-3p gene targets can be selected and investigated further using relevant functional assays, as well as using other BL cell lines. At an in vivo level, the expression of hsa-miR-200c-3p can be investigated in BL tumours from HIV positive patients and compare that to BL tumours from HIV negative patients. Ultimately, these types of studies enhance our

understanding of the role of miRNAs in cancer and their potential as biomarkers of specific human cancers, or tools for diagnosis, prognosis and therapy.

# References


ABAYOMI, E. A., SOMERS, A., GREWAL, R., SISSOLAK, G., BASSA, F., MAARTENS, D., JACOBS, P., STEFAN, C. & AYERS, L. W. 2011. Impact of the HIV epidemic and Anti-Retroviral Treatment policy on lymphoma incidence and subtypes seen in the Western Cape of South Africa, 2002-2009: preliminary findings of the Tygerberg Lymphoma Study Group. *Transfus Apher Sci,* 44**,** 161-6.

AHLFEN, S. & SCHLUMPBERGER, M. 2010. Effects of low A260/A230 ratios in RNA preparations on downstream applications. *QIAGEN Gene Expression and Function Studies*.

ALTUVIA, Y., LANDGRAF, P., LITHWICK, G., ELEFANT, N., PFEFFER, S., ARAVIN, A., BROWNSTEIN, M. J., TUSCHL, T. & MARGALIT, H. 2005. Clustering and conservation patterns of human microRNAs. *Nucleic Acids Res,* 33**,** 2697-706.

AMBROS, V., BARTEL, B., BARTEL, D. P., BURGE, C. B., CARRINGTON, J. C., CHEN, X., DREYFUSS, G., EDDY, S. R., GRIFFITHS-JONES, S., MARSHALL, M., MATZKE, M., RUVKUN, G. & TUSCHL, T. 2003. A uniform system for microRNA annotation. *RNA,* 9**,** 277-279.

ARMITAGE, J. O. 2005. Staging Non-Hodgkin Lymphoma. *CA Cancer J Clin,* 55**,** 368–376.

BLAHNA, M. T. & HATA, A. 2013. Regulation of miRNA biogenesis as an integrated component of growth factor signaling. *Curr Opin Cell Biol,* 25**,** 233-40.

BRABLETZ, S. & BRABLETZ, T. 2010. The ZEB/miR-200 feedback loop--a motor of cellular plasticity in development and cancer? *EMBO Rep,* 11**,** 670-7.

BRACKEN, C. P., GREGORY, P. A., KOLESNIKOFF, N., BERT, A. G., WANG, J., SHANNON, M. F. & GOODALL, G. J. 2008. A double-negative feedback loop between ZEB1-SIP1 and the microRNA-200 family regulates epithelial-mesenchymal transition. *Cancer Res,* 68**,** 7846-54.

BROWNE, G., SAYAN, A. E. & TULCHINSKY, E. 2010. ZEB proteins link cell motility with cell cycle control and cell survival in cancer. *Cell Cycle,* 9**,** 886-91.

BURK, U., SCHUBERT, J., WELLNER, U., SCHMALHOFER, O., VINCAN, E., SPADERNA, S. & BRABLETZ, T. 2008. A reciprocal repression between ZEB1 and members of the miR-200 family promotes EMT and invasion in cancer cells. *EMBO Rep,* 9**,** 582-9.

CALIN, G. A. & CROCE, C. M. 2006. MicroRNA signatures in human cancers. *Nat Rev Cancer,* 6**,** 857-66.

CALIN, G. A., DUMITRU, C. D., SHIMIZU, M., BICHI, R., ZUPO, S., NOCH, E., ALDLER, H., RATTAN, S., KEATING, M., RAI, K., RASSENTI, L., KIPPS, T., NEGRINI, M., BULLRICH, F. & CROCE, C. M. 2002. Frequent deletions and down-regulation of micro- RNA genes miR15 and miR16 at 13q14 in chronic lymphocytic leukemia. *Proc Natl Acad Sci U S A,* 99**,** 15524-9.

CAMPO, E., SWERDLOW, S. H., HARRIS, N. L., PILERI, S., STEIN, H. & JAFFE, E. S. 2011. The 2008 WHO classification of lymphoid neoplasms and beyond: evolving concepts and practical applications. *Blood,* 117**,** 5019-32.

CHEN, C., RIDZON, D. A., BROOMER, A. J., ZHOU, Z., LEE, D. H., NGUYEN, J. T., BARBISIN, M., XU, N. L., MAHUVAKAR, V. R., ANDERSEN, M. R., LAO, K. Q., LIVAK, K. J. & GUEGLER, K. J. 2005. Real-time quantification of microRNAs by stem-loop RT-PCR. *Nucleic Acids Res,* 33**,** e179.

CHEN, Y., GELFOND, J. A., MCMANUS, L. M. & SHIREMAN, P. K. 2009. Reproducibility of quantitative RT-PCR array in miRNA expression profiling and comparison with microarray analysis. *BMC Genomics,* 10**,** 407.

CHENDRIMADA, T. P., GREGORY, R. I., KUMARASWAMY, E., NORMAN, J., COOCH, N., NISHIKURA, K. & SHIEKHATTAR, R. 2005. TRBP recruits the Dicer complex to Ago2 for microRNA processing and gene silencing. *Nature,* 436**,** 740-4.

CHENG, A. M., BYROM, M. W., SHELTON, J. & FORD, L. P. 2005. Antisense inhibition of human miRNAs and indications for an involvement of miRNA in cell growth and apoptosis. *Nucleic Acids Res,* 33**,** 1290-7.

CHUANG, T. D. & KHORRAM, O. 2014. miR-200c regulates IL8 expression by targeting IKBKB: a potential mediator of inflammation in leiomyoma pathogenesis. *PLoS One,* 9**,** e95370.

CHUANG, T. D., PANDA, H., LUO, X. & CHEGINI, N. 2012. miR-200c is aberrantly expressed in leiomyomas in an ethnic-dependent manner and targets ZEBs, VEGFA, TIMP2, and FBLN5. *Endocr Relat Cancer,* 19**,** 541-56.

CHUGH, P. & DITTMER, D. P. 2012. Potential pitfalls in microRNA profiling. *Wiley Interdiscip Rev RNA,* 3**,** 601-16.

COCHRANE, D. R., HOWE, E. N., SPOELSTRA, N. S. & RICHER, J. K. 2010. Loss of miR-200c: A Marker of Aggressiveness and Chemoresistance in Female Reproductive Cancers. *J Oncol,* 2010**,** 821717.

COCHRANE, D. R., SPOELSTRA, N. S., HOWE, E. N., NORDEEN, S. K. & RICHER, J. K. 2009. MicroRNA-200c mitigates invasiveness and restores sensitivity to microtubule-targeting chemotherapeutic agents. *Mol Cancer Ther,* 8**,** 1055-66.

DING, L., ZHANG, Y., HAN, L., FU, L., MEI, X., WANG, J., ITKOW, J., ELABID, A. E. I., PANG, L. & YU, D. 2018. Activating and sustaining c-Myc by depletion of miR-144/451 gene locus contributes to B-lymphomagenesis. *Oncogene,* 37**,** 1293-1307.

DRAHOS, J., SCHWAMEIS, K., ORZOLEK, L. D., HAO, H., BIRNER, P., TAYLOR, P. R., PFEIFFER, R. M., SCHOPPMANN, S. F. & COOK, M. B. 2016. MicroRNA Profiles of Barrett's Esophagus and Esophageal Adenocarcinoma: Differences in Glandular Non-native Epithelium. *Cancer Epidemiol Biomarkers Prev,* 25**,** 429-37.

DUNLEAVY, K., PITTALUGA, S., SHOVLIN, M., STEINBERG, S. M., COLE, D., GRANT, C., WIDEMANN, B., STAUDT, L. M., JAFFE, E. S., LITTLE, R. F. & WILSON, W. H. 2013. Low-intensity therapy in adults with Burkitt's lymphoma. *N Engl J Med,* 369**,** 1915-25.

DUNLEAVY, K. & WILSON, W. H. 2012. How I treat HIV-associated lymphoma. *Blood* 19**,** 3245-55.

ELGAAEN, B. V., OLSTAD, O. K., HAUG, K. B. F., BRUSLETTO, B., SANDVIK, L., STAFF, A. C., GAUTVIK, K. M. & DAVIDSON, B. 2014. Global miRNA expression analysis of serous and clear cell ovarian carcinomas identifies differentially expressed miRNAs including miR200c-3p and a prognostic marker. *BMC Cancer,* 14.

ERTURK, E., CECENER, G., TEZCAN, G., EGELI, U., TUNCA, B., GOKGOZ, S., TOLUNAY, S. & TASDELEN, I. 2015. BRCA mutations cause reduction in miR-200c expression in triple negative breast cancer. *Gene,* 556**,** 163-9.

FLOYD, D. H., ZHANG, Y., DEY, B. K., KEFAS, B., BREIT, H., MARKS, K., DUTTA, A., HEROLD-MENDE, C., SYNOWITZ, M., GLASS, R., ABOUNADER, R. & PUROW, B. W. 2014. Novel anti-apoptotic microRNAs 582-5p and 363 promote human glioblastoma stem cell survival via direct inhibition of caspase 3, caspase 9, and Bim. *PLoS One,* 9**,** e96239.

FORTE, E., SALINAS, R. E., CHANG, C., ZHOU, T., LINNSTAEDT, S. D., GOTTWEIN, E., JACOBS, C., JIMA, D., LI, Q. J., DAVE, S. S. & LUFTIG, M. A. 2012. The Epstein-Barr virus (EBV)-

induced tumor suppressor microRNA MiR-34a is growth promoting in EBV-infected B cells. *J Virol,* 86**,** 6889-98.
GIT, A., DVINGE, H., SALMON-DIVON, M., OSBORNE, M., KUTTER, C., HADFIELD, J., BERTONE, P. & CALDAS, C. 2010. Systematic comparison of microarray profiling, real-time PCR, and next-generation sequencing technologies for measuring differential microRNA expression. *RNA,* 16**,** 991-1006.
GLOGHINI, A., DOLCETTI, R. & CARBONE, A. 2013. Lymphomas occurring specifically in HIV-infected patients: from pathogenesis to pathology. *Semin Cancer Biol,* 23**,** 457-67.
GOOLAM HOOSEN, T. 2017. Identifiction and characteristation of microRNAs involved in the pathogenesis of HIV-associated nonhodgkin's lymphoma. *UCT,* Masters Thesis.
GOTTWEIN, E., CORCORAN, D. L., MUKHERJEE, N., SKALSKY, R. L., HAFNER, M., NUSBAUM, J. D., SHAMULAILATPAM, P., LOVE, C. L., DAVE, S. S., TUSCHL, T., OHLER, U. & CULLEN, B. R. 2011. Viral microRNA targetome of KSHV-infected primary effusion lymphoma cell lines. *Cell Host Microbe,* 10**,** 515-26.
GRAMANTIERI, L., FERRACIN, M., FORNARI, F., VERONESE, A., SABBIONI, S., LIU, C. G., CALIN, G. A., GIOVANNINI, C., FERRAZZI, E., GRAZI, G. L., CROCE, C. M., BOLONDI, L. & NEGRINI, M. 2007. Cyclin G1 is a target of miR-122a, a microRNA frequently down-regulated in human hepatocellular carcinoma. *Cancer Res,* 67**,** 6092-9.
GREGORY, R. I., YAN, K., AMUTHAN, G., CHENDRIMADA, T., DORATOTAJ, B., COOCH, N. & SHIEKHATTAR, R. 2004. The microprocessor complex mediates the genesis of microRNAs. *Nature,* 432.
GULYAEVA, L. F. & KUSHLINSKIY, N. E. 2016. Regulatory mechanisms of microRNA expression. *J Transl Med,* 14**,** 143.
GUO, P., NIE, Q., LAN, J., GE, J., QIU, Y. & MAO, Q. 2013. C-Myc negatively controls the tumor suppressor PTEN by upregulating miR-26a in glioblastoma multiforme cells. *Biochem Biophys Res Commun,* 441**,** 186-90.
HAASE, A. D., JASKIEWICZ, L., ZHANG, H., LAINE, S., SACK, R., GATIGNOL, A. & FILIPOWICZ, W. 2005. TRBP, a regulator of cellular PKR and HIV-1 virus expression, interacts with Dicer and functions in RNA silencing. *EMBO Rep,* 6**,** 961-7.
HAN, J., LEE, Y., YEOM, K., KIM, Y., JIN, H. & KIM, V. N. 2004. The Drosha-DGCR8 complex in primary microRNA processing. *Genes Dev,* 18**,** 3016-3027.
HANAHAN, D. & WEINBERG, R. A. 2011. Hallmarks of cancer: the next generation. *Cell,* 144**,** 646-74.
HASHIMOTO, Y., AKIYAMA, Y. & YUASA, Y. 2013. Multiple-to-multiple relationships between microRNAs and target genes in gastric cancer. *PLoS One,* 8**,** e62589.
HEGARTY, S. V., SULLIVAN, A. M. & O'KEEFFE, G. W. 2015. Zeb2: A multifunctional regulator of nervous system development. *Prog Neurobiol,* 132**,** 81-95.
HILL, L., BROWNE, G. & TULCHINSKY, E. 2013. ZEB/miR-200 feedback loop: at the crossroads of signal transduction in cancer. *Int J Cancer,* 132**,** 745-54.
HOUZET, L., YEUNG, M. L., DE LAME, V., DESAI, D., SMITH, S. M. & JEANG, K. T. 2008. MicroRNA profile changes in human immunodeficiency virus type 1 (HIV-1) seropositive individuals. *Retrovirology,* 5**,** 118.
HOWE, E. N., COCHRANE, D. R. & RICHER, J. K. 2011. Targets of miR-200c mediate suppression of cell motility and anoikis resistance. *Breast Cancer Res,* 13**,** R45.
HULKOWER, K. I. & HERBER, R. L. 2011. Cell migration and invasion assays as tools for drug discovery. *Pharmaceutics,* 3**,** 107-24.

HUR, K., TOIYAMA, Y., TAKAHASHI, M., BALAGUER, F., NAGASAKA, T., KOIKE, J., HEMMI, H., KOI, M., BOLAND, C. R. & GOEL, A. 2013. MicroRNA-200c modulates epithelial-to-mesenchymal transition (EMT) in human colorectal cancer metastasis. *Gut,* 62**,** 1315-26.

IBRAHIM, F. F., JAMAL, R., SYAFRUDDIN, S. E., MUTALIB, N. S. A., SAIDIN, S., MDZIN, R. R. M. M., M. H. & MOKHTAR, N. M. 2015. microRNA-200c and microRNA-31 regulate proliferation, colony formation, migration and invasion in serous ovarian cancer. *J Ovarian Res,* 8.

IORIO, M. V., FERRACIN, M., LIU, C. G., VERONESE, A., SPIZZO, R., SABBIONI, S., MAGRI, E., PEDRIALI, M., FABBRI, M., CAMPIGLIO, M., MENARD, S., PALAZZO, J. P., ROSENBERG, A., MUSIANI, P., VOLINIA, S., NENCI, I., CALIN, G. A., QUERZOLI, P., NEGRINI, M. & CROCE, C. M. 2005. MicroRNA gene expression deregulation in human breast cancer. *Cancer Res,* 65**,** 7065-70.

KLEIN, G., GIOVANELLA, B., WESTMAN, A., STEHLIN, J. S. & MUMFORD, D. 1975. An EBV-Genome-Negative Cell Line Established from an American Burkitt Lymphoma; Receptor Characteristics. EBV Infectibility and Permanent Conversion into EBV-Positive Sublines by in vitro Infection. *Intervirology,* 5**,** 319-334.

KORPAL, M., LEE, E. S., HU, G. & KANG, Y. 2008. The miR-200 family inhibits epithelial-mesenchymal transition and cancer cell migration by direct targeting of E-cadherin transcriptional repressors ZEB1 and ZEB2. *J Biol Chem,* 283**,** 14910-4.

KUHN, D. E., MARTIN, M. M., FELDMAN, D. S., TERRY, A. V., NUOVO, G. J. & ELTON, T. S. 2008a. Experimental Validation of miRNA targets. *Methods,* 44**,** 47-54.

KUHN, D. E., MARTIN, M. M., FELDMAN, D. S., TERRY, A. V., NUOVO, G. J. & S., E. T. 2008b. Experimental Validation of miRNA targets *Methods,* 44**,** 47-54.

KWANHIAN, W., LENZE, D., ALLES, J., MOTSCH, N., BARTH, S., DOLL, C., IMIG, J., HUMMEL, M., TINGUELY, M., TRIVEDI, P., LULITANOND, V., MEISTER, G., RENNER, C. & GRASSER, F. A. 2012. MicroRNA-142 is mutated in about 20% of diffuse large B-cell lymphoma. *Cancer Med,* 1**,** 141-55.

LEE, C. T., RISOM, T. & STRAUSS, W. M. 2007. Evolutionary conservation of microRNA regulatory circuits: an examination of microRNA gene complexity and conserved microRNA-target interactions through metazoan phylogeny. *DNA Cell Biol,* 26**,** 209-18.

LEE, R. C., FEINBAUM, R. L. & AMBROS, V. 1993. The C. elegans Heterochonic Gene lin-4 Encodes small RNAs with Antisense Complementarity to lin-14. *Cell,* 75**,** 843-854.

LEE, Y., HUR, I., PARK, S., KIM, Y., SUH, M. S. & KIM, V. N. 2006. The role of PACT in the RNA silencing pathway. *EMBO J.,* 25**,** 522-533.

LENOIR, G. M., VUILLAUME, M. & BONNARDEL, C. 1985. The use of lymphomatous and lymphoblastoid cell lines in the study of Burkitt's lymphoma. *IARC Sci Publ. ,* 60**,** 309-318.

LEWIS, B. P., BURGE, C. B. & BARTEL, D. P. 2005. Conserved seed pairing, often flanked by adenosines, indicates that thousands of human genes are microRNA targets. *Cell,* 120**,** 15-20.

LI, S., DUAN, X., LI, Y., LIU, B., MCGILVRAY, I. & CHEN, L. 2014. MicroRNA-130a inhibits HCV replication by restoring the innate immune response. *J Viral Hepat,* 21**,** 121-8.

LIM, S. T., KARIM, R., NATHWANI, B. N., TULPULE, A., ESPINA, B. & LEVINE, A. M. 2005. AIDS-Related Burkitt's Lymphoma Versus Diffuse Large-Cell Lymphoma in the Pre-Highly Active Antiretroviral Therapy (HAART) and HAART Eras. *J Clin Oncol,* 23**,** 4430-38.

LITTLE, R. F. & DUNLEAVY, K. 2013. Update on the treatment of HIV-associated hematologic malignancies. *Blood*, 382-88.
LIU, B., CHE, Q., QIU, H., BAO, W., CHEN, X., LU, W., LI, B. & WAN, X. 2014. Elevated MiR-222-3p promotes proliferation and invasion of endometrial carcinoma via targeting ERalpha. *PLoS One,* 9, e87563.
LIU, S., TETZLAFF, M. T., CUI, R. & XU, X. 2012. miR-200c inhibits melanoma progression and drug resistance through down-regulation of BMI-1. *Am J Pathol,* 181, 1823-35.
LIU, X., YU, J., JIANG, L., WANG, A., SHI, F., YE, H. & ZHOU, X. 2009. MicroRNA-222 regulates cell invasion by targeting matric metalloproteinase (MMP1) in tongue squamous cell caecinoma cell lines. *Cancer Genomics Proteomics,* 6, 131-138.
LUO, Y., GUO, Z. & LI, L. 2013. Evolutionary conservation of microRNA regulatory programs in plant flower development. *Dev Biol,* 380, 133-44.
MACFARLANE, L. & MURPHY, P. R. 2010. MicroRNA: Biogenesis, Function and Role in Cancer. *Curr Genomics,* 11, 537-561.
MAGRATH, I. 2012. Epidemiology: clues to the pathogenesis of Burkitt lymphoma. *Br J Haematol,* 156, 744-56.
MALUMBRES, R., SAROSIEK, K. A., CUBEDO, E., RUIZ, J. W., JIANG, X., GASCOYNE, R. D., TIBSHIRANI, R. & S., L. I. 2009. Differentiation stage–specific expression of microRNAs in B lymphocytes and diffuse large B-cell lymphomas. *Blood,* 113, 3754-3764.
MASSIMELLI, M. J., MAJERCIAK, V., KANG, J. G., LIEWEHR, D. J., STEINBERG, S. M. & ZHENG, Z. M. 2015. Multiple regions of Kaposi's sarcoma-associated herpesvirus ORF59 RNA are required for its expression mediated by viral ORF57 and cellular RBM15. *Viruses,* 7, 496-510.
MILLER, T. E., GHOSHAL, K., RAMASWAMY, B., ROY, S., DATTA, J., SHAPIRO, C. L., JACOB, S. & MAJUMDER, S. 2008. MicroRNA-221/222 confers tamoxifen resistance in breast cancer by targeting p27Kip1. *J Biol Chem,* 283, 29897-903.
MOIR, S. & FAUCI, A. S. 2009. B cells in HIV infection and disease. *Nat Rev Immunol,* 9, 235-45.
MOORE, S. W., FIEGGEN, K., HONEY, E. & ZAAHL, M. 2016. Novel Zeb2 gene variation in the Mowat Wilson syndrome (MWS). *J Pediatr Surg,* 51, 268-71.
MORALES, S., MONZO, M. & NAVARRO, A. 2017. Epigenetic regulation mechanisms of microRNA expression. *Biomol Concepts,* 8, 203-212.
MOREY, J. S., RYAN, J. C. & VAN DOLAH, F. M. 2006. Microarray validation: factors influencing correlation between oligonucleotide microarrays and real-time PCR. *Biol Proced Online,* 8, 175-93.
NAM, E. J., KIM, S., LEE, T. S., KIM, H. J., LEE, J. Y., KIM, S. W., KIM, J. W. & KIM, Y. T. 2016. Primary and recurrent ovarian high-grade serous carcinomas display similar microRNA expression patterns relative to those of nornal ovarian tissue. *Oncotarget,* 7, 70524-70534.
NATHANS, R., CHU, C. Y., SERQUINA, A. K., LU, C. C., CAO, H. & RANA, T. M. 2009. Cellular microRNA and P bodies modulate host-HIV-1 interactions. *Mol Cell,* 34, 696-709.
NIE, Y., WAITE, J., BREWER, F., SUNSHINE, M. J., LITTMAN, D. R. & ZOU, Y. R. 2004. The role of CXCR4 in maintaining peripheral B cell compartments and humoral immunity. *J Exp Med,* 200, 1145-56.
PANDA, H., PELAKH, L., CHUANG, T. D., LUO, X., BUKULMEZ, O. & CHEGINI, N. 2012. Endometrial miR-200c is altered during transformation into cancerous states and

targets the expression of ZEBs, VEGFA, FLT1, IKKbeta, KLF9, and FBLN5. *Reprod Sci,* 19**,** 786-96.

PANNONE, G., ZAMPARESE, R., PACE, M., PEDICILLO, M. C., CAGIANO, S., SOMMA, P., ERRICO, M. E., DONOFRIO, V., R., F., DE CHIARA, A., AQUINO, G., BUCCI, P., BUCCI, E., SANTORO, A. & BUFO, P. 2014. The role of EBV in the pathogenesis of Burkitt's Lymphoma: an Italian hospital based survey. *Infect. Agents Cancer,* 9.

PARK, S. M., GAUR, A. B., LENGYEL, E. & PETER, M. E. 2008. The miR-200 family determines the epithelial phenotype of cancer cells by targeting the E-cadherin repressors ZEB1 and ZEB2. *Genes Dev,* 22**,** 894-907.

PAROO, Z., YE, X., CHEN, S. & LIU, Q. 2009. Phosphorylation of the human microRNA-generating complex mediates MAPK/Erk signaling. *Cell,* 139**,** 112-22.

PATEL, M., PHILIP, V., OMAR, T., TURTON, D., CANDY, G., LAKHA, A. & PATHER, S. 2015. The Impact of Human Immunodeficiency Virus Infection (HIV) on Lymphoma in South Africa. *Journal of Cancer Therapy,* 06**,** 527-535.

PERISE-BARRIOS, A. J., MUNOZ-FERNANDEZ, M. A. & PION, M. 2012. Direct phenotypical and functional dysregulation of primary human B cells by human immunodeficiency virus (HIV) type 1 in vitro. *PLoS One,* 7**,** e39472.

PETER, M. E. 2009. Let-7 and miR-200 microRNAs: guardians against pluripotency and cancer progression. *Cell Cycle,* 8**,** 843-52.

PFEFFER, S., SEWER, A., LAGOS-QUINTANA, M., SHERIDAN, R., SANDER, C., GRASSER, F. A., VAN DYK, L. F., HO, C. K., SHUMAN, S., CHIEN, M., RUSSO, J. J., JU, J., RANDALL, G., LINDENBACH, B. D., RICE, C. M., SIMON, V., HO, D. D., ZAVOLAN, M. & TUSCHL, T. 2005. Identification of microRNAs of the herpesvirus family. *Nat Methods,* 2**,** 269-76.

PRISLEI, S., MARTINELLI, E., MARIANI, M., RASPAGLIO, G., SIEBER, S., FERRANDINA, G., SHAHABI, S., SCAMBIA, G. & FERLINI, C. 2013. MiR-200c and HuR in ovarian cancer. *BMC Cancer,* 13**,** 72.

QIAO, J., LEE, S., PAUL, P., THEISS, L., TIAO, J., QIAO, L., KONG, A. & CHUNG, D. H. 2013. miR-335 and miR-363 regulation of neuroblastoma tumorigenesis and metastasis. *Surgery,* 154**,** 226-33.

QIU, M., LIANG, Z., CHEN, L., TAN, G., LIU, L., WANG, K., CHEN, H. & LIU, J. 2017. MicroRNA-200c suppresses cell growth and metastasis by targeting Bmi-1 and E2F3 in renal cancer cells. *Exp Ther Med,* 13**,** 1329-1336.

RANGANATHAN, K. & SIVASANKAR, V. 2014. MicroRNAs - Biology and clinical applications. *J Oral Maxillofac Pathol,* 18**,** 229-34.

ROJAS-MARQUEZ, C., VALLE-RIOS, R., LOPEZ-BAYGHEN, E. & ORTIZ-NAVARRETE, V. 2015. CRTAM is negatively regulated by ZEB1 in T cells. *Mol Immunol,* 66**,** 290-8.

ROSATO, P., ANASTASIADOU, E., GARG, N., LENZE, D., BOCCELLATO, F., VINCENTI, S., SEVERA, M., COCCIA, E. M., BIGI, R., CIRONE, M., FERRETTI, E., CAMPESE, A. F., HUMMEL, M., FRATI, L., PRESUTTI, C., FAGGIONI, A. & TRIVEDI, P. 2012. Differential regulation of miR-21 and miR-146a by Epstein-Barr virus-encoded EBNA2. *Leukemia,* 26**,** 2343-52.

ROSSIO, J. L., ESSER, M. T., SURYANARAYANA, K., SCHNEIDER, D. K., BESS, J. W., VASQUEZ, G. M., WILTROUT, T. A., CHERTOVA, E., GRIMES, M. K., SATTENTAU, Q., ARTHUR, L. O., HENDERSOM, L. E. & LIFSON, J. D. 1998. Inactivation of Human Immunodeficiency Virus Type 1 infectivity with preservation of conformational and functional integrity of virion surface proteins. *J Virol,* 72**,** 7992-8001.

ROTH, B. M., ISHIMARU, D. & HENNIG, M. 2013. The core microprocessor component DiGeorge syndrome critical region 8 (DGCR8) is a nonspecific RNA-binding protein. *J Biol Chem,* 288**,** 26785-99.

SANCHEZ-TILLO, E., FANLO, L., SILES, L., MONTES-MORENO, S., MOROS, A., CHIVA-BLANCH, G., ESTRUCH, R., MARTINEZ, A., COLOMER, D., GYORFFY, B., ROUE, G. & POSTIGO, A. 2014. The EMT activator ZEB1 promotes tumor growth and determines differential response to chemotherapy in mantle cell lymphoma. *Cell Death Differ,* 21**,** 247-57.

SÁNCHEZ-TILLÓ, E., SILES, L., DE BARRIOS, O., CUATRECASAS, M., VAQUERO, E. C., CASTELLS, A. & POSTIGO, A. 2011. Expanding roles of ZEB factors in tumorigenesis and tumor progression. *Am J Cancer Res,* 1**,** 897-912.

SISSOLAK, G., SEFTEL, M., ULDRICK, T. S., ESTERHUIZEN, T. M., MOHAMED, N. & KOTZE, D. 2017. Burkitt's Lymphoma and B-Cell Lymphoma Unclassifiable With Features

Intermediate Between Diffuse Large B-Cell Lymphoma and Burkitt's Lymphoma in Patients With HIV: Outcomes in a South African Public Hospital. *J Glob Oncol,* 3.

SKALSKY, R. L., SAMOLS, M. A., PLAISANCE, K. B., BOSS, I. W., RIVA, A., LOPEZ, M. C., BAKER, H. V. & RENNE, R. 2007. Kaposi's sarcoma-associated herpesvirus encodes an ortholog of miR-155. *J Virol,* 81**,** 12836-45.

SONG, B., YAN, J., LIU, C., ZHOU, H. & ZHENG, Y. 2015. Tumor Suppressor Role of miR-363-3p in Gastric Cancer. *Med. Sci. Monit.,* 21**,** 4074-4080.

STEFAN, D. C. & RABEEN LUTCHMAN, R. 2014. Burkitt lymphoma: epidemiological features and survival in a South African centre. *Infect Agent Cancer,* 9.

SUN, Q., ZHANG, J., CAO, W., WANG, X., XU, Q., YAN, M., WU, X. & CHEN, W. 2013. Dysregulated miR-363 affects head and neck cancer invasion and metastasis by targeting podoplanin. *Proc Natl Acad Sci U S A,* 45**,** 513-20.

THOMSON, D. W., BRACKEN, C. P. & GOODALL, G. J. 2011. Experimental strategies for microRNA target identification. *Nucleic Acids Res,* 39**,** 6845-53.

TORRE, L. A., BRAY, F., SIEGEL, R. L., FERLAY, J., LORTET-TIEULENT, J. & JEMAL, A. 2015. Global cancer statistics, 2012. *CA Cancer J Clin,* 65**,** 87-108.

TRIBOULET, R., MARI, B., LIN, Y., CHABLE-BESSIA, C., BENN ASSER, Y., LEBRIGAND, K., CARDINAUD, B., MAURIN, T., BARBRY, P., BARILLAT, V., REYNES, J., CORBEAU, P., JEANG, K. T. & BENKIRANE, M. 2007. Suppression of miRNA-silencing pathway by HIV-1 during viral replication. *Science,* 315**,** 1579-1582.

ULLAH, S., GHULAM, N., MUHAMMAD, H., REHMAN, H. U. & ZEB, J. 2015. Role of miRNAs in cancer diagnosis and therapeutics. *Merit Res. J. Med. Med. Sci.,* 3**,** 013-015.

VANDEWALLE, C., VAN ROY, F. & BERX, G. 2009. The role of the ZEB family of transcription factors in development and disease. *Cell Mol Life Sci,* 66**,** 773-87.

VELU, V. K., RAMESH, R. & SRINIVASAN, A. R. 2012. Circulating MicroRNAs as Biomarkers in Health and Disease. *J Clin Diagn Res,* 6**,** 1791-5.

VERA, O., JIMENEZ, J., PERNIA, O., RODRIGUEZ-ANTOLIN, C., RODRIGUEZ, C., SANCHEZ CABO, F., SOTO, J., ROSAS, R., LOPEZ-MAGALLON, S., ESTEBAN RODRIGUEZ, I., DOPAZO, A., ROJO, F., BELDA, C., ALVAREZ, R., VALENTIN, J., BENITEZ, J., PERONA, R., DE CASTRO, J. & IBANEZ DE CACERES, I. 2017. DNA Methylation of miR-7 is a Mechanism Involved in Platinum Response through MAFG Overexpression in Cancer Cells. *Theranostics,* 7**,** 4118-4134.

VISONE, R., RUSSO, L., PALLANTE, P., I., D. M., FERRARO, A., LEONE, V., BORBONE, E., PETROCCA, F., ALDER, H., CROCE, C. M. & A., F. 2007. MicroRNAs mir-221 and miR-

222, both overexpressed in human thyroid papillary carcinomas, regulate p27 protein levels and cell cycle. *Endocr Relat Cancer,* 14**,** 791-798.
WANG, H., YAN, C., SHI, X., ZHENG, J., DENG, L., YANG, L., YU, F., YANG, Y. & SHAO, Y. 2015. MicroRNA-575 targets BLID to promote growth and invasion of non-small cell lung cancer cells. *FEBS Lett,* 589**,** 805-11.
WANG, X., ZHAO, X., GAO, P. & WU, M. 2013. c-Myc modulates microRNA processing via the transcriptional regulation of Drosha. *Sci Rep,* 3**,** 1942.
WARNER, M. J., BRIDGE, K. S., HEWITSON, J. P., HODGKINSON, M. R., HEYAM, A., MASSA, B. C., HASLAM, J. C., CHATZIFRANGKESKOU, M., EVANS, G. J., PLEVIN, M. J., SHARP, T. V. & LAGOS, D. 2016. S6K2-mediated regulation of TRBP as a determinant of miRNA expression in human primary lymphatic endothelial cells. *Nucleic Acids Res,* 44**,** 9942-9955.
WIGHTMAN, B., HA, I. & RUVKUN, G. 1993. Posttranscriptional Regulation of the Heterochonic Gene lin-14 by lin-4 Mediates Temphoral Pattern Formation in C. elegans. *Cell,* 75**,** 855-862.
YAN, Q., MA, X., SHEN, C., CAO, X., FENG, N., QIN, D., ZENG, Y., ZHU, J., GAO, S. & LUA, C. 2014. Inhibition of Kaposi's sarcoma-associated herpesvirus lytic replication by HIV-1 nef and cellular microRNA hsa-miR-1258. *J. Virol,* 88**,** 4987–5000.
YAO, Y., SUO, A. L., LI, Z. F., LIU, L. Y., TIAN, T., NI, L., ZHANG, W. G., NAN, K. J., SONG, T. S. & HUANG, C. 2009. MicroRNA profiling of human gastric cancer. *Mol Med Rep,* 2**,** 963-70.
YI, R., QIN, Y., MACARA, I. G. & CULLEN, B. R. 2003. Exportin-5 mediates nuclear export of pre-microRNAs and short hairpin RNAs. *Genes Dev,* 17**,** 3011-3016.
ZHANG, H., SUN, Z., LI, Y., FAN, D. & JIANG, H. 2017. MicroRNA-200c binding to FN1 suppresses the proliferation, migration and invasion of gastric cancer cells. *Biomed Pharmacother,* 88**,** 285-292.
ZHANG, P., SUN, Y. & MA, L. 2015. ZEB1: at the crossroads of epithelial-mesenchymal transition, metastasis and therapy resistance. *Cell Cycle,* 14**,** 481-7.
ZHANG, P., WEI, Y., WANG, L., DEBEB, B. G., YUAN, Y., ZHANG, J., YUAN, J., WANG, M., CHEN, D., SUN, Y., WOODWARD, W. A., LIU, Y., DEAN, D. C., LIANG, H., HU, Y., ANG, K. K., HUNG, M. C., CHEN, J. & MA, L. 2014. ATM-mediated stabilization of ZEB1 promotes DNA damage response and radioresistance through CHK1. *Nat Cell Biol,* 16**,** 864-75.
ZHOU, X., WANG, Y., SHAN, B., HAN, J., ZHU, H., LV, Y., FAN, X., SANG, M., LIU, X.-D. & LIU, W. 2015. The downregulation of miR-200c/141 promotes ZEB1/2 expression and gastric cancer progression. *Med Oncol,* 32.

# Appendices

## Appendix A: Recipes and Reagents

**Tissue culture**

**Complete growth media for Ramos and BL41 cell lines**
Add 5ml of FBS (10%) and 0.5ml P/S (1%) to a 50ml Falcon tube
Fill up to 50ml with RPMI media and mix well
Store at $4^0$C

**Freezing media for Ramos and BL41 cell lines**
10% DMSO and 10% FBS in RPMI media (as needed for immediate use)
Place on ice in fume hood until use

**Antibiotic-free media for mycoplasma testing**
10% FBS in RPMI media (make fresh for immediate use, as needed)

**Low serum media for pre-treatment**
Add 0.1 ml (0.5%) of FBS and 0.2ml (1%) of P/S in a 50ml Falcon tube
Fill up to 20ml with RPMI media
Mix well before using for plating cells

**Mycoplasma Testing**

**Fixative**
Mix glacial acetic acid and methanol in a ratio of 1:3 in a 50ml Falcon tube
Cover the tube with foil and store at 4°C

**Mounting Fluid**
22.2ml 0.1 M citric acid
27.8ml 0.2 M Na2HPO4.2H2O
50ml glycerol
Mix and adjust to pH 5.5
Aliquot and store at $4^0$C

**RNA Extraction**

**0.1% diethyl pyrocarbonate- (DEPC) treated water**
Fill a large bottle with deionized water and add 1ml of DEPC per 1l of water

Add a stirrer bar and place in stirrer for a few hours (3-5 hours)
Place the bottle in the fume hood overnight
Remove stirrer bar and autoclave to inactivate the remaining DEPC
Store the water at room temperature

**0.1% diethyl pyrocarbonate- (DEPC) treatment of plasticware**
Fill a big beaker with deionised water and add 1ml of DEPC per 1l of water
Add a stirrer bar and plasticware (pipette tips, centrifuge tubes, etc.) and cover with foil
Place the beaker in the stirrer for a few hours (3-5 hours) and transfer to the fume hood for overnight storage
Remove the plasticware from the water and airdry
Place the plasticware in autoclave bags and autoclave to inactivate the remaining DEPC

**1X Phosphate-buffered saline (PBS)**
Dissolve tablets in deionised water per manufacturer's instructions
Autoclave and store a $4^0$C

**10X Tris/Borate/EDTA (TBE) buffer**
108g Tris
55g Boric acid
Dissolve in 900ml DEPC-treated water.
Add 40ml EDTA (0.5M, pH 8)
Adjust to 1L and store at room temperature

**1X TBE**
100ml of 10X TBE stock
900ml DEPC-treated water
Mix and store at room temperature

**2X RNA loading buffer**
900µl formamide
99µl sucrose
0.5µl Bromophenol Blue
0.5µl Xylene Cyanol
Mix and store at room temperature

**10X DNA loading buffer**
0.025g Xylene cyanol
0.025g Bromophenol Blue
1.25ml 10% SDS

12.5ml glycerol
Dissolve in 6.25 mL of deionised
Store at room temperature

**1%/1.5% agarose gel**
1g/1.5g agarose
100ml 1x TBE
Dissolve all the agarose by heating.
Allow cooling and then add 2µl Ethidium Bromide (EtBr, 0.5mg/ml) per 30ml of gel
Pour gel on tray and allow to set

**Protein Extraction**

**RIPA buffer**
Dissolve 0.5g (1%) deoxycholate powder in 40ml deionized water
1.5ml 5M NaCl (150mM)
0.5 ml Triton X100 (1%)
0.25ml 20% SDS (0.1%)
0.5ml 1M Tris **(**pH 7.5) (10mM)
Mix and top up to 50 mL with deionized water
Store at $4^0$C

**7X protease inhibitor**
Dissolve 1 protease inhibitor tablet in 2.5 mL 1X PBS
Store at $-20^0$C

**RIPA solution**
Mix 423µl RIPA buffer and 71µl 7X protease inhibitor
Store on ice until use

**Western blot analysis**

**SDS-PAGE reagents**

**30% acryl-bisacrilamide**
29g acrylamide
1g N.N'-methylenbisacrylamide
Dissolve in 60ml deionised water
Heat the solution to $37^0$C
Adjust volume 100ml and cover with foil to protect from light

Store at $4^0$C

**1.5M Tris buffer (pH 6.8)**
Dissolve 60.5g Tris in 300ml deionised water
Adjust pH to 6.8 with HCl
Fill up to 500ml with deionised water
Store at $4^0$C

**1.5M Tris buffer (pH 8.8)**
Dissolve 60.5g Tris in 300ml deionised water
Adjust pH to 8.8 with HCl
Fill up to 500ml with deionised water
Store at $4^0$C

**10% Sodium dodecyl (SDS)**
Dissolve 5g SDS in 40ml deionised water
Fill up to 50ml with deionised water
Store at room temperature

**0.1% SDS**
Dissolve 0.05g SDS in 40ml deionised water
Adjust volume to 50ml with deionised water
Store at room temperature

**10% Ammonium persulfate (APS)**
Dissolve 0.1g APS in 1ml deionised water
Cover tube with foil and store at $4^0$C

**8% resolving gel for SDS-PAGE**
3.45ml deionised water
1.95ml 30% acryl-bisacrylamide
1.95ml 1.5M Tris (pH 8.8)
0.075ml 10% SDS
0.075ml 10% APS
0.0045ml tetramethylethylenediamine (TEMED) (under the fume hood)
Mix and pour between the glass plates in gel casting apparatus using a ml pipette, minimising exposure to air
Add 0.1% SDS on top to even the gel out and allow to set.
Pour out the SDS after the gel has set.

**5% Stacking gel for SDS-PAGE**
2.1ml deionised water
0.5ml 30% acryl-bisacrylamide
0.38ml 1.5M Tris (pH 6.8)
0.03ml 10% SDS
0.03ml 10% APS
0.003ml tetramethylethylenediamine (TEMED) (under the fume hood)
Mix and pour on top of the resolving gel between the glass plates
Add comb and allow to set

**5X SDS loading dye**
0.04g Bromophenol blue (0.04%)
10g SDS (10%)
Dissolved in 52.5ml deionised water
12.5ml 2M Tris (pH 6.8)
30ml 100% glycerol
5ml β-mercaptoethanol
Mix, aliquot and store at room temperature

**10X SDS-PAGE running buffer**
10g SDS
30.3g Tris
144.1g glycine
Dissolve in 800ml deionised water
Adjust to 1l with deionised water and store at room temperature

**1X SDS-PAGE running buffer**
100ml of 10X SDS-PAGE running buffer stock
900ml deionised water
Mix and store at room temperature

**10X SDS-PAGE transfer buffer**
38g Tris
144g glycine
Dissolve in 800ml deionised water
Adjust volume to 1l with deionised water and store at room temperature

**1X SDS-PAGE transfer buffer**
100ml 10X SDS-PAGE transfer buffer stock
700ml deionised water

200ml isopropanol
Make on the same day to be used, store at $4^0$C

**Protein detection and washing**

**0.1% (w/v) Ponceau S staining solution, in 5% (v/v) acetic acid**
0.05g Ponceau S
2.5ml acetic acid (5%)
Dissolve and adjust volume to 50ml with deionised water
Cover with foil to protect from light and store at room temperature

**1X PBS/0.1% Tween (PBS-Tween)**
1ml Tween 20 in 1l 1X PBS
Add stirrer bar and place on stirrer
Mix well, remove stirrer bar and store at $4^0$C

**Blocking buffer**
41.7ml fat-free milk (5%)
58.3ml PBS-Tween
Mix and store at $4^0$C

**Stripping buffer**
0.69ml 100Mm β-mercaptoethanol
10ml 2% SDS
6.25ml 62.5mM Tris (pH 6.7)
Adjust to 100ml with deionised water
Store at room temperature

**Migration assay reagents**

**0.1% (w/v) Crystal violet solution, in 2% (v/v) ethanol**
0.04g Crystal violet
0.4ml 100% ethanol
Dissolve and adjust volume to 20ml with deionised water
Mix and store at room temperature

**50% Acetic acid**
Mix ml 100% glacial acetic acid with 5ml deionised water
Store at room temperature

Appendix B: Additional data

**Table B1: Stem loop primer sequences for selected miRNAs and controls**

| miRNA | Sequence |
|---|---|
| **RNU48** | 5'-GAUGACCCCAGGUAACUCUGAGUGUGUCGCUGAUGCCAUCACCGCAGCGCUCUG ACC-3' |
| **RNU6B** | 5'-GUGCUCGCUUCGGCAGCACAUAUACUAAAAUUGGAACGAUACAGAGAAGAUUAG CAUGGCCCCUGCGCAAGGAUGACACGCAAAUUCGUGAAGCGUUCCAUAUUUU-3' |
| **Hsa-miR-200c-3p** | 5'-UAAUACUGCCGGGUAAUGAUGGA-3' |
| **Hsa-miR-222-3p** | 5'-AGCUACAUCUGGCUACUGGGU-3' |
| **Hsa-miR-363-3p** | 5'-AAUUGCACGGUAUCCAUCUGUA-3' |
| **Hsa-miR-575** | 5'-GAGCCAGUUGGACAGGAGC-3' |

Hsa- homo sapiens, miR- microRNA

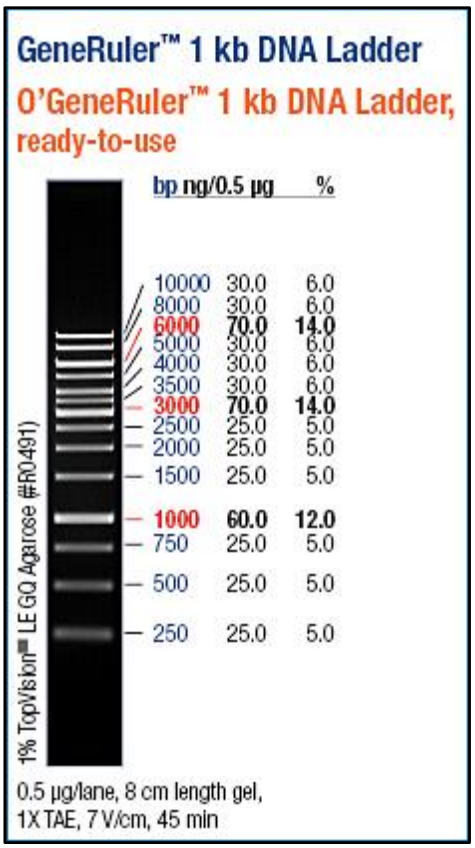


**Figure B1: 1Kb pre-stained DNA ladder**

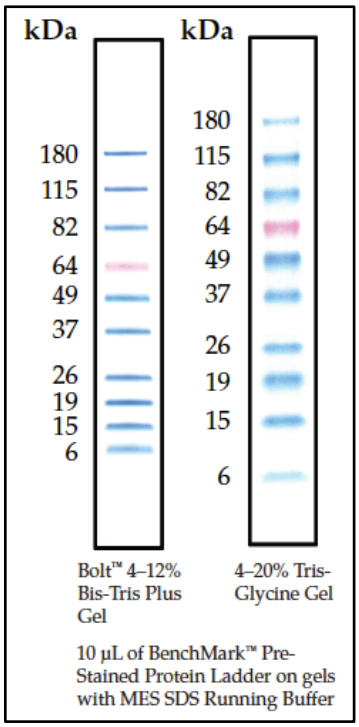


**Figure B2: BenchMark™ Pre-Stained Protein Ladder**

**Table B2: Raw data Ct values obtained from validation* experiment to measure expression levels of hsa-miR-200c-3p, hsa-miR-222-3p, hsa-miR-363-3p, and hsa-miR-575 in Ramos cells**

| Sample | Hsa-miR-575 | | Hsa-miR-222-3p | | Hsa-miR-200c-3p | | Hsa-miR-363-3p | |
|---|---|---|---|---|---|---|---|---|
| | Ct (rep 1) | Ct (rep 2) | Ct (rep 1) | Ct (rep 2) | Ct (rep 1) | Ct (rep 2) | Ct (rep 1) | Ct (rep 2) |
| UT1_R | 32.904457 | 33.557125 | 36.26741 | 34.806908 | 35,196262 | 40 | 40.00 | 31.382 |
| UT2_R | 34.39949 | 34.660065 | 39.317074 | 34.79593 | 35,639393 | 35,43049 | 11.924 | 31.830 |
| MV1_R | 34.16631 | 38.288887 | 36.62299 | 33.508793 | 36,51687 | 36,404068 | 40.00 | 31.380 |
| MV2_R | 35.351856 | 34.766544 | 34.419777 | 35.221294 | 37,365463 | 37,61949 | 40.00 | 32.426 |
| HIV1_R | 34.841084 | 33.409992 | 40 | 39.10493 | 36,746952 | 36,440174 | 40.00 | 31.748 |
| HIV2_R | 33.83914 | 34.717674 | 34,994736 | 40 | 35,13842 | 35,306335 | 40.00 | 31.479 |

* The Applied Biosystems 7900HT Fast Real-time PCR system was used for these experiments. UT-untreated cells, MV-microvesicle-treated cells, HIV-HIV-treated cells, rep-technical replicate

**Table B3: Raw data Ct values obtained from qPCR experiments* performed to determine expression of hsa-miR-200c-3p in Ramos and BL41 cell lines**

| Sample | Ramos | | BL41 | |
|---|---|---|---|---|
| | RNU48 | Hsa-miR-200c-3p | RNU48 | Hsa-miR-200c-3p |
| MV_rep1 | 11.68 | 16.60 | 11.48 | 15.92 |
| MV_rep2 | 11.72 | 16.44 | 11.05 | 16.94 |
| MV_rep3 | 11.94 | 15.85 | 11.24 | 16.39 |
| HIV_rep1 | 11.81 | 17.28 | 11.27 | 18.03 |
| HIV_rep2 | 11.62 | 17.38 | 11.24 | 15.45 |
| HIV_rep3 | 11.43 | 16.85 | 11.29 | 17.42 |

*Roche RotorGene Q platform used. MV- microvesicle-treated cells, HIV- HIV treated cells

**Table B4: Fold change in hsa-miR-200c-3p expression in Ramos cells when normalised to RNU6B**

| Sample | Fold change |
|---|---|
| Rep 1.1 | 0.59 |
| Rep 1.2 | 0.93 |
| Rep 2.1 | 0.87 |
| Rep 2.2 | 0.67 |

**Table B5: Raw Ct values obtained from qPCR experiment performed to measure expression levels of ZEB1 and ZEB2 in Ramos and BL41 cell lines**

| Sample | Ramos | | | BL41 | | |
|---|---|---|---|---|---|---|
| | ZEB1 | ZEB2 | GAPDH | ZEB1 | ZEB2 | GAPDH |
| MV_rep1 | 17.33 | 21.30 | 11.99 | 20.35 | 21.32 | 16.30 |
| MV_rep2 | 17.28 | 20.70 | 11.98 | 20.17 | 21.23 | 15.64 |
| MV_rep3 | 16.95 | 20.60 | 11.96 | 20.06 | 21.15 | 16.11 |
| HIV_rep1 | 18.13 | 22.28 | 12.00 | 20.27 | 21.58 | 17.74 |
| HIV_rep2 | 18.38 | 21.83 | 11.99 | 20.37 | 21.36 | 15.69 |
| HIV_rep3 | 17.66 | 21.72 | 12.08 | 20.25 | 21.40 | 16.07 |